

Root cause discovery via permutations and Cholesky decomposition

Jinzhou Li, Benjamin B. Chu, Ines F. Scheller,
Julien Gagneur, Marloes H. Maathuis

November 25, 2024

Abstract

This work is motivated by the following problem: Can we identify the disease-causing gene in a patient affected by a monogenic disorder? This problem is an instance of root cause discovery. In particular, we aim to identify the intervened variable in one interventional sample using a set of observational samples as reference. We consider a linear structural equation model where the causal ordering is unknown. We begin by examining a simple method that uses squared z-scores and characterize the conditions under which this method succeeds and fails, showing that it generally cannot identify the root cause. We then prove, without additional assumptions, that the root cause is identifiable even if the causal ordering is not. Two key ingredients of this identifiability result are the use of permutations and the Cholesky decomposition, which allow us to exploit an invariant property across different permutations to discover the root cause. Furthermore, we characterize permutations that yield the correct root cause and, based on this, propose a valid method for root cause discovery. We also adapt this approach to high-dimensional settings. Finally, we evaluate the performance of our methods through simulations and apply the high-dimensional method to discover disease-causing genes in the gene expression dataset that motivates this work.

1 Introduction

1.1 Motivation and problem statement

Rare diseases can stem from mutations in a single gene (also known as Mendelian or monogenic disorders). Typically, such mutations affect the expression of the gene itself, and of further downstream genes, ultimately leading to the disease (e.g., Yépez et al., 2021, 2022). Discovering the disease-causing gene is important, as it enhances our understanding of the disease mechanism and is a critical step toward developing potential cures. This motivates us to consider the problem of root cause discovery, which aims to find the ultimate cause of an observed effect.

Specifically, we distinguish between observational samples (e.g., gene expression data from healthy individuals) and interventional samples (e.g., gene expression data from patients), with the former serving as a reference to detect the root cause variable in the latter. While we assume that observational samples are independent and identically distributed, we do not make this assumption for interventional samples, since disease-causing genes often differ among rare

disease patients, even among those with very similar phenotypes as in the case of mitochondrial disorders (Gusic and Prokisch, 2021). Consequently, we conduct root cause discovery for rare disease patients in a personalized manner, focusing on one interventional sample at a time. This presents a unique challenge and distinguishes the problem from most related problems in the literature where identically distributed interventional samples are available.

To formalize the problem, we consider n i.i.d. observational samples $\mathbf{x}_1, \dots, \mathbf{x}_n$ of X (e.g., data of healthy individuals) and one interventional sample \mathbf{x}^I of X^I (e.g., data of a patient) generated from the following two linear structural equation models (SEMs), respectively:

$$X \leftarrow b + BX + \varepsilon \quad (1)$$

and

$$X^I \leftarrow b + BX^I + \varepsilon + \delta, \quad (2)$$

where X, X^I, b, ε and $\delta \in \mathbb{R}^p$ and $B \in \mathbb{R}^{p \times p}$. Here, b is an intercept term. B encodes the underlying causal structure. It can be visualized in a causal directed acyclic graph (DAG) on vertices $\{1, \dots, p\}$, where there is an edge from i to j if the edge weight $B_{ji} \neq 0$. Further, ε is an error term that follows an arbitrary distribution with mean 0 and diagonal covariance matrix. Finally, $\delta = (0, \dots, 0, \delta_r, 0, \dots, 0)^T$ represents a mean-shift intervention. It has only one non-zero entry δ_r in the r -th position, indicating that the variable X_r^I is intervened upon by a mean shift δ_r , modeling a mutation that results in over- or under-expression of the gene. We refer to r or X_r^I as the *root cause* of X^I . We assume this model throughout the paper.

Our goal is to discover the root cause of X^I by comparing $\mathbf{x}^I = (x_1^I, \dots, x_p^I)^T$ with the observational samples $\mathbf{x}_1, \dots, \mathbf{x}_n$. Intuitively, when $|\delta_r|$ is large compared to the noise variance, x_r^I will stand out as prominently aberrant compared to the values of the r -th variable in the observational samples. But the intervention effect on x_r^I can also propagate to downstream variables, causing many other variables to appear aberrant as well. This propagation can make it difficult to identify the root cause.

For a quick illustration, we look at a simulated dataset shown in Figure 1(b), where we use $b = (0, 0, 0, 0, 0)^T$, $B = \begin{pmatrix} 0 & 1 & -1 & -2 & 0 \\ 0 & 0 & -1 & 1 & 0 \\ 0 & 0 & 0 & -2 & 0 \\ 0 & 0 & 0 & 0 & 0 \\ 0 & -2 & 1 & 3 & 0 \end{pmatrix}$, $\text{Cov}(\varepsilon) = \text{Diag}(3, 2, 3, 2, 3)$, and $\delta = (0, 0, 10, 0, 0)^T$.

The causal DAG in plot (a) represents the generating process. The vector δ indicates that X_3^I is the root cause for the interventional sample (visualized by the lightning symbol in the DAG). All variables except for X_4^I are descendants of X_3^I , meaning that the intervention effect propagates to X_1^I , X_2^I , and X_5^I . This is reflected in plot (b), where 100 observational samples (in gray) and one interventional sample (in color) show that, except for X_4^I , all variables of the interventional sample appear aberrant compared to the observational samples.

1.2 Our contribution

In this paper, we start by studying a commonly used quantity for detecting aberrancy: the squared z-score (see (3) in Section 2). We characterize when the squared z-score can and cannot successfully identify the root cause, as the observational sample size and the intervention strength tend to infinite. In particular, we show that the squared z-score can consistently identify the root cause if $\text{Var}(X_k) > \alpha_{r \rightarrow k} \text{Var}(X_r)$ for all k , where $\alpha_{r \rightarrow k}$ is the total causal effect of X_r on X_k . Three sufficient conditions on the generating mechanism that ensure this are: (1) for any descendants of the root cause, there is no common ancestor that has a directed path to the

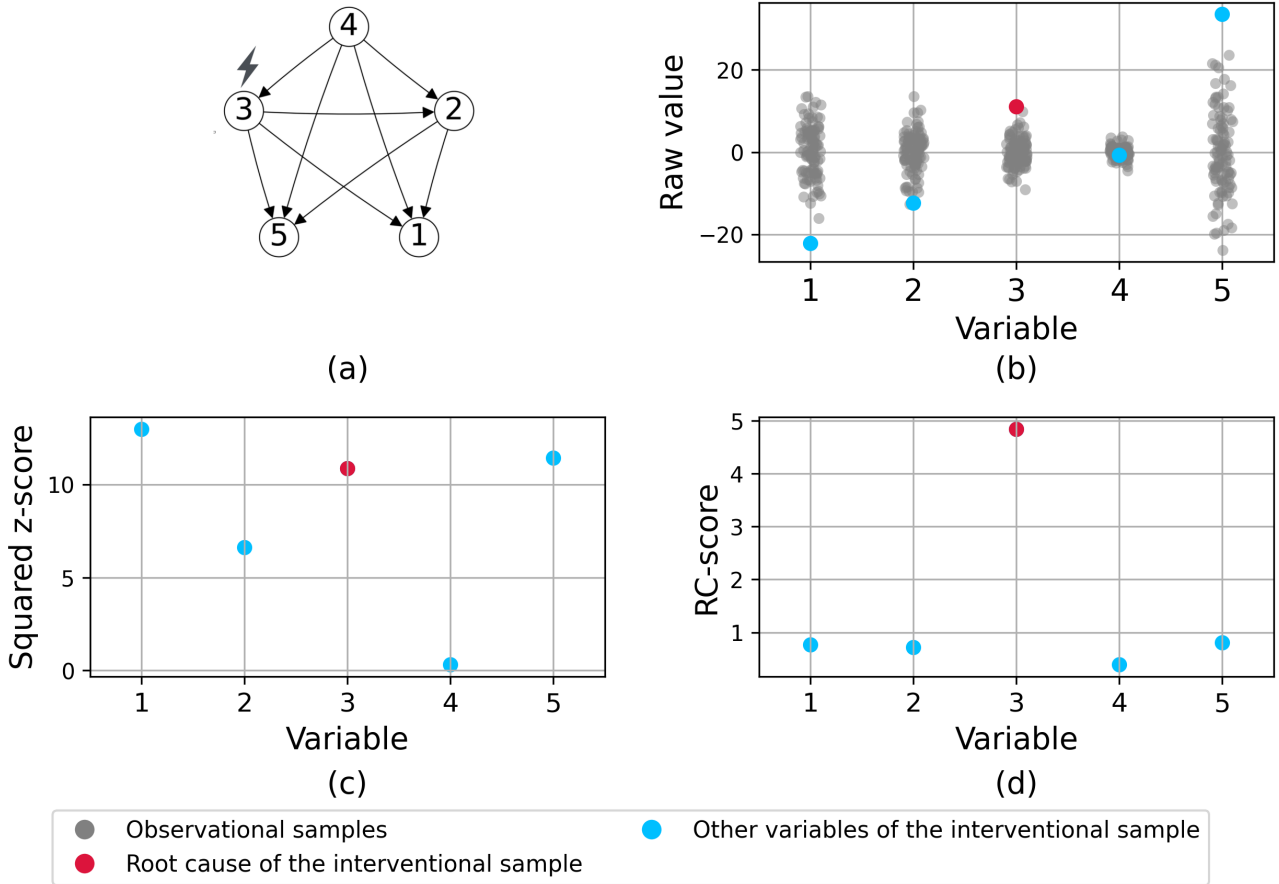


Figure 1: (a) The causal DAG that generates the samples shown in plot (b). (b) A simulated dataset based on the causal DAG in plot (a). Gray points represent 100 observational samples, while colored points denote the data of one interventional sample. (c) The squared z-score for each variable in the interventional sample. (d) The RC-score for each variable in the interventional sample.

descendant without passing through the root cause; (2) the causal DAG is a polytree (see, e.g., Jakobsen et al., 2022; Tramontano et al., 2022, 2023); and (3) all entries of the matrix B are nonnegative. On the other hand, if there exists a k such that $\text{Var}(X_k) < \alpha_{r \rightarrow k} \text{Var}(X_r)$, then the squared z-score cannot consistently identify the root cause.

In Section 3, we study the fundamental question of whether the root cause is identifiable based on the observational distribution and the first moment of the interventional distribution. We consider the observational distribution as it can theoretically be estimated with n i.i.d. observational samples, and we consider only the first moment of the interventional distribution because only one interventional sample is available. The answer to this question is not immediately clear, as even the causal ordering may be non-identifiable in this setting. We prove, however, that the root cause is in fact identifiable in this setting. This identifiability result stems from an invariant property involving permutations of variables and the Cholesky decomposition.

The above identifiability result leads to a valid root cause discovery method which requires trying all permutations of the variables. Considering $p!$ permutations, however, quickly becomes infeasible when the number of variables p increases. To alleviate this problem, we characterize so-

called “sufficient” permutations that allow us to identify the root cause. In particular, sufficient permutations are those where the parents of the root cause are positioned before it and the true descendants are positioned after it. This leads to the second valid root cause discovery algorithm with a smaller computational burden (see Algorithm 2). At last, we develop a heuristic root cause discovery method designed for high-dimensional settings (Algorithm 3), building on our previously proposed Algorithm 2.

As a preview, plots (c) and (d) in Figure 1 show the performance of both the squared z-scores and our proposed RC-scores (Algorithm 2) on the simulated dataset in plot (b). We see that our method successfully identifies the root cause X_3^I by assigning it the highest score, whereas the squared z-score method fails to do so. More simulations are conducted in Section 4 to examine the performance of our methods.

In Section 5, we revisit the problem of discovering disease-causing genes in the high-dimensional gene expression dataset that motivates our study. We apply the high-dimensional method (Algorithm 3), yielding very promising results. We conclude the paper with discussions in Section 6.

1.3 Related ideas and work

Recall that we assume that the underlying causal structure is unknown. If the DAG or causal ordering were known, there are two natural methods for root cause discovery: (1) first identify all aberrant variables and then select the one that appears first in the causal ordering; (2) leverage invariance: only the root cause will exhibit a changed conditional distribution given its parents (see, e.g., Haavelmo, 1944; Peters et al., 2016; Budhathoki et al., 2021; Li et al., 2022).

One may try to estimate the DAG or causal ordering from observational samples and then apply the ideas of the previous paragraph. However, it is well-known that these estimation problems are highly challenging and often requires very large sample sizes (see, e.g., Evans, 2020). More importantly, causal orderings and DAGs may be unidentifiable (see, e.g., Spirtes et al., 2001; Pearl, 2009b), which presents a fundamental issue that cannot be resolved regardless of sample size. Nevertheless, in Section 4, we implement methods based on these two ideas, using LiNGAM (Shimizu et al., 2006), and compare their performance to that of our method.

When the DAG is unknown, there is a line of work that combines both observational and interventional samples, with the primary goal of either estimating the intervened variables (i.e., root causes) or learning the causal structure with the estimated root cause as a by-product. However, these methods rely on aspects of the interventional distributions like the second moments (Rothenhäusler et al., 2015; Varici et al., 2021, 2022), likelihoods (Eaton and Murphy, 2007; Taeb and Bühlmann, 2021), or the entire interventional distribution (Squires et al., 2020; Jaber et al., 2020; Ikram et al., 2022; Yang et al., 2024). These approaches cannot be applied to our problem, where only a single interventional sample is available.

Our method relies on the Cholesky decomposition, which has been used before in causal structure learning (Ye et al., 2020; Raskutti and Uhler, 2018) and for estimating the effects of joint interventions (Nandy et al., 2017). In particular, Raskutti and Uhler (2018) also combine permutations with the Cholesky decomposition to find the sparsest Cholesky factorization. Our approach differs fundamentally from these works: we combine permutations and the Cholesky decomposition to search for an invariant property related to the root cause.

Finally, there is related work that treats root cause analysis as a causal contribution problem (see, e.g., Budhathoki et al., 2022; Okati et al., 2024), as well as work that focuses on root cause analysis for microservice-based applications (see Hardt et al. (2023) and the references therein).

These works either require knowledge of the causal DAG or estimate it based on data, then proceed similarly to the two ideas discussed above, but with a specific focus on microservice-based applications.

To the best of our knowledge, no formal method currently exists in the literature to address our problem, where only a single interventional sample is available, and the causal ordering may be unidentifiable.

2 Squared z-scores are not generally valid

The squared z-score is commonly used to quantify aberrancy. Instead of simply examining raw values, it adjusts for the marginal mean and variance of each variable. It is intuitively expected that the squared z-score cannot identify the root cause in general, as it does not account for the causal relationships between variables. In this section, we formally verify this intuition by characterizing when the squared z-score succeeds and fails.

For $j \in [p] = \{1, \dots, p\}$, the z-score of X_j^I is defined as

$$\widehat{Z}_{n,j} = \frac{X_j^I - \widehat{\mu}_{n,j}}{\widehat{\sigma}_{n,j}}, \quad (3)$$

where $\widehat{\mu}_{n,j} = \frac{1}{n} \sum_{i=1}^n x_{ij}$ and $\widehat{\sigma}_{n,j} = \sqrt{\frac{1}{n-1} \sum_{i=1}^n (x_{ij} - \widehat{\mu}_{n,j})^2}$ are the sample mean and standard deviation of the observational samples.

We first consider the z-score with population mean and standard deviation of the observational distribution:

$$Z_j = \frac{X_j^I - \mu_j}{\sigma_j},$$

where μ_j and σ_j are the mean and standard deviation of X_j , respectively.

Let $r \in [p]$ be the root cause and $k \in [p] \setminus \{r\}$. For the linear SEMs (1) and (2), we have

$$X_r^I = X_r + \delta_r \quad \text{and} \quad X_k^I = X_k + \alpha_{r \rightarrow k} \delta_r, \quad (4)$$

where $\alpha_{r \rightarrow k} = (I - B)_{kr}^{-1}$ is the total causal effect of X_r on X_k . Then, using (4), we have

$$Z_r = \frac{X_r - \mu_r}{\sigma_r} + \frac{\delta_r}{\sigma_r} \quad \text{and} \quad Z_k = \frac{X_k - \mu_k}{\sigma_k} + \frac{\alpha_{r \rightarrow k} \delta_r}{\sigma_k}.$$

Here the first terms on the right hand sides are standardized random variables. Hence, for δ_r large, the deterministic terms will dominant and $Z_r^2 > Z_k^2$ if $\sigma_k^2 > \alpha_{r \rightarrow k}^2 \sigma_r^2$.

The corresponding sample version result is given in Theorem 2.1.

Theorem 2.1. *Let $r \in [p]$ be the root cause. For any $k \in [p] \setminus \{r\}$, the following two statements hold:*

(i) *If $\sigma_k^2 > \alpha_{r \rightarrow k}^2 \sigma_r^2$, then $\lim_{\substack{n \rightarrow \infty \\ \delta_r \rightarrow \infty}} P\left(\widehat{Z}_{n,r}^2 > \widehat{Z}_{n,k}^2\right) = 1$.*

(ii) *If $\sigma_k^2 < \alpha_{r \rightarrow k}^2 \sigma_r^2$, then $\lim_{\substack{n \rightarrow \infty \\ \delta_r \rightarrow \infty}} P\left(\widehat{Z}_{n,r}^2 < \widehat{Z}_{n,k}^2\right) = 1$.*

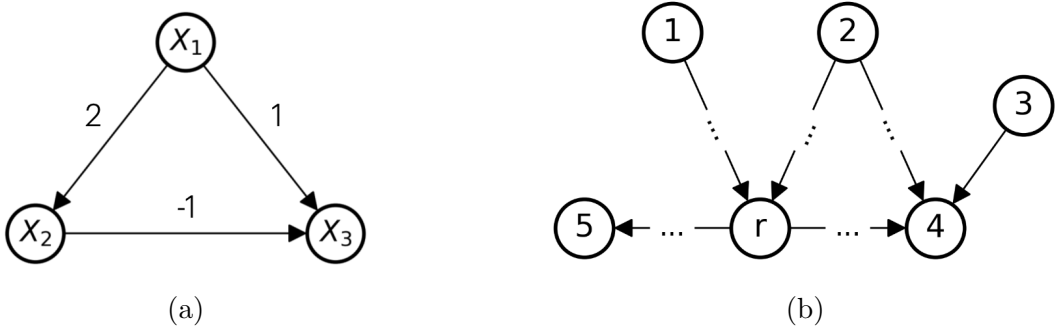


Figure 2: (a) The DAG corresponding to the SEM in Example 2.1. (b) DAG used to illustrate Proposition 2.1, where r denotes the root cause, and the edges with dots represent directed paths.

As a direct corollary, if the condition $\sigma_k^2 > \alpha_{r \rightarrow k}^2 \sigma_r^2$ holds for all $k \in [p] \setminus r$, the squared z-score can consistently identify the root cause.

In the above theorem, $n \rightarrow \infty$ allows us to obtain consistent estimators for the population mean and standard deviation of the observational distribution. However, since there is only one interventional sample, which is used to estimate μ_j^I , the variance of this estimator does not vanish. To account for this, we let $\delta_r \rightarrow \infty$. Based on our proof in Appendix A.1, one can also obtain non-asymptotic high-probability results with a more precise characterization of δ_r , but we refrain from doing so here for simplicity.

To give a concrete illustration of the conditions in Theorem 2.1, we present a simple example.

Example 2.1. Consider a linear SEM

$$\begin{pmatrix} X_1 \\ X_2 \\ X_3 \end{pmatrix} \leftarrow \begin{pmatrix} 1 \\ 1 \\ 1 \end{pmatrix} + \begin{pmatrix} 0 & 0 & 0 \\ 2 & 0 & 0 \\ 1 & -1 & 0 \end{pmatrix} \begin{pmatrix} X_1 \\ X_2 \\ X_3 \end{pmatrix} + \begin{pmatrix} \varepsilon_1 \\ \varepsilon_2 \\ \varepsilon_3 \end{pmatrix},$$

where $\varepsilon_1, \varepsilon_2$ and ε_3 follow standard Gaussian distribution. The corresponding causal DAG with edge weights is shown in Figure 2(a). It easily follows from this model that $\sigma_1^2 = 1$, $\sigma_2^2 = 5$, $\sigma_3^2 = 3$, $\alpha_{1 \rightarrow 2} = 2$, $\alpha_{1 \rightarrow 3} = -1$, $\alpha_{2 \rightarrow 3} = -1$, and that all other $\alpha_{j \rightarrow k}$ equal 0. Hence, when X_1 or X_3 is the root cause, condition (i) in Theorem 2.1 holds for all $k \neq r$, so we should be able to identify the root cause. In contrast, when X_2 is the root cause, we have $\sigma_3^2 < \alpha_{2 \rightarrow 3}^2 \sigma_2^2$, so X_3 will have a larger squared z-score than X_2 with high probability.

We conduct simulations to verify these theoretical results. We generate 100 observational samples and 30 interventional samples with an intervention strength $\delta_r = 10$. Specifically, the first 10 interventional samples correspond to $r = 1$ (i.e., X_1 being the root cause), the next 10 correspond to $r = 2$, and the final 10 correspond to $r = 3$. We use the 100 observational samples to calculate the sample mean and standard deviation and obtain squared z-scores for each individual interventional sample based on formula (3).

Figure 3 shows the results, with the first row displaying the squared z-scores for these 30 interventional samples. As expected from the theoretical results, the squared z-scores successfully identify the root cause for X_1 and X_3 (see the first and third plots containing interventional samples 1–10 and 21–30, respectively), but fail to identify the root cause for X_2 (see the middle plot containing interventional samples 11–20). In the second row, we present the performance

of our RC-scores that we will introduce in Section 3. They successfully identify the root cause in all cases.

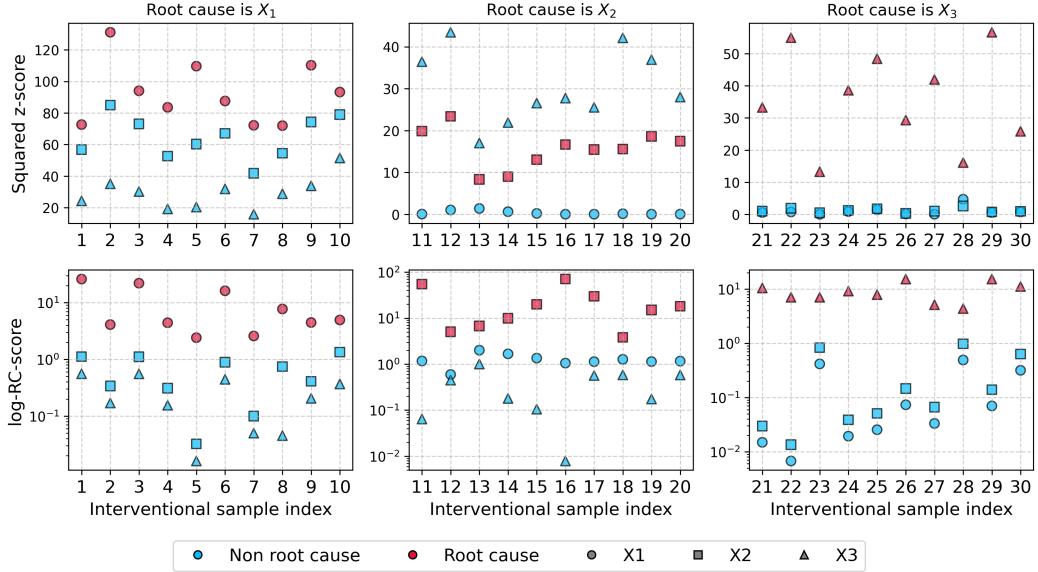


Figure 3: Simulation results based on Example 2.1. The three plots in the first row show the squared z-scores of the interventional samples, with root causes X_1 , X_2 , and X_3 , respectively. The three plots in the second row display the RC-scores (in log scale) for the same interventional samples. For each interventional sample, red denotes the root cause while blue represents non-root cause variables, and X_1 , X_2 , and X_3 are represented by circles, squares, and triangles, respectively.

A natural follow-up question is: Can we give sufficient conditions on the generating model that ensure $\sigma_k^2 > \alpha_{r \rightarrow k}^2 \sigma_r^2$ for some or all $k \in [p] \setminus \{r\}$? To answer this question, we first introduce some notation. For $j \in [p]$ and a DAG G , let the set of its ancestors and descendants be

$$\begin{aligned} \text{An}(j) &= \{l \in [p] \setminus \{j\} : \text{there is a directed path from } l \text{ to } j \text{ in } G\}, \\ \text{De}(j) &= \{l \in [p] \setminus \{j\} : \text{there is a directed path from } j \text{ to } l \text{ in } G\}. \end{aligned}$$

In addition, for $k \in [p] \setminus \{r\}$, define

$$O(r, k) = \{j \in \text{An}(r) \cap \text{An}(k) : \text{there is a directed path from } j \text{ to } k \text{ in } G \text{ that does not through } r\}.$$

Then, we have the following Proposition 2.1:

Proposition 2.1. *Let $r \in [p]$ be the root cause and let $k \in [p] \setminus \{r\}$. If (i) $k \notin \text{De}(r)$, or (ii) $k \in \text{De}(r)$ and $O(r, k) = \emptyset$, then $\sigma_k^2 > \alpha_{r \rightarrow k}^2 \sigma_r^2$.*

In other words, a variable X_k may only be problematic in the sense of having a larger asymptotic squared z-score than X_r if $k \in \text{De}(r)$ and $O(r, k) \neq \emptyset$. For illustration, consider Figure 2 (b), where r is the root cause and the edges with dots represent directed paths, variables 1, 2, 3 and 5 are considered safe because $1, 2, 3 \notin \text{De}(r)$ and $5 \in \text{De}(r)$ with $O(r, 5) = \emptyset$. The only unsafe variable is 4, as $4 \in \text{De}(r)$ with $O(r, 4) = \{2\} \neq \emptyset$. Similarly, in Figure 2 (a), all variables

are safe when $r = 1$ or $r = 3$. But if $r = 2$, X_3 is unsafe as $3 \in \text{De}(2)$ and $O(2, 3) = \{1\}$. We saw in Figure 3 that this was indeed the only case where the squared z-score failed.

Let us look at Example 2.1 a bit more closely to obtain better understanding. In the case where X_2 is the root cause, if the edge $X_1 \rightarrow X_3$ were absent, the variance of X_3 would be larger, namely 6, which would result in a smaller squared z-score than that of the root cause. However, due to the additional path $X_1 \rightarrow X_3$, which has the opposite sign of $X_1 \rightarrow X_2 \rightarrow X_3$, the variance of X_3 becomes smaller, namely 3, causing its squared z-score to be larger than that of the root cause. If we change the SEM to $X_3 = 1 + X_1 + X_2 + \varepsilon_3$, i.e., changing the sign of the edge weight of $X_1 \rightarrow X_3$, then X_3 is still unsafe according to Proposition 2.1, but $\sigma_3^2 > \alpha_{2 \rightarrow 3}^2 \sigma_2^2$. This shows that Proposition 2.1 only provides a sufficient condition. Another sufficient condition is shown in the following proposition.

Proposition 2.2. *Let $r \in [p]$ be the root cause. If all edge weights are nonnegative, then $\sigma_k^2 > \alpha_{r \rightarrow k}^2 \sigma_r^2$ for all $k \in [p] \setminus \{r\}$.*

Corollary 2.1 directly follows from Propositions 2.1 and 2.2.

Corollary 2.1. *Let $r \in [p]$ be the root cause. If the underlying DAG is a polytree or if all edge weights are nonnegative, then $\lim_{\substack{n \rightarrow \infty \\ \delta_r \rightarrow \infty}} P(\widehat{Z}_r^2 > \widehat{Z}_k^2) = 1$ for all $k \in [p] \setminus \{r\}$.*

In summary, using the squared z-score identifies the root cause in some cases, but not in general.

3 Root cause discovery via permutations and Cholesky decomposition

3.1 Is the root cause identifiable?

At this point, it is unclear whether the root cause is identifiable based solely on the observational distribution and the first moment of the interventional distribution. As mentioned in the introduction, we focus on these two quantities because the former can be estimated from n i.i.d. observational samples, while a single interventional sample only allows us to estimate the first moment of the interventional distribution. This question is fundamental and not immediately clear, given that the causal ordering and the causal DAG are generally non-identifiable.

In the following, we give a positive answer to this question. In particular, we prove that the root cause is identifiable from the mean and covariance matrix of the observational distribution (denoted by μ_X and Σ_X) and the mean of the interventional distribution (denoted by μ_{X^I}). We focus on population quantities to address the identifiability question for now, and the sample version algorithm will be introduced in the next section.

Note that the population version of the z-score can be written as $\text{Diag}(\sigma_1, \dots, \sigma_p)^{-1}(\mu_{X^I} - \mu_X)$. Considering the generalization that takes the full covariance matrix into account, we introduce the following key term:

$$\xi := L_X^{-1}(\mu_{X^I} - \mu_X), \quad (5)$$

where L_X is the lower-triangular matrix with real and positive diagonals obtained by the Cholesky decomposition of Σ_X , i.e., $\Sigma_X = L_X L_X^T$.

To motivate the reason of using the Cholesky decomposition, we look at the special case where (X_1, \dots, X_p) is sorted by a causal ordering. In this case, the matrix B in model (1) is lower triangular. From model (1), we have $\Sigma_X = (I - B)^{-1} D_\varepsilon (I - B)^{-T}$, where $D_\varepsilon = \text{Diag}(\sigma_{\varepsilon_1}^2, \dots, \sigma_{\varepsilon_p}^2)$ is the diagonal covariance matrix of ε . Hence, $L_X = (I - B)^{-1} D_\varepsilon^{1/2}$ by the uniqueness of the Cholesky decomposition. Additionally, since $\mu_{X^I} = (I - B)^{-1}(b + \delta)$ and $\mu_X = (I - B)^{-1}b$, we have

$$\xi = L_X^{-1}(\mu_{X^I} - \mu_X) = D_\varepsilon^{-1/2} \delta = (0, \dots, 0, \delta_r / \sigma_{\varepsilon_r}, 0, \dots, 0)^T. \quad (6)$$

Therefore, for this special permutation of (X_1, \dots, X_p) , we can distinguish the root cause based on ξ because it is the only entry with a non-zero value.

However, since (X_1, \dots, X_p) is generally not in a causal ordering, the matrix B is not lower triangular and L_X does not equal $(I - B)^{-1} D_\varepsilon^{1/2}$. As a result, ξ may not exhibit the informative pattern seen in (6). Therefore, the root cause cannot be identified using only the Cholesky decomposition.

Remarkably, based on a linear algebra result (see Lemma B.1 in Appendix B.1), there is actually an invariant property related to the root cause that involves ξ and the permutations of (X_1, \dots, X_p) , as shown in Theorem 3.1. This property allows us to identify the root cause by combining permutations and the Cholesky decomposition.

Theorem 3.1 (Identifiability of the root cause). *Let (X_1, \dots, X_p) be sorted in any ordering (not necessarily a causal ordering). The corresponding ξ must have at least one nonzero element. Furthermore, if ξ has exactly one nonzero element, then this element must be the root cause.*

Theorem 3.1 enables us to exploit an invariant property to identify the root cause: by trying all permutations of (X_1, \dots, X_p) , we are guaranteed to find at least one permutation (since a causal ordering must exist) for which the corresponding ξ has only one non-zero entry, which must be the root cause. This verifies the identifiability of the root cause.

Note that Theorem 3.1 implies that the root cause is identifiable even if the causal ordering is not. From this perspective, discovering the root cause is a fundamentally simpler task than estimating the causal ordering or learning the causal DAG.

3.2 Root cause discovery algorithm based on all permutations

Theorem 3.1 inspires a root cause discovery algorithm by trying all permutations of variables. Before presenting this algorithm, we first introduce some notation.

For a permutation $\pi = (\pi(1), \dots, \pi(p))$, let $X^\pi = (X_{\pi(1)}, \dots, X_{\pi(p)})^T$ and $X^{I\pi} = (X_{\pi(1)}^I, \dots, X_{\pi(p)}^I)^T$, with their corresponding means and covariance matrix denoted by μ_{X^π} , $\mu_{X^{I\pi}}$ and Σ_{X^π} , respectively. We introduce the following notation to make the dependence of ξ (see (5)) on the permutation π explicit:

$$\xi(\pi) := L_{X^\pi}^{-1}(\mu_{X^{I\pi}} - \mu_{X^\pi}), \quad (7)$$

where L_{X^π} is the lower triangular matrix obtained from the Cholesky decomposition of Σ_{X^π} . Note that $\xi(\pi)$ is not simply a permuted version of ξ due to the presence of $L_{X^\pi}^{-1}$.

By Theorem 3.1, if $\xi(\pi)$ has only one non-zero element, it must be in the $\pi^{-1}(r)$ -th position, corresponding to the root cause's new position after the permutation. We call a permutation π *sufficient* if $\xi(\pi)$ has only one non-zero element, indicating that this permutation is sufficient

to identify the root cause. Otherwise we call it *insufficient*, in which case $\xi(\pi)$ contains more than one non-zero element. The existence of a sufficient π is clear because a causal ordering is sufficient. As we will show in Section 3.3, non-causal orderings can also be sufficient.

Now we introduce the sample version algorithm. Let $\mathbf{x}_1^\pi, \dots, \mathbf{x}_n^\pi$ be n i.i.d. observational samples of X^π , and let $\mathbf{x}^{I\pi}$ be one interventional sample of $X^{I\pi}$. Denote the estimators of L_{X^π} and μ_{X^π} based on these observational samples by \widehat{L}_{X^π} and $\widehat{\mu}_{X^\pi}$. Then, we estimate $\xi(\pi)$ by

$$\widehat{\xi}(\pi) = \widehat{L}_{X^\pi}^{-1}(\mathbf{x}^{I\pi} - \widehat{\mu}_{X^\pi}). \quad (8)$$

To quantify the extent to which $\widehat{\xi}(\pi)$ exhibits the “only one non-zero entry” pattern, we use

$$\widehat{c}(\pi) = \frac{|\widehat{\xi}(\pi)|_{(1)} - |\widehat{\xi}(\pi)|_{(2)}}{|\widehat{\xi}(\pi)|_{(2)}}, \quad (9)$$

where $|\widehat{\xi}(\pi)|_{(i)}$ denotes the i -th largest entry in $|\widehat{\xi}(\pi)|$. Note that $\widehat{c}(\pi)$ is infinite if $\widehat{\xi}(\pi)$ has only one non-zero entry, so a large value of $\widehat{c}(\pi)$ indicates that $\widehat{\xi}(\pi)$ is close to having the desired “only one non-zero entry” pattern.

By Theorem 3.1, if π is sufficient, then the root cause is likely to have the largest value in $|\widehat{\xi}(\pi)|$. Therefore, we define the potential root cause with respect to a permutation π as

$$\widehat{u}(\pi) = \pi(\operatorname{argmax}_{j \in [p]} |\widehat{\xi}(\pi)|_j).$$

Let

$$\widehat{U} = \cup_{\pi \in \Pi_{\text{all}}} \widehat{u}(\pi) \quad (10)$$

be the set of all potential root causes, where Π_{all} is the set of all permutations of $(1, \dots, p)$.

Based on \widehat{U} , we assign a score to each variable i as a measure of its likelihood of being the root cause. This score, which we call the *RC-score*, is defined as:

$$\widehat{C}_i = \begin{cases} \max_{\pi: \widehat{u}(\pi)=i} \widehat{c}(\pi), & \text{if } i \in \widehat{U} \\ \widehat{w}_i \widehat{c}_{\min}, & \text{if } i \in [p] \setminus \widehat{U}, \end{cases} \quad (11)$$

where $\widehat{c}_{\min} = \min_{i \in \widehat{U}} \widehat{C}_i / 2$ is half of the smallest RC-score among potential root causes, and $\widehat{w}_i = \widehat{Z}_{n,i}^2 / \sum_{j \in [p] \setminus \widehat{U}} \widehat{Z}_{n,j}^2$ is the weight based on the squared z-scores. This ensures that RC-scores for variables unlikely to be the root cause (i.e., not in \widehat{U}) remain smaller than the scores for all potential root causes. A large \widehat{C}_i value indicates that variable i is more likely to be the root cause.

We note that while an alternative approach that assigns a score of zero to all variables not in \widehat{U} is simpler and does not affect the theoretical consistency of the method, using $\widehat{w}_i \widehat{c}_{\min}$ has an advantage of assigning the root cause a better score in the unfavorable case where it falls outside \widehat{U} . For example, when the root cause has no children, even if it happens to be outside \widehat{U} , using (11) may still assign it a large score compared to other variables, as it might be the only aberrant variable with the largest squared z-score.

The following theorem shows that if the estimators \widehat{L}_{X^π} and $\widehat{\mu}_{X^\pi}$ are both consistent, then using the RC-score (11) will consistently identify the root cause as the sample size and intervention strength go to infinity.

Theorem 3.2. *Let r be the root cause and \widehat{C}_i be obtained by (11). If $\widehat{L}_{X^\pi} \xrightarrow[n \rightarrow \infty]{p} L_{X^\pi}$ and $\widehat{\mu}_{X^\pi} \xrightarrow[n \rightarrow \infty]{p} \mu_{X^\pi}$, then*

$$\lim_{\substack{n \rightarrow \infty \\ \delta_r \rightarrow \infty}} P\left(\widehat{C}_r > \max_{k \in [p] \setminus \{r\}} \widehat{C}_k\right) = 1.$$

We apply the RC-score (11) to the previous Example 2.1. Figure 3 shows our RC-score successfully identifies all root causes, which aligns with our expectations based on the theoretical results.

3.3 Characterization of sufficient permutations and an efficient root cause discovery algorithm

Calculating the RC-score using (11) requires evaluating $p!$ permutations, which becomes computationally infeasible when p is large. The purpose of considering all permutations is to ensure that at least one sufficient permutation is found. Therefore, to reduce the search space, it is crucial to understand which permutations are sufficient. To this end, we give a complete characterization of sufficient permutations in Theorem 3.3.

Before presenting the theorem, we introduce two notation to be used. For $j \in [p]$, we define its parents and real descendants as

$$\text{Pa}(j) = \{k \in [p] \setminus \{j\} : B_{jk} \neq 0\} \quad \text{and} \quad \text{rDe}(j) = \{k \in [p] \setminus \{j\} : (I - B)_{kj}^{-1} \neq 0\},$$

respectively. Recall that $(I - B)_{kj}^{-1} = \alpha_{j \rightarrow k}$ is the total causal effect X_j on X_k (see (4)).

Theorem 3.3. *Let r be the root cause. A permutation π is sufficient if and only if the following two conditions hold:*

- (i) $\pi^{-1}(k) < \pi^{-1}(r)$ for all $k \in \text{Pa}(r)$,
- (ii) $\pi^{-1}(k) > \pi^{-1}(r)$ for all $k \in \text{rDe}(r)$.

Theorem 3.3 shows that sufficient permutations are those where the parents of the root cause are positioned before it, and the real descendants of the root cause are positioned after it. This characterization enables us to develop a method that significantly reduces the search space of permutations.

Specifically, let $D = \{r\} \cup \text{rDe}(r)$ be the set comprising the root cause and its real descendants. If D is known (though the exact root cause r within D does not need to be known), then we can generate $|D|$ permutations that are guaranteed to include a sufficient permutation. Specifically, we generate $|D|$ permutations by

$$\pi = ([p] \setminus D, i, D \setminus \{i\}), \quad i \in D, \tag{12}$$

where the orderings within $[p] \setminus D$ and $D \setminus \{i\}$ are arbitrary. Then, it is clear that the permutation with $i = r$ is sufficient, as it satisfies the conditions in Theorem 3.3. Although we cannot directly target this sufficient permutation due to not knowing which variable is r , it is enough for our purpose that one of the $|D|$ permutations is sufficient.

Algorithm 1 : Obtain permutations based on squared z-scores

Input: Observational samples $\mathbf{x}_1, \dots, \mathbf{x}_n$, the interventional sample \mathbf{x}^I , and the number of random permutations v .

Output: A set of permutations.

- 1: Calculate the squared z-scores $\widehat{Z}_{n,1}^2, \dots, \widehat{Z}_{n,p}^2$ based on formula (3) and initialize an empty set $\widehat{\Pi}$ to record permutations.
 - 2: **for** $i = 1, \dots, p$ **do**
 Obtain the set of aberrant variables $D = \{j \in [p] : \widehat{Z}_{n,j}^2 \geq \widehat{Z}_{n,i}^2\} := \{d_1, \dots, d_u\}$.
 - 3: **for** $l = 1, \dots, u$ **do**
 - 4: **for** $k = 1, \dots, v$ **do**
 Randomly permute $[p] \setminus D$ and $D \setminus \{d_l\}$ to generate a permutation $\pi = ([p] \setminus D, d_l, D \setminus \{d_l\})$, and add π to the permutation set $\widehat{\Pi}$.
 - 5: **Return** $\widehat{\Pi}$.
-

As a concrete example, consider the case where $p = 6$, the root cause is 3, and $D = \{1, 3, 6\}$. First, we put $[p] \setminus D = \{2, 4, 5\}$ in the front positions of the permutation. Then, we generate 3 permutations by placing 1, 3, and 6 in turn in the fourth position (i.e., the first available position after $\{2, 4, 5\}$) and randomly placing the remaining two elements. An example of these 3 permutations could be: $(2, 4, 5, 1, 3, 6)$, $(4, 5, 2, 3, 1, 6)$, and $(2, 5, 4, 6, 3, 1)$. In this case, the second permutation $(4, 5, 2, 3, 1, 6)$ is sufficient.

The set D is unknown in practice. However, since the root cause and its real descendants are expected to be aberrant due to the intervention, while the other variables are not, we can estimate D using the set of aberrant variables. One way is to use the squared z-scores $\widehat{Z}_{n,i}^2$ (see (3)) to form an estimate $\widehat{D} = \{j \in [p] : \widehat{Z}_{n,j}^2 \geq \tau\}$ for some threshold τ . It is important to note that our primary goal is to reduce the search space of permutations, and trying more permutations is generally beneficial for root cause discovery. Therefore, we are not restricted to using just $|D|$ permutations generated from a single estimator of D . Instead, we can use multiple thresholds to obtain several sets \widehat{D} and generate more permutations accordingly. For instance, we could use all the squared z-scores $\widehat{Z}_{n,1}^2, \dots, \widehat{Z}_{n,p}^2$ as thresholds. Because of this, we are not facing the difficult issue of choosing an optimal threshold.

For the same reason, when generating the permutation $\pi = ([p] \setminus D, i, D \setminus \{i\})$ for a certain i (see (12)), we can record additional permutations by using different random orderings of $[p] \setminus D$ and $D \setminus \{i\}$. Although using more permutations does not bring any advantage from an asymptotic perspective, it tends to be beneficial for finite sample performance. The reason is that using only one such permutation might result in the undesired case where the root cause is out of \widehat{U} (see (10)), whereas trying more permutations increases the possibility that the root cause is included in \widehat{U} . See Appendix C.1 for an illustration.

We summarize the method for obtaining permutations in Algorithm 1. In Theorem 3.4, we show that as the sample size and intervention strength tend to infinity, one of the permutations outputted by this algorithm is guaranteed to be sufficient with a probability tending to one. Algorithm 1 generates a total of $vp(p+1)/2$ permutations. In practice, to reduce computational time, one can use some reasonable thresholds such as $\{1.5, 2, 2.5, \dots, 5\}$ instead of using all squared z-scores in step 2 of Algorithm 1.

Theorem 3.4. Let $\widehat{\Pi}$ be the set of permutations obtained by Algorithm 1, then

$$\lim_{\substack{n \rightarrow \infty \\ \delta_r \rightarrow \infty}} P\left(\widehat{\Pi} \text{ contains at least one sufficient permutation}\right) = 1.$$

Algorithm 2 : Root cause discovery

Input: Observational samples $\mathbf{x}_1, \dots, \mathbf{x}_n$ and the interventional sample \mathbf{x}^I , and the number of random permutations v .

Output: RC-score \widehat{C}_i for all variables.

- 1: Obtain $\widehat{\Pi}$ by implementing Algorithm 1 with the same inputs as this algorithm.
 - 2: Initialize an empty set \widehat{U} .
 - 3: **for** $\pi \in \widehat{\Pi}$ **do**:
 - (i) Obtain permuted samples $\mathbf{x}_1^\pi, \dots, \mathbf{x}_n^\pi$ and $\mathbf{x}^{I\pi}$.
 - (ii) Obtain estimators \widehat{L}_{X^π} and $\widehat{\mu}_{X^\pi}$ based on $\mathbf{x}_1^\pi, \dots, \mathbf{x}_n^\pi$.
 - (iii) Get $\widehat{\xi}(\pi) = \widehat{L}_{X^\pi}^{-1}(\mathbf{x}^{I\pi} - \widehat{\mu}_{X^\pi})$, $\widehat{c}(\pi) = \frac{|\widehat{\xi}(\pi)|_{(1)} - |\widehat{\xi}(\pi)|_{(2)}}{|\widehat{\xi}(\pi)|_{(2)}}$, and $\widehat{u}(\pi) = \pi(\operatorname{argmax}_{j \in [p]} |\widehat{\xi}(\pi)|_j)$.
 - (iv) Add $\widehat{u}(\pi)$ into \widehat{U} .
 - 4: **for** $i \in \widehat{U}$ **do**: Let $\widehat{C}_i = \max_{\pi: \pi \in \widehat{\Pi} \text{ and } \widehat{u}(\pi)=i} \widehat{c}(\pi)$.
 - 5: **for** $i \in [p] \setminus \widehat{U}$ **do**: Let $\widehat{C}_i = \widehat{w}_i \widehat{c}_{\min}$, where $\widehat{c}_{\min} = \min_{j \in \widehat{U}} \widehat{C}_j / 2$ and $\widehat{w}_i = \widehat{Z}_{n,i}^2 / \sum_{j \in [p] \setminus \widehat{U}} \widehat{Z}_{n,j}^2$ with $\widehat{Z}_{n,j}^2$ defined by (3).
 - 6: Return \widehat{C}_i for all $i \in [p]$.
-

By applying Algorithm 1, we replace the set of all permutations in (10) with those generated by the algorithm. This significantly reduces computational expense and leads to our main root cause discovery method (Algorithm 2). As shown in the following Theorem 3.5, if both \widehat{L}_{X^π} and $\widehat{\mu}_{X^\pi}$ are consistent, Algorithm 2 is also consistent, in the sense that as the sample size and intervention strength increase to infinity, the algorithm is guaranteed to identify the root cause with a probability approaching one.

Theorem 3.5. Let r be the root cause and \widehat{C}_i be obtained by Algorithm 2. If $\widehat{L}_{X^\pi} \xrightarrow[n \rightarrow \infty]{p} L_{X^\pi}$ and $\widehat{\mu}_{X^\pi} \xrightarrow[n \rightarrow \infty]{p} \mu_{X^\pi}$, then

$$\lim_{\substack{n \rightarrow \infty \\ \delta_r \rightarrow \infty}} P\left(\widehat{C}_r > \max_{k \in [p] \setminus \{r\}} \widehat{C}_k\right) = 1.$$

3.4 An adapted root cause discovery algorithm for high-dimensional settings

For Algorithm 2 to perform well, it is important to obtain an accurate estimate of the covariance matrix, as it is used in the Cholesky decomposition to get \widehat{L}_{X^π} . We found that obtaining a good covariance matrix is particularly challenging for the high-dimensional gene expression data analyzed in Section 5, which involves around 20,000 variables and 400 samples. Estimating covariance matrices in high-dimensional settings is known to be difficult and is an independent

research topic from our problem (see, e.g., Cai et al. (2016) and Fan et al. (2016) for reviews on this topic). We therefore propose a special adaptation of our method that circumvents estimating a high-dimensional covariance matrix. We build on Algorithm 2 and incorporating Lasso (Tibshirani, 1996) for dimension reduction in a node-wise manner.

We first present the main idea. We treat a variable as the response and consider a subsystem containing only this variable and its Markov blanket (i.e., the set of variables that are conditionally dependent on the response given the remaining variables). Then, two key observations are: (1) If the variable treated as the response is not the root cause, then it is not the root cause within the subsystem. This is because if this variable is affected by the intervention, its parents, which are included in the Markov blanket, must also be affected, indicating that this variable cannot be the root cause within the subsystem. If this variable is not affected by the intervention, then it is clear that it cannot be the root cause within the subsystem. (2) If the variable treated as the response is the root cause, then it remains the root cause within the subsystem because it is affected by the intervention while its parents are not.

Building on these observations, we treat each variable i as the response and apply cross-validated Lasso to estimate its Markov blanket, then implement the first three steps of Algorithm 2 to the subdataset corresponding to the subsystem containing variable i and its estimate Markov blanket. Then, if i is the root cause, it is still the root cause in this subsystem. Therefore, there should be a permutation π such that the corresponding $\xi(\pi)$ (see (8)) follows the “only one non-zero entry” pattern, with $|\xi(\pi)|_{\pi^{-1}(i)}$ having the largest value. Hence, the corresponding $\hat{c}(\pi)$ (see (9)) is a reasonable choice as the root cause score for variable i . In fact, we should take the largest $\hat{c}(\pi)$ from all possible permutations π where $|\xi(\pi)|_{\pi^{-1}(i)}$ has the highest value, as done in Algorithm 2.

Following the above description and the previously mentioned ideas regarding assigning scores to variables outside \hat{U} (see (11)), we propose Algorithm 3 for root cause discovery in high-dimensional settings. Treating all p variables as responses in its step 2 guarantees that the root cause will be treated as a response. In practice, to reduce computational time, one can select a subset of variables that are likely to contain the root cause to treat as responses, for example, by selecting a subset of variables with a squared z-scores larger than a certain value.

We point out a caveat regarding Algorithm 3: after dimension reduction, latent variables may be introduced into the subsystem before applying Algorithm 2. To assess the robustness of Algorithm 2 to the presence of latent variables, we conduct simulations in latent variable settings in Section 4.4. We also examine the performance of Algorithm 3 in high-dimensional settings in Section 4.5.

We note that Algorithm 3 is a heuristic algorithm, and no theoretical guarantees are provided in this paper. We present it here because it performs very well in discovering the disease-causing gene in the gene expression dataset (see Section 5). While it would be interesting to explore its theoretical properties in high-dimensional settings, this would require studying the theoretical behavior of Algorithm 2 in the latent variable settings, which is beyond the scope of this paper. So we leave this for future research.

4 Simulations

We now evaluate the finite sample performance of our proposed RC-score (Algorithm 2). Additionally, we empirically examine its robustness in the presence of latent variables and eval-

Algorithm 3 : Root cause discovery (high-dimensional version)

Input: Observational samples $\mathbf{x}_1, \dots, \mathbf{x}_n$ and the interventional sample \mathbf{x}^I , and the number of random permutations v .

Output: RC-score \widehat{C}_i for all variables.

- 1: Initialize $\widetilde{U} = \emptyset$.
 - 2: **for** $i = 1, \dots, p$ **do**:
 - (i) Treat X_i as the response and other variables as covariates, run the cross-validated Lasso using observational samples to obtain an estimated Markov blanket \widehat{S} . Let $\mathbf{x}_{\text{new},1}, \dots, \mathbf{x}_{\text{new},n}$ and $\mathbf{x}_{\text{new}}^I$ be the new observational and interventional samples with variables in $\{i\} \cup \widehat{S}$.
 - (ii) Using $\mathbf{x}_{\text{new},1}, \dots, \mathbf{x}_{\text{new},n}$, $\mathbf{x}_{\text{new}}^I$ and v as inputs, run the first three steps of Algorithm 2 to obtain \widehat{U} , $\widehat{\Pi}$, $\widehat{c}(\pi)$, and $\widehat{u}(\pi)$ for $\pi \in \widehat{\Pi}$.
 - (iii) If $i \in \widehat{U}$, let $\widehat{C}_i = \max_{\pi: \pi \in \widehat{\Pi} \text{ and } \widehat{u}(\pi)=i} \widehat{c}(\pi)$ and include i in \widetilde{U} .
 - 3: **for** $i \in [p] \setminus \widetilde{U}$ **do**: Let $\widehat{C}_i = \widehat{w}_i \widehat{c}_{\min}$, where $\widehat{c}_{\min} = \min_{i \in \widetilde{U}} \widehat{C}_i / 2$ and $\widehat{w}_i = \widehat{Z}_{n,i}^2 / \sum_{j \in [p] \setminus \widetilde{U}} \widehat{Z}_{n,j}^2$ with $\widehat{Z}_{n,j}^2$ defined by (3).
 - 4: Return \widehat{C}_i for all $i \in [p]$.
-

uate the performance of Algorithm 3 in high-dimensional settings. All simulations were carried out in Python, and the code is available at GitHub (<https://github.com/Jinzhou-Li/RootCauseDiscovery>).

4.1 Simulation setup

We generate observational and interventional samples according to models (1) and (2), respectively. Specifically, for the intercept term b , we randomly sample its entries from the uniform distribution $U(-10, 10)$. For the error term ε , we consider two distributions: a Gaussian distribution with mean zero and variances randomly sampled from $U(1, 5)$, and a uniform distribution $U(-5, 5)$. For the matrix B , we consider two types corresponding to the following two DAGs:

- **Hub DAG:** This DAG is motivated by genetic interactions where certain genes, known as hub genes, act as central points of connection and significantly influence the overall network behavior. In our simulations, we consider 4 hub nodes, each with an upper node block of size 15, where the nodes point to the hub node, and a lower node block of size 10, to which the hub node points. Additionally, each hub node is pointed to by 4 nodes from other upper node blocks and points to 3 nodes from other lower node blocks. Nodes within the upper and lower node blocks form a random DAG, as described below, with a sparsity level s . In total, there are $p = 104$ variables. The corresponding matrix B is constructed based on this setup as a lower-triangular matrix to ensure acyclicity, and we randomly sample values from $U(-1, 1)$ as edge weights.
- **Random DAG:** This is a commonly used DAG where nodes are connected in a completely random manner. Specifically, to ensure acyclicity, we generate a lower-triangular matrix B of size $p = 100$ with a sparsity level s . We randomly select positions for the non-zero entries and assign random values from $U(-1, 1)$ as edge weights.

To ensure the marginal variances of $X = (X_1, \dots, X_p)$ do not increase along the causal ordering and to prevent our method from implicitly making use of this information (Reisach et al., 2021; Ng et al., 2024), we first randomly sample some target variances for X from $U(10, 50)$. We then rescale the matrix B to ensure that the final variances of X are close to the target variances. Finally, we randomly permute the ordering of the variables so that they are not sorted according to a causal ordering (with b , ε and B permuted accordingly).

Given b , ε and B , we independently generate n observational samples and one interventional sample. The root cause of the interventional sample is chosen randomly, and the intervention effect is set to δ_r . We randomly generate 20 matrices B . For each B , we generate n observational samples and 50 interventional samples with different root causes. These n observational samples are then used for root cause discovery on the 50 interventional samples. In total, there are $m = 1000$ interventional samples. To investigate the effects of sample size n , the intervention strength δ_r , and the sparsity level s , we consider the following scenarios:

- Vary $n \in \{100, 200, 300\}$ while fixing $s = 0.4$ and $\delta_r = 16$.
- Vary $\delta_r \in \{12, 16, 20\}$ while fixing $s = 0.4$ and $n = 200$.
- Vary $s \in \{0.2, 0.4, 0.6\}$ while fixing $n = 200$ and $\delta_r = 16$.

In total, we consider four settings: a random DAG with Gaussian errors, a random DAG with uniform errors, a hub DAG with Gaussian errors, and a hub DAG with uniform errors. For each setting, we consider the nine scenarios as described above.

4.2 Implemented methods

Given n observational samples and one interventional sample, we calculate the squared z-scores and our proposed RC-scores (Algorithm 2) for each variable in the interventional sample. In addition, we implement two methods mentioned in Section 1.3 that require estimating the causal ordering or DAG, for which we use LiNGAM (Shimizu et al., 2006). LiNGAM can consistently estimate a causal ordering or DAG in linear non-Gaussian settings, which are part of our simulation setup. However, in linear Gaussian settings, which are also part of our simulation setup, the causal ordering and DAG are generally non-identifiable. Below, we give a detailed description of the implementation of these two methods.

The first method estimates a causal ordering and an aberrant variable set, and then ranks the variables based on these estimates. Specifically, we estimate the aberrant variable set based on squared z-scores. A threshold is required to obtain this set. The optimal (oracle) threshold would be the squared z-score of the root cause, because any other threshold would yield a root cause rank that is at most as good as using the squared z-score of the root cause. However, determining this optimal threshold in a data-dependent manner is challenging. In our simulations, we use this optimal threshold to assess the best possible performance of the approach, though it is important to note that this is infeasible in practice due to the requirement of prior knowledge of the root cause. We also use two fixed thresholds 2 and 5 for comparison. Lastly, based on the aberrant variable set and the estimated causal ordering, we assign ranks to the aberrant variables: an aberrant variable receives a smaller rank if it appears earlier in the estimated causal ordering. Variables not in the aberrant set are ranked after the aberrant ones based on their squared z-scores.

The second method uses an estimated DAG and residuals. For each variable X_i , let $\widehat{\text{Pa}}_i$ denote its estimated parents. We then apply cross-validated Lasso to fit a linear model $\hat{f}(X_{\widehat{\text{Pa}}_i})$ based on observational data, with X_i as the response variable and $X_{\widehat{\text{Pa}}_i}$ as the covariates. Next, we compute the absolute residual $|X_i^I - \hat{f}(X_{\widehat{\text{Pa}}_i}^I)|$ based on the interventional sample, and use this value as the score for this variable. The logic behind it is that if X_i^I is not the root cause (i.e., it is not intervened upon), the distribution of X_i^I given its parents remains invariant across different environments, so the residual should be small. On the other hand, if X_i^I is the root cause (i.e., it is intervened upon), its value should be quite different from $\hat{f}(X_{\widehat{\text{Pa}}_i}^I)$, leading to a large residual.

We summarize the implemented methods as follows:

1. Squared z-score: Based on formula (3). This method is denoted as “Z-score” in the plots.
2. The approach based on an estimated causal ordering and aberrant set: The causal ordering is estimated using the Python package *lingam* (Ikeuchi et al., 2023). We denote the three methods with the optimal threshold and thresholds of 2 and 5 for obtaining the aberrant variable set as “LiNGAM-opt”, “LiNGAM-2”, and “LiNGAM-5”, respectively, in the plots.
3. The approach based on an estimated DAG and residuals: The DAG is estimated using the same Python package *lingam* as above. We denote the method as “LiNGAM-Inva” in the plots.
4. RC-score: Implemented using Algorithm 2 with the random permutation number $v = 10$ and thresholds $(0.1, 0.3, \dots, 5)$ in its first step. The estimator \widehat{L}_{X^π} in step 2 is obtained by applying the Cholesky decomposition on the estimated covariance matrix, for which the sample covariance matrix is used when $n > p$, and a shrinkage estimator is used when $n < p$ (Schäfer and Strimmer (2005), we use the Python function *sklearn.covariance.ShrunkCovariance* for its implementation). This method is denoted as “RC-score” in the plots.

4.3 Simulation results

Based on the obtained scores, we calculate and record the rank of the root cause for each interventional sample. A smaller rank indicates a larger score for the root cause, so rank 1 is the best. LiNGAM-opt, LiNGAM-2, and LiNGAM-5 directly provide the rank of the root cause, so we simply record it. In total, we obtain 1000 ranking values for each method, where smaller values indicate better performance. To compare their performances, we plot the cumulative distribution function (CDF) of the root cause rank for each method. The value of the CDF at $x = k$ represents the percentage of times the root cause is ranked in the top k among the 1000 interventional samples. Generally, a method is considered better if its corresponding CDF has a larger area under the curve.

The simulation results for the setting with a hub DAG and uniform errors are shown in Figure 4, where the top, middle, and bottom plots display results with different sample sizes, intervention strengths, and sparsity levels, respectively. As expected, the performance of all methods improves with larger sample sizes or stronger interventions. However, with higher sparsity levels, the performance of both our RC-score and LiNGAM-based approaches decreases because estimating the covariance matrix, causal ordering, and DAG becomes more difficult in

denser graphs. Our proposed RC-score outperforms other methods across almost all settings, even surpassing LiNGAM-opt, which utilizes oracle information.

The RC-score outperforms the squared z-score for different intervention strengths. For large intervention strength (e.g., $\delta_r = 20$), the performance difference is mainly due to fundamental identifiability issues. For intermediate or small intervention strengths, one potential reason for the RC-score to be better is that it accounts for covariance information, whereas the squared z-score method does not.

LiNGAM-2 and LiNGAM-5 perform worse than or similarly to the squared z-score, while LiNGAM-opt consistently outperforms the squared z-score as expected. The optimal thresholds used in LiNGAM-opt across all settings are plotted in Appendix C.3. These plots show significant variation in the optimal thresholds across the 1000 interventional samples, indicating that no single fixed optimal threshold exists for all scenarios.

The performance of LiNGAM-Inva can be good if the DAG is well-estimated, such as when a large sample size is used for estimation (see the plot with $n = 300$). It even has larger CDF values for x approximately between 5 and 20 than our method in the setting with $\delta_r = 12$ (although our method performs better in other ranges of x). However, it is important to note that these settings use the uniform error, which is particularly favorable for LiNGAM. With Gaussian errors, however, the performance of LiNGAM-Inva can deteriorate because the estimated DAG is less accurate. Please see the related simulation results in Appendix C.2, which also contains the results for three other settings with different combinations of DAGs and error types.

4.4 Robustness in latent variable settings

In this section, we empirically examine the robustness of our proposed RC-scores (Algorithm 2) in the presence of latent variables. Since squared z-scores are calculated marginally and are not affected by latent variables, we use them for comparison. We consider random and hub DAGs with Gaussian errors as described in Section 4.1. We generate samples in the same manner as in Section 4.1, with the only difference that we introduce latent variables by randomly discarding η percent of the variables in the generated samples. We fix the sample size at $n = 200$ and the intervention strength at $\delta_r = 12$ in our simulations, and we vary the latent proportion η and the sparsity level s to investigate their effects. To this end, we consider the following scenarios:

- Vary $\eta \in \{0.1, 0.3, 0.5, 0.7\}$ while fixing $s = 0.2$.
- Vary $s \in \{0.1, 0.3, 0.5, 0.7\}$ while fixing $\eta = 0.3$.

The results are shown in Figure 5, with different line types representing different simulation settings. We observe that the RC-score outperforms the squared z-score across all settings, maintaining stable performance as the latent proportion η and sparsity level s vary, demonstrating its robustness to latent variables. The performance of the squared z-score seem improve as η increases, but this occurs because with more latent variables, the root cause is compared to fewer variables, leading to an increase in its rank. Hence this is not a real improvement. The CDF of the RC-score remains relatively stable across different values of η because the root cause already has a small rank.

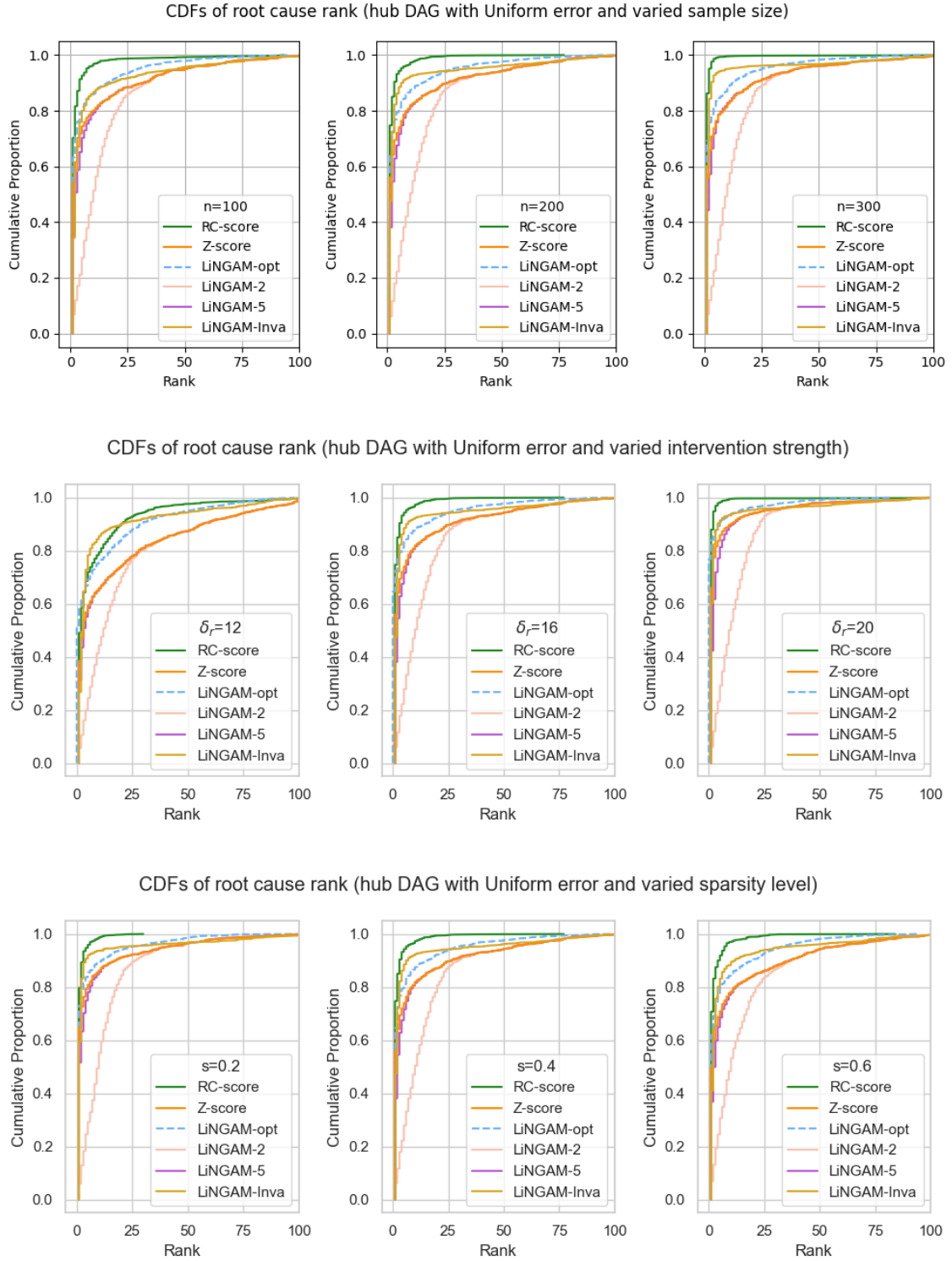


Figure 4: CDFs of the root cause rank using the squared z-score, RC-score, and LiNGAM-based approaches in the setting with a hub DAG and uniform errors. The top, middle, and bottom plots display results for varying sample sizes, intervention strengths, and sparsity levels, respectively.

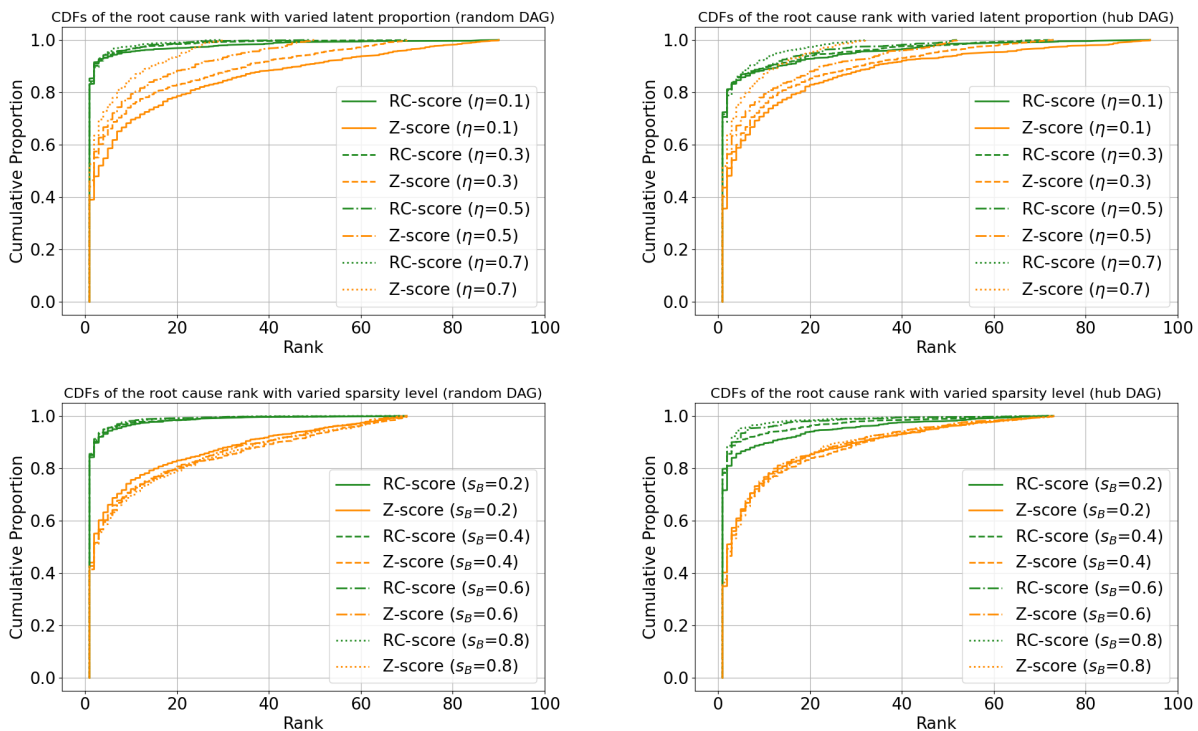


Figure 5: CDFs of the root cause rank using the squared z-score and RC-score in the presence of latent variables. The left and right columns display results for random and hub DAGs, respectively. Different line types represent various simulation settings. The top and bottom plots show results for different latent proportions and sparsity levels, respectively.

4.5 Simulations in high-dimensional settings

We conduct simulations to evaluate the performance of Algorithm 3 in high-dimensional settings (denoted by “RC-score-hd” Figure 6), alongside calculating the squared z-scores for comparison. We set the random permutation number $v = 10$ for Algorithm 3. To reduce computational time, we only treat variables with a squared z-score larger than 1.5 as the response in step 2 of Algorithm 3. Additionally, as in previous simulations, we use thresholds $(0.1, 0.3, \dots, 5)$ in the first step of Algorithm 2 when it is called by Algorithm 3. We consider a hub graph for our simulations as it is inspired by genetic applications which involves high-dimensional data, and we use Gaussian errors. The simulation setup follows the description in Section 4.1, but we now consider a larger hub graph. Specifically, we consider 20 hub nodes. Each hub node has an upper node block of size 30, where the nodes point to the hub node, and a lower node block of size 20, to which the hub node points. Additionally, each hub node is pointed to by 9 nodes from other upper node blocks and points to 6 nodes from other lower node blocks. This results in a total of $p = 1020$ variables. As in Section 4.1, we randomly generate 20 matrices B , and for each B , we generate n observational samples and 50 interventional samples with different root causes. This results in a total of $m = 1000$ interventional samples. We consider the following scenarios to investigate the effects of sample size n and intervention strength δ_r :

- Vary $n \in \{100, 200, 300, 400\}$ while fixing $\delta_r = 12$.
- Vary $\delta_r \in \{8, 12, 16, 20\}$ while fixing $n = 200$.

The simulation results is shown in Figure 6. We can see that Algorithm 3 performs better than the squared z-scores in all settings. As expected, with larger sample size and intervention strength, the performances become better.

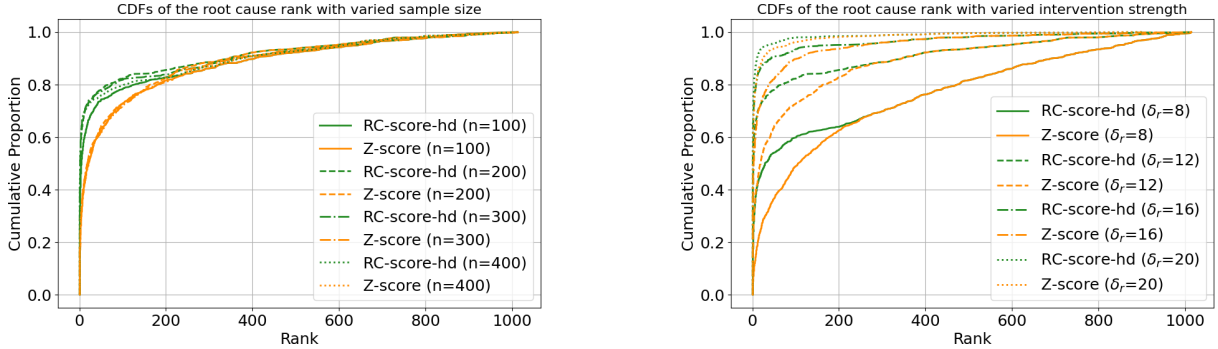


Figure 6: CDFs of the root cause rank using the squared z-score and RC-score based on Algorithm 3 in high-dimensional settings with a hub DAG and Gaussian errors. Different line types represent various simulation settings. The left plot shows results for different sample sizes, while the right plot presents results for varying intervention strengths.

5 Real application on a gene expression dataset

5.1 Data description

In this section, we analyze the gene expression dataset mentioned in Section 1, which motivates this paper. The dataset comprises gene expression data in form of RNA-sequencing read counts from skin fibroblasts of 423 individuals with a suspected Mendelian disorder, including 154 non-strand-specific and 269 strand-specific RNA-sequencing samples. The non-strand-specific dataset is available at <https://zenodo.org/records/4646823> (Yepez et al., 2021), and the strand-specific dataset is available at <https://zenodo.org/records/7510836> (Yepez et al., 2023). We combine the two datasets to increase sample size before applying our method. However, it is worth noting that if sample size is sufficiently large, it is preferable to separate these datasets due to differences in how gene expression levels are measured.

Among these 423 patients, 23 with aberrant expression have known genetic mutations that were diagnosed by whole exome sequencing (see Table S4 in Additional file 1 of Yépez et al. (2022)). Additionally, this study reports 25 newly diagnosed patients with aberrant expression and their corresponding genetic causes (see Table S2 in the same file). Another 10 patients with candidate causes, which are potential genetic causes of the disease, are also reported (see Table S3 in the same file). In total, we have 58 patients. We apply our method to identify the disease-causing gene in these patients and compare the results with the aforementioned genetic causes and candidate genes, which serve as the ground truth.

When applying our method to one patient, we treat the other patients as observational samples. While this approach may not be ideal for detecting aberrancy and identifying the root cause, it is reasonable in this application because the aberrant genes in these rare disease patients are likely to be different. Therefore, for any given variable, the majority of patients

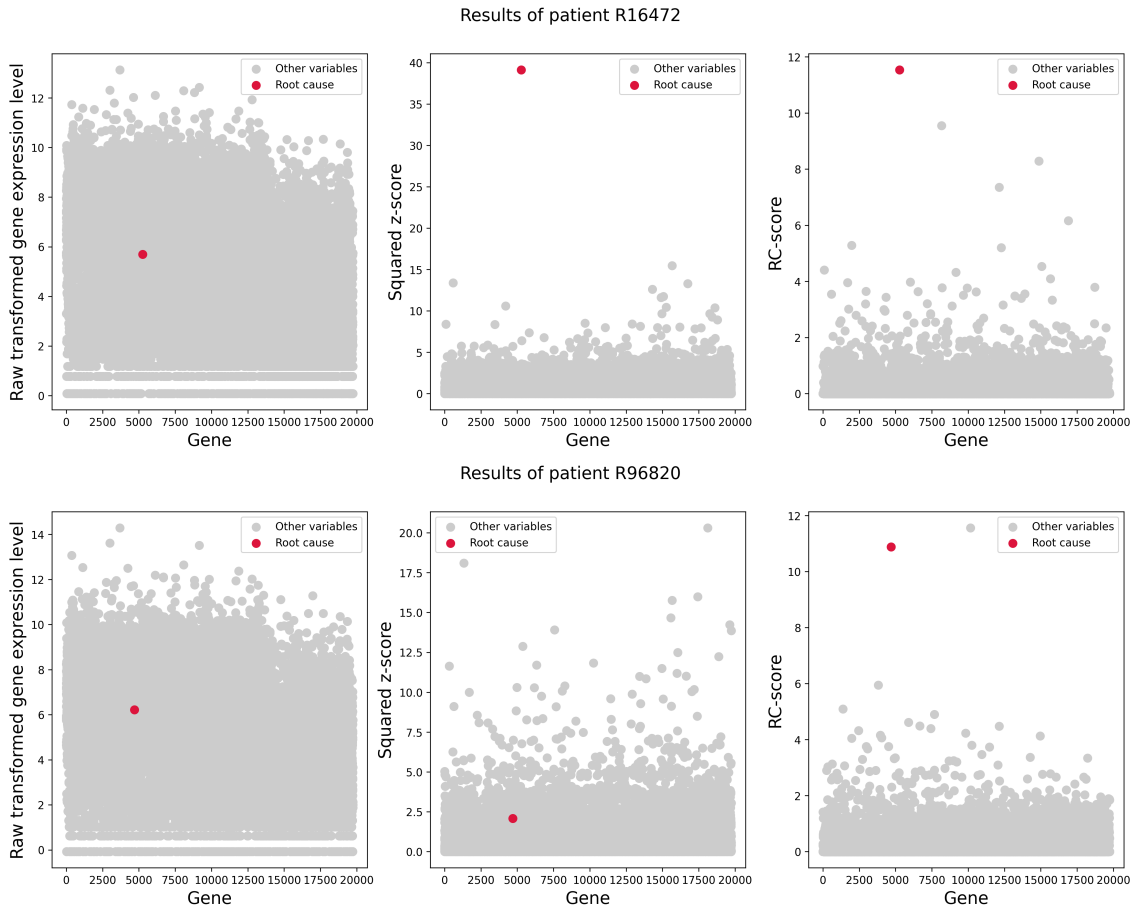


Figure 7: The raw transformed gene expression levels, squared z-scores, and RC-scores of genes for patients *R16472* and *R96820*.

should still exhibit normal expression levels. Better results are expected if gene expression data from healthy individuals were available as a reference.

We first apply the following pre-processing and quality control steps to the raw gene expression data. Specifically, we filter out genes with counts less than 10 in more than 90% of the samples and remove genes that are highly correlated with others (marginal correlation greater than 0.999). For the remaining genes, we follow the preprocessing procedure described by (Brechtmann et al., 2018), applying a log-transformation to better satisfy the linear assumption and dividing by a size factor (Anders and Huber, 2010) to account for sequencing depth. This results in $p = 19736$ genes and $n = 423$ samples in the pre-processed gene expression data.

5.2 Results

We apply Algorithm 3 with the random permutation number $v = 20$ to the gene expression data to discover the root cause for 58 patients. To reduce computational time, in step 2 of Algorithm 3, we treat only the variables with squared z-scores greater than 1.5 as responses. For comparison, we also implement the squared z-score method.

We first examine the raw transformed gene expression levels, squared z-scores, and RC-scores

of genes for two representative patients, *R16472* and *R96820*, as shown in Figure 7. In both cases, the raw gene expression values of the root cause are obscured by other genes due to the propagation of the intervention effect, which leads to many aberrant genes. For patient *R16472*, the squared z-score method successfully identifies the root cause, as suggested by our results in Section 2, which show that this method can be effective in some cases. Our method also assigns the root cause the highest score for this patient. However, for patient *R96820*, the squared z-score fails to distinguish the root cause while our method was able to assign the root cause the highest score. Plots for other patients are provided in Appendix C.4.

We present a table in Figure 8 showing the rank of the root cause based on the squared z-score and the RC-score for all patients. In this table, for 18 out of 58 patients, both the squared z-score and the RC-score assign the same rank to the root cause. For 30 patients, the RC-score assigns a smaller rank to the root cause, indicating that it performs better than the squared z-score. In contrast, for 10 patients, the squared z-score outperforms the RC-score. It is worth noting that the RC-score often improves by a significant margin compared to the squared z-score. For example, for patients *R59185* and *R34834*, the RC-score assigns the root cause a rank of 1, whereas the squared z-score gives ranks of 3057 and 1657, respectively. In cases where the squared z-score performs better, the rank differences are relatively small.

We also count how many patients have the true root cause ranked in the top k for each method, and show it in Figure 9. It is evident that the RC-score method outperforms the squared z-score. Specifically, using the RC-score, the root cause is ranked first in 28 out of 58 patients, in the top 5 in 38 patients, in the top 10 in 46 patients, and in the top 20 in 51 patients. Our method does not work well for the patients *R18626*, *R46723*, and *R12128*. One potential reason is that the genetic correlation structures around the root causes and their descendants in these patients are particularly complex, leading to inaccurate estimates of the associated Markov blankets and covariance matrices. Additionally, the ground truth for patient *R12128* is only a candidate genetic cause, so it would be interesting to further investigate whether our discovered root cause is a reasonable disease-causing gene.

Overall, these results show that our proposed method can be useful for discovering disease-causing genes based on gene expression data. In particular, considering that we are not in the ideal scenario where gene expression data from healthy individuals are available and with a large sample size, we expect our method to be even more effective if such a better reference is available.

6 Discussion

Motivated by the challenge of discovering disease-causing genes in rare disease patients, we study the problem of root cause discovery in this paper. We focus on linear structural equation models where the causal ordering is unknown, aiming to identify the root cause (i.e., the intervened variable) of a single interventional sample by comparing it to n i.i.d. observational samples. We begin by studying a simple method that uses the squared z-score and provide conditions under which this method can successfully identify the root cause, as well as scenarios where it fails. In addition, we present three sufficient conditions under which using the squared z-score can consistently discover the root cause: (i) there is no common ancestor of the root cause and any of its descendants that has a directed path to the descendant without passing through the root cause; (ii) the causal DAG is a polytree; and (iii) all entries of the matrix B are nonnegative.

Patient ID	R19100	R61100	R77611	R16472	R28774	R64921	R80184	R59185	R91273	R60537
RC-score rank	1	1	1	1	1	1	1	1	1	1
Squared z-score rank	1	2	10	1	1	3	11	3057	2	1
Patient ID	R82353	R34834	R30367	R45867	R31640	R55237	R34820	R19907	R27473	R30525
RC-score rank	1	1	1	1	1	1	1	1	1	1
Squared z-score rank	1	1657	1	1	1	1	5	1	38	1
Patient ID	R64055	R15748	R66814	R77365	R42505	R64948	R21470	R47816	R62943	R96820
RC-score rank	1	1	1	1	1	1	1	1	2	2
Squared z-score rank	1	1	1	1	1	9	19	1	770	1633
Patient ID	R91016	R54158	R21147	R64046	R25473	R52016	R21993	R11258	R36605	R95723
RC-score rank	2	2	3	3	4	4	4	5	6	6
Squared z-score rank	2	1	1	15	91	1	2002	31	262	115
Patient ID	R15264	R24289	R76358	R89912	R44456	R20754	R72253	R70186	R98254	R75000
RC-score rank	7	7	7	8	8	9	13	14	17	18
Squared z-score rank	1	21	6	60	83	718	2	2	2289	585
Patient ID	R51757	R78764	R29620	R80346	R26710	R18626	R46723	R12128		
RC-score rank	19	25	52	71	95	610	1028	4475		
Squared z-score rank	29	4	268	1799	576	227	1326	1011		

Figure 8: Table showing the rank of the root cause for 58 patients based on the squared z-score and the RC-score. A smaller rank indicates the root cause has a larger score, with rank 1 being the best.

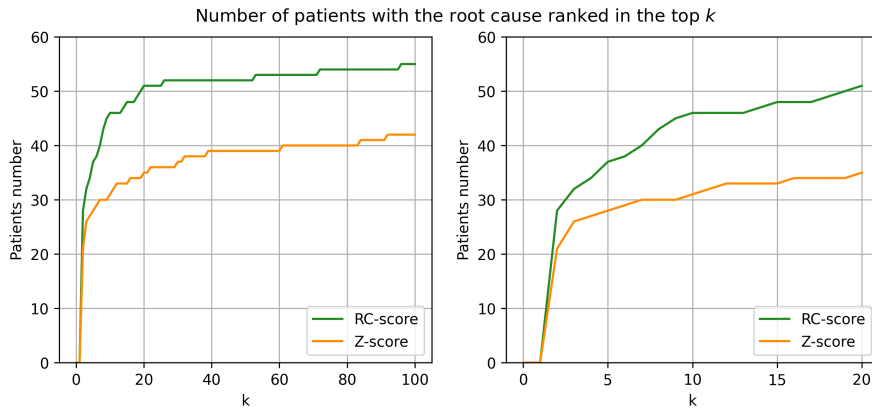


Figure 9: The number of patients with the root cause ranked in the top k based on the squared z-score and the RC-score. The right plot is the zoom-in version of the left plot for $k = 1, \dots, 20$.

Next, we take a step back to consider the identifiability problem of the root cause. Through a novel application of Cholesky decomposition combined with variable permutations, we exploit a (conditional) invariant property related to the root cause: conditional on $\xi(\pi)$ (see (7)) having only one non-zero entry, the variable corresponding to this entry is invariant and must be the root cause. This implies that the root cause is identifiable based on the first two moments of the observational distribution and the first moment of the interventional distribution. Notably, this identifiability result holds even the causal ordering is not identifiable. The proof of this result gives rise to a method for discovering the root cause based on all permutations, but this method becomes intractable when the number of variables is large. To address this, we characterize the sufficient permutations that yield the correct root cause and propose a valid and efficient method

for root cause discovery. Finally, we revisit and analyze the high-dimensional gene expression data. We propose a new root discovery method tailored for high-dimensional settings, building on our previously proposed method and incorporating Lasso for dimension reduction. Applying this method to discover disease-causing genes yields very promising results, showing its potential to many other applications.

As a first step, this paper focuses on the fundamental issue of identifiability and proposes an efficient method for root cause discovery in the simplest settings of linear SEMs without cycle or latent variables. There are many interesting directions for follow-up research.

One direction involves cases with latent variables. Although our simulations demonstrated the robustness of our method to latent variables, a formal study is important and desired. This is also closely related to a deeper understanding of the theoretical properties of Algorithm 3, which is designed for high-dimensional settings. With respect to the intervention types, we focus on mean-shift interventions in this paper because they are reasonable in genetic applications. There are also other types of interventions in the causal literature, such as do-intervention and variance-shift intervention (see, e.g., Eberhardt and Scheines, 2007; Pearl, 2009a). Investigating how to conduct root cause discovery in these settings is an interesting topic for future research. Furthermore, in many applications, there may be multiple root causes, non-linear relationships between variables, or feedback loops. Thus, generalizing the current methodology to address these complexities would be important. Additionally, quantifying the uncertainty in the output from our method is valuable, and developing a method to achieve this would be of great interest. The main idea of using Cholesky decomposition and permutations to exploit an invariant property opens up new possibilities of utilizing interventional samples. It would be interesting to leverage this idea to develop new methods in structural learning, active causal learning, and experimental design where interventional samples are available.

Acknowledgments

Jinzhou Li gratefully acknowledges support by the SNSF Grant P500PT-210978.

References

- Anders, S. and Huber, W. (2010). Differential expression analysis for sequence count data. *Nature Precedings*, pages 1–1.
- Brechtmann, F., Mertes, C., Matusevičiūtė, A., Yépez, V. A., Avsec, Ž., Herzog, M., Bader, D. M., Prokisch, H., and Gagneur, J. (2018). Outrider: a statistical method for detecting aberrantly expressed genes in rna sequencing data. *The American Journal of Human Genetics*, 103(6):907–917.
- Budhathoki, K., Janzing, D., Bloebaum, P., and Ng, H. (2021). Why did the distribution change? In *International Conference on Artificial Intelligence and Statistics*, pages 1666–1674. PMLR.
- Budhathoki, K., Minorics, L., Blöbaum, P., and Janzing, D. (2022). Causal structure-based root cause analysis of outliers. In *International Conference on Machine Learning*, pages 2357–2369. PMLR.

- Cai, T. T., Ren, Z., and Zhou, H. H. (2016). Estimating structured high-dimensional covariance and precision matrices: Optimal rates and adaptive estimation. *Electronic Journal of Statistics*, 10:1–59.
- Eaton, D. and Murphy, K. (2007). Exact bayesian structure learning from uncertain interventions. In *International Conference on Artificial Intelligence and Statistics*, pages 107–114. PMLR.
- Eberhardt, F. and Scheines, R. (2007). Interventions and causal inference. *Philosophy of Science*, 74(5):981–995.
- Evans, R. J. (2020). Model selection and local geometry. *The Annals of Statistics*, 48(6):3513–3544.
- Fan, J., Liao, Y., and Liu, H. (2016). An overview of the estimation of large covariance and precision matrices. *The Econometrics Journal*, 19(1):C1–C32.
- Gusic, M. and Prokisch, H. (2021). Genetic basis of mitochondrial diseases. *FEBS letters*, 595(8):1132–1158.
- Haavelmo, T. (1944). The probability approach in econometrics. *Econometrica: Journal of the Econometric Society*, pages iii–115.
- Hardt, M., Orchard, W., Blöbaum, P., Kasiviswanathan, S., and Kirschbaum, E. (2023). The petshop dataset—finding causes of performance issues across microservices. *arXiv preprint arXiv:2311.04806*.
- Ikeuchi, T., Ide, M., Zeng, Y., Maeda, T. N., and Shimizu, S. (2023). Python package for causal discovery based on lingam. *Journal of Machine Learning Research*, 24(14):1–8.
- Ikram, A., Chakraborty, S., Mitra, S., Saini, S., Bagchi, S., and Kocaoglu, M. (2022). Root cause analysis of failures in microservices through causal discovery. *Advances in Neural Information Processing Systems*, 35:31158–31170.
- Jaber, A., Kocaoglu, M., Shanmugam, K., and Bareinboim, E. (2020). Causal discovery from soft interventions with unknown targets: Characterization and learning. *Advances in Neural Information Processing Systems*, 33:9551–9561.
- Jakobsen, M. E., Shah, R. D., Bühlmann, P., and Peters, J. (2022). Structure learning for directed trees. *Journal of Machine Learning Research*, 23:159.
- Li, M., Li, Z., Yin, K., Nie, X., Zhang, W., Sui, K., and Pei, D. (2022). Causal inference-based root cause analysis for online service systems with intervention recognition. In *Proceedings of the 28th ACM SIGKDD Conference on Knowledge Discovery and Data Mining*, pages 3230–3240.
- Nandy, P., Maathuis, M. H., and Richardson, T. S. (2017). Estimating the effect of joint interventions from observational data in sparse high-dimensional settings. *The Annals of Statistics*, pages 647–674.

- Ng, I., Huang, B., and Zhang, K. (2024). Structure learning with continuous optimization: A sober look and beyond. In *Causal Learning and Reasoning*, pages 71–105. PMLR.
- Okati, N., Mejia, S. H. G., Orchard, W. R., Blöbaum, P., and Janzing, D. (2024). Root cause analysis of outliers with missing structural knowledge. *arXiv preprint arXiv:2406.05014*.
- Pearl, J. (2009a). Causal inference in statistics: An overview. *Statistics Surveys*, 3(none):96 – 146.
- Pearl, J. (2009b). *Causality*. Cambridge university press.
- Peters, J., Bühlmann, P., and Meinshausen, N. (2016). Causal inference by using invariant prediction: identification and confidence intervals. *Journal of the Royal Statistical Society: Series B (Statistical Methodology)*, 78(5):947–1012.
- Raskutti, G. and Uhler, C. (2018). Learning directed acyclic graph models based on sparsest permutations. *Stat*, 7(1):e183.
- Reisach, A., Seiler, C., and Weichwald, S. (2021). Beware of the simulated dag! causal discovery benchmarks may be easy to game. *Advances in Neural Information Processing Systems*, 34:27772–27784.
- Rothenhäusler, D., Heinze, C., Peters, J., and Meinshausen, N. (2015). Backshift: Learning causal cyclic graphs from unknown shift interventions. *Advances in Neural Information Processing Systems*, 28.
- Schäfer, J. and Strimmer, K. (2005). A shrinkage approach to large-scale covariance matrix estimation and implications for functional genomics. *Statistical Applications in Genetics and Molecular Biology*, 4(1).
- Shimizu, S., Hoyer, P. O., Hyvärinen, A., Kerminen, A., and Jordan, M. (2006). A linear non-gaussian acyclic model for causal discovery. *Journal of Machine Learning Research*, 7(10).
- Spirtes, P., Glymour, C., and Scheines, R. (2001). *Causation, prediction, and search*. MIT press.
- Squires, C., Wang, Y., and Uhler, C. (2020). Permutation-based causal structure learning with unknown intervention targets. In *Conference on Uncertainty in Artificial Intelligence*, pages 1039–1048. PMLR.
- Taeb, A. and Bühlmann, P. (2021). Perturbations and causality in gaussian latent variable models. *arXiv preprint arXiv:2101.06950*.
- Tibshirani, R. (1996). Regression shrinkage and selection via the lasso. *Journal of the Royal Statistical Society Series B: Statistical Methodology*, 58(1):267–288.
- Tramontano, D., Monod, A., and Drton, M. (2022). Learning linear non-gaussian polytree models. In *Conference on Uncertainty in Artificial Intelligence*, pages 1960–1969. PMLR.
- Tramontano, D., Waldmann, L., Drton, M., and Duarte, E. (2023). Learning linear gaussian polytree models with interventions. *IEEE Journal on Selected Areas in Information Theory*, pages 1–1.

- Varici, B., Shanmugam, K., Sattigeri, P., and Tajer, A. (2021). Scalable intervention target estimation in linear models. *Advances in Neural Information Processing Systems*, 34:1494–1505.
- Varici, B., Shanmugam, K., Sattigeri, P., and Tajer, A. (2022). Intervention target estimation in the presence of latent variables. In *Conference on Uncertainty in Artificial Intelligence*, pages 2013–2023. PMLR.
- Yang, Y., Salehkaleybar, S., and Kiyavash, N. (2024). Learning unknown intervention targets in structural causal models from heterogeneous data. In *International Conference on Artificial Intelligence and Statistics*, pages 3187–3195. PMLR.
- Ye, Q., Amini, A. A., and Zhou, Q. (2020). Optimizing regularized cholesky score for order-based learning of bayesian networks. *IEEE Transactions on Pattern Analysis and Machine Intelligence*, 43(10):3555–3572.
- Yepez, V., Gusic, M., Kopajtich, R., Meitinger, T., Prokisch, H., and Gagneur, J. (2023). Gene expression and splicing counts from the Yepez, Gusic et al study - fibroblast, hg19, strand-specific, high seq depth.
- Yepez, V. A., Gusic, M., Kopajtich, R., Meitinger, T., Gagneur, J., and Prokisch, H. (2021). Gene expression and splicing counts from the Yepez, Gusic et al study - non strand-specific.
- Yépez, V. A., Gusic, M., Kopajtich, R., Mertes, C., Smith, N. H., Alston, C. L., Ban, R., Beblo, S., Berutti, R., Blessing, H., et al. (2022). Clinical implementation of rna sequencing for mendelian disease diagnostics. *Genome Medicine*, 14(1):38.
- Yépez, V. A., Mertes, C., Müller, M. F., Klapproth-Andrade, D., Wachutka, L., Frésard, L., Gusic, M., Scheller, I. F., Goldberg, P. F., Prokisch, H., et al. (2021). Detection of aberrant gene expression events in rna sequencing data. *Nature Protocols*, 16(2):1276–1296.

SUPPLEMENTARY MATERIAL

A Proofs for Section 2

A.1 Proof of Theorem 2.1

Proof. (Theorem 2.1)

Recall that $\alpha_{r \rightarrow j} = (I - B)_{jr}^{-1}$,

$$X = (I - B)^{-1}(b + \varepsilon) \quad \text{and} \quad X^I = (I - B)^{-1}(b + \varepsilon + \delta) = X + (I - B)^{-1}\delta.$$

Hence, for $j \in [p]$, we have

$$X_j^I = X_j + \alpha_{r \rightarrow j}\delta_r, \tag{13}$$

with $\alpha_{r \rightarrow r} = 1$.

Recall that $Z_j = (X_j^I - \mu_j)/\sigma_j$ is the population version of the z-score of the interventional variable X_j^I , and let $Z_j^o = (X_j - \mu_j)/\sigma_j$ be the corresponding term for the observational variable X_j .

Let $k \in [p] \setminus \{r\}$, by (13), we have

$$\begin{aligned} Z_r^2 - Z_k^2 &= \left(\frac{X_r^I - \mu_r}{\sigma_r} \right)^2 - \left(\frac{X_k^I - \mu_k}{\sigma_k} \right)^2 \\ &= \left(\frac{X_r + \delta_r - \mu_r}{\sigma_r} \right)^2 - \left(\frac{X_k + \alpha_{r \rightarrow k}\delta_r - \mu_k}{\sigma_k} \right)^2 \\ &= \left(Z_r^o + \frac{\delta_r}{\sigma_r} \right)^2 - \left(Z_k^o + \frac{\alpha_{r \rightarrow k}\delta_r}{\sigma_k} \right)^2 \\ &= (Z_r^o)^2 - (Z_k^o)^2 + \delta_r \left(\frac{2Z_r^o}{\sigma_r} - \frac{2Z_k^o\alpha_{r \rightarrow k}}{\sigma_k} \right) + \delta_r^2 \left(\frac{\sigma_k^2 - \alpha_{r \rightarrow k}^2\sigma_r^2}{\sigma_r^2\sigma_k^2} \right) \\ &:= H_1 + \delta_r H_2 + \delta_r^2 h_3, \end{aligned}$$

where $H_1 = (Z_r^o)^2 - (Z_k^o)^2$, $H_2 = \frac{2Z_r^o}{\sigma_r} - \frac{2Z_k^o\alpha_{r \rightarrow k}}{\sigma_k}$, and $h_3 = \frac{\sigma_k^2 - \alpha_{r \rightarrow k}^2\sigma_r^2}{\sigma_r^2\sigma_k^2}$. Note that $\delta_r^2 h_3$ is the leading term if $\delta_r \rightarrow \infty$.

In the first case of $\sigma_k^2 > \alpha_{r \rightarrow k}^2\sigma_r^2$, we have $h_3 > 0$. Fix a small positive η , so for a sufficiently

large δ_r , we have $\delta_r^2 h_3 > \eta$. For any $\epsilon > 0$, when δ_r is large enough, we have

$$\begin{aligned}
\mathrm{P}(Z_r^2 - Z_k^2 \leq \eta) &= \mathrm{P}(H_1 + \delta_r H_2 \leq -\delta_r^2 h_3 + \eta) \\
&\leq \mathrm{P}(|H_1 + \delta_r H_2| \geq \delta_r^2 h_3 - \eta) \\
&\leq \frac{\mathrm{E}[|H_1 + \delta_r H_2|]}{\delta_r^2 h_3 - \eta} \\
&\leq \frac{\mathrm{E}[|H_1|] + \mathrm{E}[|\delta_r H_2|]}{\delta_r^2 h_3 - \eta} \\
&= \frac{\mathrm{E}[(Z_r^o)^2 - (Z_k^o)^2] + \mathrm{E}\left[\frac{2\delta_r Z_r^o}{\sigma_r} - \frac{2\delta_r Z_k^o \alpha_{r \rightarrow k}}{\sigma_k}\right]}{\delta_r^2 h_3 - \eta} \\
&\leq \frac{\mathrm{E}[(Z_r^o)^2] + \mathrm{E}[(Z_k^o)^2] + \frac{2|\delta_r|}{\sigma_r} \mathrm{E}[|Z_r^o|] + \frac{2|\delta_r \alpha_{r \rightarrow k}|}{\sigma_k} \mathrm{E}[|Z_k^o|]}{\delta_r^2 h_3 - \eta} \\
&\leq \frac{2}{\delta_r^2 h_3 - \eta} \left(1 + \frac{|\delta_r|}{\sigma_r} + \frac{|\delta_r \alpha_{r \rightarrow k}|}{\sigma_k}\right) \\
&\leq \epsilon/3,
\end{aligned} \tag{14}$$

where we used Markov's inequality in the second inequality, and $\mathrm{E}[(Z_j^o)^2] = 1$ and $\mathrm{E}[|Z_j^o|] \leq 1$ for $j \in [p]$ in the second last inequality, as Z_j^o is a standardized random variable with mean 0 and variance 1.

Because $\widehat{\mu}_{n,j} \xrightarrow{p} \mu_j$ and $\widehat{\sigma}_{n,j} \xrightarrow{p} \sigma_j$ as $n \rightarrow \infty$, we have $\widehat{Z}_{n,j}^2 \xrightarrow{p} Z_j^2$ as $n \rightarrow \infty$ by the continuous mapping theorem. Hence, for any $\epsilon > 0$ and large enough n , we have

$$\mathrm{P}\left(|\widehat{Z}_{n,r}^2 - Z_r^2| > \eta/4\right) \leq \epsilon/3 \quad \text{and} \quad \mathrm{P}\left(|\widehat{Z}_{n,k}^2 - Z_k^2| > \eta/4\right) \leq \epsilon/3. \tag{15}$$

Therefore, for any $\epsilon > 0$, when δ_r and n are sufficiently large, we have

$$\begin{aligned}
\mathrm{P}\left(\widehat{Z}_{n,r}^2 > \widehat{Z}_{n,k}^2\right) &\geq \mathrm{P}\left(Z_r^2 - Z_k^2 > \eta, |\widehat{Z}_{n,r}^2 - Z_r^2| \leq \eta/4, |\widehat{Z}_{n,k}^2 - Z_k^2| \leq \eta/4\right) \\
&\geq 1 - \mathrm{P}\left(Z_r^2 - Z_k^2 \leq \eta\right) - \mathrm{P}\left(|\widehat{Z}_{n,r}^2 - Z_r^2| > \eta/4\right) - \mathrm{P}\left(|\widehat{Z}_{n,k}^2 - Z_k^2| > \eta/4\right) \\
&\geq 1 - \epsilon,
\end{aligned}$$

which by definition proves that

$$\lim_{\substack{n \rightarrow \infty \\ \delta_r \rightarrow \infty}} \mathrm{P}\left(\widehat{Z}_{n,r}^2 > \widehat{Z}_{n,k}^2\right) = 1.$$

The second case of $\sigma_k^2 - \alpha_{r \rightarrow k}^2 \sigma_r^2 < 0$ can be proved similarly. \square

A.2 Proof of Propositions 2.1 and 2.2

Proof. (Propositions 2.1 and 2.2) We start with the proof of Propositions 2.1.

For (i), when $k \notin \mathrm{De}(r)$, we have $\alpha_{r \rightarrow k} = 0$, so $\sigma_k^2 > \alpha_{r \rightarrow k}^2 \sigma_r^2 = 0$.

For (ii), recall that $X = (I - B)^{-1}(b + \epsilon)$ and $\alpha_{j \rightarrow k} = (I - B)_{kj}^{-1}$, so

$$X_k = \mu_k + \sum_{j \neq k} \alpha_{j \rightarrow k} \epsilon_j + \epsilon_k,$$

where $\mu_k = \mathbb{E}[X_k]$.

From now on, without loss of generality, we assume that X_1, \dots, X_p is sorted by a causal ordering. That is, $i < j$ for $j \in \text{De}(i)$, where $\text{De}(i)$ denotes the descendants of i . Then, we have

$$X_k = \mu_k + \sum_{j=1}^{k-1} \alpha_{j \rightarrow k} \varepsilon_j + \varepsilon_k.$$

Denote $\theta_j^2 = \text{Var}(\varepsilon_j)$, then

$$\sigma_k^2 = \text{Var}(X_k) = \sum_{j=1}^{k-1} \alpha_{j \rightarrow k}^2 \theta_j^2 + \theta_k^2.$$

For $k \in \text{De}(r)$, we have $k > r$. The condition

$$\begin{aligned} & \sigma_k^2 - \alpha_{r \rightarrow k}^2 \sigma_r^2 \\ &= \sum_{j=1}^{k-1} \alpha_{j \rightarrow k}^2 \theta_j^2 + \theta_k^2 - \alpha_{r \rightarrow k}^2 \left(\sum_{j=1}^{r-1} \alpha_{j \rightarrow r}^2 \theta_j^2 + \theta_r^2 \right) \\ &= \alpha_{1 \rightarrow k}^2 \theta_1^2 + \dots + \alpha_{k-1 \rightarrow k}^2 \theta_{k-1}^2 + \theta_k^2 - (\alpha_{r \rightarrow k}^2 \alpha_{1 \rightarrow r}^2 \theta_1^2 + \dots + \alpha_{r \rightarrow k}^2 \alpha_{r-1 \rightarrow r}^2 \theta_{r-1}^2) - \alpha_{r \rightarrow k}^2 \theta_r^2 \\ &= (\alpha_{1 \rightarrow k}^2 - \alpha_{r \rightarrow k}^2 \alpha_{1 \rightarrow r}^2) \theta_1^2 + \dots + (\alpha_{r-1 \rightarrow k}^2 - \alpha_{r \rightarrow k}^2 \alpha_{r-1 \rightarrow r}^2) \theta_{r-1}^2 \\ & \quad + \alpha_{r \rightarrow k}^2 \theta_r^2 - \alpha_{r \rightarrow k}^2 \theta_r^2 \\ & \quad + \mathbb{1}_{\{k \geq r+2\}} (\alpha_{r+1 \rightarrow k}^2 \theta_{r+1}^2 + \dots + \alpha_{k-1 \rightarrow k}^2 \theta_{k-1}^2) + \theta_k^2 \\ & := U + V, \end{aligned}$$

where

$$U = (\alpha_{1 \rightarrow k}^2 - \alpha_{1 \rightarrow r}^2 \alpha_{r \rightarrow k}^2) \theta_1^2 + \dots + (\alpha_{r-1 \rightarrow k}^2 - \alpha_{r-1 \rightarrow r}^2 \alpha_{r \rightarrow k}^2) \theta_{r-1}^2$$

and

$$V = \mathbb{1}_{\{k \geq r+2\}} (\alpha_{r+1 \rightarrow k}^2 \theta_{r+1}^2 + \dots + \alpha_{k-1 \rightarrow k}^2 \theta_{k-1}^2) + \theta_k^2 > 0.$$

Consider the terms in U and note that $\alpha_{j \rightarrow k}$ is the total causal effect of X_j on X_k , and $\alpha_{j \rightarrow r} \alpha_{r \rightarrow k}$ is the total causal effect of X_j on X_k through X_r . Hence, if $O(r, k) = \emptyset$, then $\alpha_{j \rightarrow k} = \alpha_{j \rightarrow r} \alpha_{r \rightarrow k}$ for all $j < r$. This implies that $U = 0$ and $\sigma_k^2 > \alpha_{r \rightarrow k}^2 \sigma_r^2$.

Next, we prove Propositions 2.2.

We only need to consider the case where $k \in \text{De}(r)$. If all edge weights are nonnegative, then the causal effects along all paths are nonnegative, hence

$$\alpha_{j \rightarrow k} \geq \alpha_{j \rightarrow r} \alpha_{r \rightarrow k}.$$

This implies $U \geq 0$ and $\sigma_k^2 > \alpha_{r \rightarrow k}^2 \sigma_r^2$. □

B Proofs of Section 3

We first introduce some notation that will be used in the following proofs.

For a permutation π , let P^π be the permutation matrix that permutes the rows of the identity matrix according to π . Then, for the permuted X^π and $X^{I\pi}$ (see Section 3.2), we have

$$X^\pi = (I - B^\pi)^{-1}(b^\pi + \varepsilon^\pi) \quad \text{and} \quad X^{I\pi} = (I - B^\pi)^{-1}(b^\pi + \varepsilon^\pi + \delta^\pi),$$

where $b^\pi = P^\pi b$, $\varepsilon^\pi = P^\pi \varepsilon$, and $B^\pi = P^\pi B (P^\pi)^T$. It then follows that $\mu_{X^\pi} = (I - B^\pi)^{-1}b^\pi$, $\mu_{X^{I\pi}} = (I - B^\pi)^{-1}(b^\pi + \delta^\pi)$, and $\Sigma_{X^\pi} = (I - B^\pi)^{-1}D_{\varepsilon^\pi}(I - B^\pi)^{-T}$. Hence, for the $\xi(\pi)$ defined in Section 3.2, we have

$$\xi(\pi) = L_{X^\pi}^{-1}(\mu_{X^{I\pi}} - \mu_{X^\pi}) = L_{X^\pi}^{-1}(I - B^\pi)^{-1}\delta^\pi. \quad (16)$$

B.1 Proof of Theorem 3.1

Before proving Theorem 3.1, we introduce the following Lemma B.1, whose proof will be provided after the proof of Theorem 3.1.

Lemma B.1. *Let $A \in \mathbb{R}^{p \times p}$ be an invertible matrix for which there exists a permutation matrix $P \in \mathbb{R}^{p \times p}$ such that PAP^T is lower-triangular. Let L be the lower-triangular matrix obtained by the Cholesky decomposition of AA^T . For any fixed $j \in [p]$, if the j -th column of $L^{-1}A$ has exactly one non-zero element, then this non-zero element must be in the j -th position of this column.*

We first prove Theorem 3.1.

Proof. (Theorem 3.1) Using the notation $\xi(\pi) = L_{X^\pi}^{-1}(\mu_{X^{I\pi}} - \mu_{X^\pi})$ (see Section 3.2), proving Theorem 3.1 is equivalent to proving that for any permutation π :

- (i) $\xi(\pi)$ must have at least one nonzero element;
- (ii) If $\xi(\pi)$ has exactly one nonzero element, then this element must be in the $\pi^{-1}(r)$ -th position, that is, the position of the root cause.

We prove these two statements by applying Lemma B.1.

Let $A = (I - B^\pi)^{-1}D_{\varepsilon^\pi}^{1/2}$ which satisfies the conditions in Lemma B.1. Note that $\Sigma_{X^\pi} = AA^T$, so L_{X^π} is the lower-triangular matrix obtained by implementing the Cholesky decomposition of AA^T .

By (16), we have that $\xi(\pi) = L_{X^\pi}^{-1}(I - B^\pi)^{-1}\delta^\pi$. Since δ^π has only one nonzero entry in the $\pi^{-1}(r)$ -th position and D_{ε^π} is a diagonal matrix with positive diagonals, $\xi(\pi)$ has the same support as the $\pi^{-1}(r)$ -th column of $L_{X^\pi}^{-1}A = L_{X^\pi}^{-1}(I - B^\pi)^{-1}D_{\varepsilon^\pi}^{1/2}$.

Because $L_{X^\pi}^{-1}A$ is invertible, its $\pi^{-1}(r)$ -th column must contain at least one nonzero element, hence $\xi(\pi)$ must have at least one nonzero element. This proves statement (i).

Statement (ii) follows by applying Lemma B.1 with $j = \pi^{-1}(r)$. □

Now we give the proof of Lemma B.1.

Proof. (Lemma B.1) Denote

$$A = \begin{pmatrix} a_{11} & a_{12} & \cdots & a_{1p} \\ a_{21} & a_{22} & \cdots & a_{2p} \\ \vdots & \vdots & \ddots & \vdots \\ a_{p1} & a_{p2} & \cdots & a_{pp} \end{pmatrix} = \begin{pmatrix} a_1^T \\ a_2^T \\ \vdots \\ a_p^T \end{pmatrix} = [a^{(1)}, a^{(2)}, \dots, a^{(p)}],$$

so

$$A^T = [a_1, a_2, \dots, a_p].$$

Since A is invertible and PAP^T is lower-triangular, it follows that all diagonal elements of A are non-zero.

Let $A^T = QR$ be the QR decomposition of A^T , where

$$Q = \begin{pmatrix} q_{11} & q_{12} & \cdots & q_{1p} \\ q_{21} & q_{22} & \cdots & q_{2p} \\ \vdots & \vdots & \ddots & \vdots \\ q_{p1} & q_{p2} & \cdots & q_{pp} \end{pmatrix} = [q^{(1)}, \dots, q^{(p)}]$$

is an orthogonal matrix (i.e., $QQ^T = Q^TQ = I$, where I is the identity matrix) and

$$R = \begin{pmatrix} \langle q^{(1)}, a_1 \rangle & \langle q^{(1)}, a_2 \rangle & \cdots & \langle q^{(1)}, a_p \rangle \\ 0 & \langle q^{(2)}, a_2 \rangle & \cdots & \langle q^{(2)}, a_p \rangle \\ \vdots & \vdots & \ddots & \vdots \\ 0 & 0 & \cdots & \langle q^{(p)}, a_p \rangle \end{pmatrix} \quad (17)$$

is an upper-triangular matrix with positive diagonal elements. We have $LL^T = AA^T = R^TQ^TQR = R^TR$, so $L = R^T$ by the uniqueness of the Cholesky decomposition for a positive-definite matrix.

We now consider the j -th column of $L^{-1}A$, i.e., $L^{-1}Ae_j$, where $e_j = (0, \dots, 0, 1, 0, \dots, 0)^T \in \mathbb{R}^p$ with the non-zero element 1 in the j -th position. Suppose that this column contains one non-zero element, i.e., $L^{-1}Ae_j = ce_k$ for some $c \neq 0$ and $k \in [p]$. We need to show that this non-zero element is in the j -th position, i.e., $k = j$.

First note that $L^{-1}Ae_j = ce_k$, $L = R^T$ and the form of R (see (17)) imply

$$a^{(j)} = Ae_j = cLe_k = cR^T e_k = c \begin{pmatrix} 0 \\ \vdots \\ 0 \\ \langle q^{(k)}, a_k \rangle \\ \vdots \\ \langle q^{(k)}, a_p \rangle \end{pmatrix}.$$

Since $a_{jj} \neq 0$, we must have $k \leq j$.

Next, note that

$$ce_k = L^{-1}Ae_j = L^{-1}R^TQ^T e_j = L^{-1}LQ^T e_j = Q^T e_j,$$

so that

$$e_j = cQe_k = cq^{(k)}.$$

Since $1 = \|e_j\|_2 = \|cq^{(k)}\|_2 = |c|$, we have $c = \pm 1$ and $q^{(k)} = \pm e_j$.

It is well-known by the Gram-Schmidt process that $q^{(k)}$ can be written as a linear combination of vectors a_1, \dots, a_k , so there exists $b_{h_1}, \dots, b_{h_m} \neq 0$ such that $q^{(k)} = b_{h_1}a_{h_1} + \dots + b_{h_m}a_{h_m}$, where $1 \leq m \leq k$ and $h_1, \dots, h_m \leq k$.

Now assume $k < j$, we will show that this leads to a contradiction, which then concludes that $k = j$.

We have $h_1, \dots, h_m \leq k < j$ and hence the h_1, \dots, h_m -th elements of $q^{(k)}$ equal zero as $q^{(k)} = \pm e_j$. Looking at these elements, we have

$$\begin{pmatrix} 0 \\ \vdots \\ 0 \end{pmatrix} = b_{h_1} \begin{pmatrix} a_{h_1 h_1} \\ \vdots \\ a_{h_1 h_m} \end{pmatrix} + \dots + b_{h_m} \begin{pmatrix} a_{h_m h_1} \\ \vdots \\ a_{h_m h_m} \end{pmatrix} = \begin{pmatrix} a_{h_1 h_1} & \dots & a_{h_m h_1} \\ \vdots & \ddots & \vdots \\ a_{h_1 h_m} & \dots & a_{h_m h_m} \end{pmatrix} \begin{pmatrix} b_{h_1} \\ \vdots \\ b_{h_m} \end{pmatrix}.$$

Denote

$$\tilde{A} = \begin{pmatrix} a_{h_1 h_1} & \dots & a_{h_m h_1} \\ \vdots & \ddots & \vdots \\ a_{h_1 h_m} & \dots & a_{h_m h_m} \end{pmatrix},$$

then \tilde{A} must be non-invertible, otherwise $b_{h_1} = \dots = b_{h_m} = 0$ and $q^{(k)} = 0$. However, \tilde{A} is obtained by taking the h_1, \dots, h_m -th rows and columns of A^T , whose diagonal elements are non-zero and for which there exists a permutation matrix P such that $PA^T P^T$ is upper-triangular, hence \tilde{A} must be invertible, which contradicts the previous conclusion. \square

B.2 Proof of Theorem 3.2

Proof. (Theorem 3.2) The proof is almost the same as the proof of Theorem 3.5, with the only difference that we now directly have

$$P(\Pi_{\text{all}} \text{ contains at least one sufficient permutation}) = 1.$$

Hence we omit the proof. \square

B.3 Proof of Theorem 3.3

Before proving Theorem 3.3, we present Lemma B.2, with its proof given after the proof of Theorem 3.3.

Lemma B.2. *Let $A \in \mathbb{R}^{p \times p}$ be an invertible matrix for which there exists a permutation matrix $P \in \mathbb{R}^{p \times p}$ such that PAP^T is lower-triangular. Let L be the lower-triangular matrix obtained by the Cholesky decomposition of AA^T . For any fixed $j \in [p]$, if*

(i) $A_{kj} = 0$ for all $k < j$, and

(ii) $(A^{-1})_{jk} = 0$ for all $k > j$

hold, then the j -th column of $L^{-1}A$ has exactly one non-zero element in the j -th position. If one of the above two conditions does not hold, then the j -th column of $L^{-1}A$ has at least two non-zero elements.

We first give the proof of Theorem 3.3.

Proof. (Theorem 3.3) We prove this theorem by applying Lemma B.2.

Let $A = (I - B^\pi)^{-1}D_{\varepsilon^\pi}^{1/2}$ which satisfies the conditions in Lemma B.2. Note that $\Sigma_{X^\pi} = AA^T$, so L_{X^π} is the lower-triangular matrix obtained by implementing the Cholesky decomposition of AA^T .

Because D_{ε^π} is a diagonal matrix with positive diagonals, A has the same support as $(I - B^\pi)^{-1}$ and the off-diagonal part of A^{-1} has the same support as B^π . Hence, we have

$$\begin{aligned} \pi^{-1}(k) < \pi^{-1}(r) \text{ for all } k \in \text{Pa}(r) &\iff B_{\pi^{-1}(r)j}^\pi = 0 \text{ for all } j > \pi^{-1}(r) \\ &\iff (A^{-1})_{\pi^{-1}(r)j} = 0 \text{ for all } j > \pi^{-1}(r), \end{aligned}$$

$$\begin{aligned} \pi^{-1}(k) > \pi^{-1}(r) \text{ for all } k \in \text{rDe}(r) &\iff (I - B^\pi)_{j\pi^{-1}(r)}^{-1} = 0 \text{ for all } j < \pi^{-1}(r) \\ &\iff A_{j\pi^{-1}(r)} = 0 \text{ for all } j < \pi^{-1}(r). \end{aligned}$$

By (16), we have that $\xi(\pi) = L_{X^\pi}^{-1}(I - B^\pi)^{-1}\delta^\pi$. Since δ^π has only one nonzero entry in the $\pi^{-1}(r)$ -th position and D_{ε^π} is a diagonal matrix with positive diagonals, $\xi(\pi)$ has the same support as the $\pi^{-1}(r)$ -th column of $L_{X^\pi}^{-1}A = L_{X^\pi}^{-1}(I - B^\pi)^{-1}D_{\varepsilon^\pi}^{1/2}$.

The results then follow from applying Lemma B.2 with $j = \pi^{-1}(r)$. \square

Now we prove Lemma B.2.

Proof. (Lemma B.2) First, we prove that if conditions (i) and (ii) hold for some fixed $j \in [p]$, then the j -th column of $L^{-1}A$ has exactly one non-zero element in the j -th position.

Let $c = (c_1, \dots, c_p)^T$ be the j -th column of $L^{-1}A$. It suffices to prove that $c_j \neq 0$ and $c_l = 0$ for any $l \in [p] \setminus \{j\}$. We prove this case by case.

Case 1: $l < j$. Because L is lower-triangular, we have $(L^{-1})_{ik} = 0$ for all $k > i$, so $c_l = \sum_{k=1}^p (L^{-1})_{lk}A_{kj} = \sum_{k=1}^l (L^{-1})_{lk}A_{kj}$. Then, by condition (i) that $A_{kj} = 0$ for all $k < j$, we have $c_l = \sum_{k=1}^l (L^{-1})_{lk}A_{kj} = 0$ as $l < j$.

Case 2: $l = j$. Following the same arguments as above, we have $c_l = c_j = (L^{-1})_{jj}A_{jj}$. A is invertible and PAP^T is lower-triangular implies that all diagonal elements of A are non-zero, and L is lower-triangular with positive diagonals implies that all diagonal elements of L^{-1} are non-zero. Therefore, $c_j = (L^{-1})_{jj}A_{jj} \neq 0$.

Case 3: $l > j$. Note that $L^{-1}A = L^T A^{-T}$ as $AA^T = LL^T$, so $c_l = \sum_{k=1}^p (L^T)_{lk}(A^{-T})_{kj}$. L is lower-triangular implies that $(L^T)_{lk} = 0$ for all $l > k$, so $c_l = \sum_{k=1}^p (L^T)_{lk}(A^{-T})_{kj} = \sum_{k=l}^p (L^T)_{lk}(A^{-T})_{kj}$. Additionally, condition (ii) that $(A^{-1})_{jk} = 0$ for all $k > j$ implies that $(A^{-T})_{kj} = 0$ for all $k > j$, hence $c_l = \sum_{k=l}^p (L^T)_{lk}(A^{-T})_{kj} = 0$ as $l > j$.

The claim is then proved by combining the above three cases.

Next, we prove that if conditions (i) or (ii) does not hold, then the j -th column of $L^{-1}A$ has at least two non-zero elements.

If condition (i) does not hold, that is, there exists some $k < j$ such that $A_{kj} \neq 0$. Denote the smallest such k by m , then $c_m = (L^{-1})_{mm}A_{mj} \neq 0$. Because $m \neq j$, there must exist another non-zero element $c_{m'}$ for some $m' \in [p] \setminus \{m\}$, otherwise it contradicts Lemma B.1.

Similarly, if condition (ii) does not hold, that is, there exists some $k > j$ such that $(A^{-1})_{jk} \neq 0$, which is equivalent to $(A^{-T})_{kj} \neq 0$. Denote the largest such k by u , then $c_u = (L^T)_{uu}(A^{-T})_{uj} \neq 0$. Because $u \neq j$, there must exist another non-zero element $c_{u'}$ for some $u' \in [p] \setminus \{u\}$, otherwise it contradicts Lemma B.1. \square

B.4 Proof of Theorem 3.4

Proof. (Theorem 3.4) If we obtain an aberrant set $D = \{r\} \cup \text{rDe}(r)$ in step 2 of Algorithm 1, then by steps 3 and 4 of Algorithm 1 and Theorem 3.3, $\widehat{\Pi}$ contains at least one sufficient permutation. Therefore, we prove the result by showing that $D = \{r\} \cup \text{rDe}(r)$ happens with a probability tending to one as n and δ_r tend to infinity.

In the case of $\{r\} \cup \text{rDe}(r) = [p]$, $D = \{r\} \cup \text{rDe}(r) = [p]$ occurs when $\min_{j \in [p]} \widehat{Z}_{n,j}^2$ is used as a threshold in step 2 of Algorithm 1, hence

$$\mathbb{P}\left(\widehat{\Pi} \text{ contains at least one sufficient permutation}\right) \geq \mathbb{P}(D = \{r\} \cup \text{rDe}(r)) = 1.$$

Now consider the case where $\{r\} \cup \text{rDe}(r) \neq [p]$. Let $R = \{r\} \cup \text{rDe}(r)$ for simplicity of notation. We will show that for large enough n and δ_r , all $\widehat{Z}_{n,j}^2$ with $j \in R$ are larger than $\widehat{Z}_{n,k}^2$, $k \notin R$, hence when $\min_{j \in R} \widehat{Z}_{n,j}^2$ is used as a threshold in step 2 of Algorithm 1, we have $D = R$.

We first consider the population version terms. For $i \in [p]$, recall that

$$Z_i = \frac{X_i^I - \mu_i}{\sigma_i}, \quad Z_i^o = \frac{X_i - \mu_i}{\sigma_i}, \quad \text{and} \quad X_i^I = X_i + \alpha_{r \rightarrow i} \delta_r,$$

where $\alpha_{r \rightarrow i}$ is the total causal effect of X_r on X_i , and μ_i and σ_i are the population mean and standard deviation of X_i , respectively. Note that Z_i^o is a standardized random variable with mean 0 and variance 1.

For any $j \in R$ and $k \notin R$, we have $\alpha_{r \rightarrow j} \neq 0$ and $\alpha_{r \rightarrow k} = 0$ (here we use the convention that $\alpha_{r \rightarrow r} = 1$). Hence,

$$Z_j^2 = (Z_j^o)^2 + \delta_r \frac{2\alpha_{r \rightarrow j} Z_j^o}{\sigma_j} + \delta_r^2 \frac{\alpha_{r \rightarrow j}^2}{\sigma_j^2}, \quad Z_k^2 = (Z_k^o)^2,$$

and

$$Z_j^2 - Z_k^2 = (Z_j^o)^2 - (Z_k^o)^2 + \delta_r \frac{2\alpha_{r \rightarrow j} Z_j^o}{\sigma_j} + \delta_r^2 \frac{\alpha_{r \rightarrow j}^2}{\sigma_j^2} := J_1 + \delta_r J_2 + \delta_r^2 J_3,$$

where $J_1 = (Z_j^o)^2 - (Z_k^o)^2$, $J_2 = \frac{2\alpha_{r \rightarrow j} Z_j^o}{\sigma_j}$, and $J_3 = \frac{\alpha_{r \rightarrow j}^2}{\sigma_j^2} > 0$.

Fix a small positive η . For sufficiently large δ_r , we have $-\delta_r^2 J_3 + \eta < 0$. Then, for any $\epsilon > 0$,

when δ_r is large enough, we have

$$\begin{aligned}
\mathrm{P}(Z_j^2 - Z_k^2 \leq \eta) &= \mathrm{P}(J_1 + \delta_r J_2 \leq -\delta_r^2 J_3 + \eta) \\
&\leq \mathrm{P}(|J_1 + \delta_r J_2| \geq \delta_r^2 J_3 - \eta) \\
&\leq \frac{\mathrm{E}[|J_1 + \delta_r J_2|]}{\delta_r^2 J_3 - \eta} \\
&\leq \frac{\mathrm{E}[(Z_j^o)^2] + \mathrm{E}[(Z_k^o)^2] + \frac{|2\alpha_{r \rightarrow j} \delta_r|}{\sigma_j} \mathrm{E}[|Z_j^o|]}{\delta_r^2 \frac{\alpha_{r \rightarrow j}^2}{\sigma_j^2} - \eta} \\
&\leq \frac{2\sigma_j^2 + \sigma_j |2\alpha_{r \rightarrow j} \delta_r|}{\delta_r^2 \alpha_{r \rightarrow j}^2 - \eta \sigma_j^2} \\
&\leq \frac{\epsilon}{3|R|(p - |R|)},
\end{aligned} \tag{18}$$

where we used Markov's inequality in the second inequality. Therefore, for any $\epsilon > 0$ and sufficiently large δ_r , we have

$$\begin{aligned}
&\mathrm{P}\left(\min_{j \in R} Z_j^2 - \max_{k \notin R} Z_k^2 > \eta\right) \\
&= \mathrm{P}\left(\bigcap_{j \in R} \bigcap_{k \notin R} \{Z_j^2 - Z_k^2 > \eta\}\right) \\
&\geq \sum_{j \in R} \sum_{k \notin R} \mathrm{P}(Z_j^2 - Z_k^2 > \eta) - |R|(p - |R|) + 1 \\
&\geq \sum_{j \in R} \sum_{k \notin R} \left(1 - \frac{\epsilon}{3|R|(p - |R|)}\right) - |R|(p - |R|) + 1 \\
&= 1 - \epsilon/3,
\end{aligned} \tag{19}$$

where we used (18) in the last inequality.

Now we consider the sample version terms. Because $\hat{\mu}_{n,j} \xrightarrow[n \rightarrow \infty]{p} \mu_j$ and $\hat{\sigma}_{n,j} \xrightarrow[n \rightarrow \infty]{p} \sigma_j$, we have $\min_{j \in R} \hat{Z}_{n,j}^2 \xrightarrow[n \rightarrow \infty]{p} \min_{j \in R} Z_j^2$ and $\max_{k \notin R} \hat{Z}_{n,k}^2 \xrightarrow[n \rightarrow \infty]{p} \max_{k \notin R} Z_k^2$ by the continuous mapping theorem. Hence, for any $\epsilon > 0$ and large enough n , we have

$$\mathrm{P}\left(\left|\min_{j \in R} \hat{Z}_{n,j}^2 - \min_{j \in R} Z_j^2\right| \leq \eta/4\right) \geq 1 - \epsilon/3 \quad \text{and} \quad \mathrm{P}\left(\left|\max_{k \notin R} \hat{Z}_{n,k}^2 - \max_{k \notin R} Z_k^2\right| \leq \eta/4\right) \geq 1 - \epsilon/3. \tag{20}$$

Therefore, by (19) and (20), for any $\epsilon > 0$ and sufficiently large δ_r and n , we have

$$\begin{aligned}
& \mathbb{P} \left(\widehat{\Pi} \text{ contains at least one sufficient permutation} \right) \\
& \geq \mathbb{P} (D = R) \\
& \geq \mathbb{P} \left(\min_{j \in R} \widehat{Z}_{n,j}^2 > \max_{k \notin R} \widehat{Z}_{n,k}^2 \right) \\
& \geq \mathbb{P} \left(\min_{j \in R} Z_j^2 - \max_{k \notin R} Z_k^2 > \eta, \left| \min_{j \in R} \widehat{Z}_{n,j}^2 - \min_{j \in R} Z_j^2 \right| \leq \eta/4, \left| \max_{k \notin R} \widehat{Z}_{n,k}^2 - \max_{k \notin R} Z_k^2 \right| \leq \eta/4 \right) \\
& \geq \mathbb{P} \left(\min_{j \in R} Z_j^2 - \max_{k \notin R} Z_k^2 > \eta \right) + \mathbb{P} \left(\left| \min_{j \in R} \widehat{Z}_{n,j}^2 - \min_{j \in R} Z_j^2 \right| \leq \eta/4 \right) + \mathbb{P} \left(\left| \max_{k \notin R} \widehat{Z}_{n,k}^2 - \max_{k \notin R} Z_k^2 \right| \leq \eta/4 \right) \\
& \quad - 2 \\
& \geq 1 - \epsilon,
\end{aligned}$$

which by definition proves that

$$\lim_{\substack{n \rightarrow \infty \\ \delta_r \rightarrow \infty}} \mathbb{P} \left(\widehat{\Pi} \text{ contains at least one sufficient permutation} \right) = 1.$$

□

B.5 Proof of Theorem 3.5

Before giving the proof, we first introduce some notation and two lemmas that will be used in the proof of Theorem 3.5. Let

$$\widetilde{\xi}(\pi) := L_{X^\pi}^{-1}(\mathbf{x}^{I^\pi} - \mu_{X^\pi}),$$

which has mean $\mathbb{E}[\widetilde{\xi}(\pi)] = L_{X^\pi}^{-1}(\mu_{X^{I^\pi}} - \mu_{X^\pi}) = L_{X^\pi}^{-1}(I - B^\pi)^{-1}\delta^\pi = \xi(\pi)$ (see (16)). Recall that $\delta^\pi = (0, \dots, 0, \delta_r, 0, \dots, 0)^T$, where δ_r is in the $\pi^{-1}(r)$ -th position. Let

$$\tilde{c}(\pi) = \frac{|\widetilde{\xi}(\pi)|_{(1)} - |\widetilde{\xi}(\pi)|_{(2)}}{|\widetilde{\xi}(\pi)|_{(2)}} \quad \text{and} \quad \tilde{u}(\pi) = \pi(\operatorname{argmax}_{j \in [p]} |\widetilde{\xi}(\pi)|_j),$$

where $|\widetilde{\xi}(\pi)|_{(i)}$ denotes the i -th largest entry in $|\widetilde{\xi}(\pi)|$. Then, we have the following two lemmas showing some properties of $\tilde{u}(\pi)$ and $\tilde{c}(\pi)$ for sufficient and insufficient π , respectively.

Lemma B.3. *Let r be the root cause. For a sufficient permutation π , we have*

$$\tilde{c}(\pi) \xrightarrow[\delta_r \rightarrow \infty]{p} \infty \quad \text{and} \quad \tilde{u}(\pi) \xrightarrow[\delta_r \rightarrow \infty]{p} r. \tag{21}$$

Lemma B.4. *There exists some constant $C > 0$ such that for any insufficient permutation π , we have*

$$\lim_{\delta_r \rightarrow \infty} P(\tilde{c}(\pi) < C) = 1. \tag{22}$$

We now give the proof of Theorem 3.5, followed by the proofs of the above two lemmas.

Proof. (Theorem 3.5) We divide the proof into two parts. In the first part, we show some properties for sufficient and insufficient π that will be used later. In the second part, we prove the main result.

Part 1: Prove some properties related to π .

First, because

$$\widehat{L}_{X^\pi} \xrightarrow[n \rightarrow \infty]{p} L_{X^\pi} \quad \text{and} \quad \widehat{\mu}_{X^\pi} \xrightarrow[n \rightarrow \infty]{p} \mu_{X^\pi},$$

we have by the continuous mapping theorem that

$$\widehat{\mu}_{\widetilde{\xi}(\pi)} = \widehat{L}_{X^\pi}^{-1}(\mathbf{x}^{I^\pi} - \widehat{\mu}_{X^\pi}) \xrightarrow[n \rightarrow \infty]{p} L_{X^\pi}^{-1}(\mathbf{x}^{I^\pi} - \mu_{X^\pi}) = \widetilde{\xi}(\pi),$$

$$\hat{c}(\pi) = \frac{\left| \widehat{\mu}_{\widetilde{\xi}(\pi)} \right|_{(1)} - \left| \widehat{\mu}_{\widetilde{\xi}(\pi)} \right|_{(2)}}{\left| \widehat{\mu}_{\widetilde{\xi}(\pi)} \right|_{(2)}} \xrightarrow[n \rightarrow \infty]{p} \frac{|\widetilde{\xi}(\pi)|_{(1)} - |\widetilde{\xi}(\pi)|_{(2)}}{|\widetilde{\xi}(\pi)|_{(2)}} = \tilde{c}(\pi), \quad (23)$$

and

$$\hat{u}(\pi) = \pi(\operatorname{argmax}_{j \in [p]} |\widehat{\mu}_{\widetilde{\xi}(\pi)}|_j) \xrightarrow[n \rightarrow \infty]{p} \pi(\operatorname{argmax}_{j \in [p]} |\widetilde{\xi}(\pi)|_j) = \tilde{u}(\pi). \quad (24)$$

Part 1-1: Prove some properties related to sufficient π .

For a sufficient π , because

$$\mathbb{P}(\hat{u}(\pi) = r) \geq \mathbb{P}(\tilde{u}(\pi) = r, |\hat{u}(\pi) - \tilde{u}(\pi)| < 1/2) \geq \mathbb{P}(\tilde{u}(\pi) = r) + \mathbb{P}(|\hat{u}(\pi) - \tilde{u}(\pi)| < 1/2) - 1,$$

by (24) and Lemma B.3, we have

$$\hat{u}(\pi) \xrightarrow[n, \delta_r \rightarrow \infty]{p} r. \quad (25)$$

In addition, for any $M > 0$, we have

$$\begin{aligned} & \mathbb{P}(\hat{c}(\pi) \mathbb{1}_{\{\hat{u}(\pi)=r\}} \geq M) \\ & \geq \mathbb{P}(\tilde{c}(\pi) \geq 2M, \tilde{u}(\pi) = r, |\hat{u}(\pi) - \tilde{u}(\pi)| < 1/2, |\hat{c}(\pi) - \tilde{c}(\pi)| < M/2) \\ & \geq \mathbb{P}(\tilde{c}(\pi) \geq 2M) + \mathbb{P}(\tilde{u}(\pi) = r) + \mathbb{P}(|\hat{u}(\pi) - \tilde{u}(\pi)| < 1/2) + \mathbb{P}(|\hat{c}(\pi) - \tilde{c}(\pi)| < M/2) - 3, \end{aligned}$$

so by (23), (24) and Lemma B.3, we have

$$\hat{c}(\pi) \mathbb{1}_{\{\hat{u}(\pi)=r\}} \xrightarrow[n, \delta_r \rightarrow \infty]{p} \infty. \quad (26)$$

Furthermore, for any $M > 0$ and $k \in [p] \setminus \{r\}$, we have

$$\begin{aligned} \mathbb{P}(\hat{c}(\pi) \mathbb{1}_{\{\hat{u}(\pi)=k\}} < M) & \geq \mathbb{P}(\hat{u}(\pi) = r) \\ & \geq \mathbb{P}(\tilde{u}(\pi) = r, |\hat{u}(\pi) - \tilde{u}(\pi)| < 1/2) \\ & \geq \mathbb{P}(\tilde{u}(\pi) = r) + \mathbb{P}(|\hat{u}(\pi) - \tilde{u}(\pi)| < 1/2) - 1, \end{aligned}$$

so by Lemma B.3 and (24), we have

$$\lim_{\substack{n \rightarrow \infty \\ \delta_r \rightarrow \infty}} \mathbb{P}(\hat{c}(\pi) \mathbb{1}_{\{\hat{u}(\pi)=k\}} < M) = 1. \quad (27)$$

Part 1-2: Prove some properties related to insufficient π .

For an insufficient π and any $j \in [p]$, let C be the constant from Lemma B.4, we have

$$\begin{aligned} \mathbb{P}(\hat{c}(\pi) \mathbb{1}_{\{\hat{u}(\pi)=j\}} < 2C) &\geq \mathbb{P}(\hat{c}(\pi) < 2C) \\ &\geq \mathbb{P}(\tilde{c}(\pi) < C, |\hat{c}(\pi) - \tilde{c}(\pi)| < C/2) \\ &\geq \mathbb{P}(\tilde{c}(\pi) < C) + \mathbb{P}(|\hat{c}(\pi) - \tilde{c}(\pi)| < C/2) - 1, \end{aligned}$$

so by (23) and Lemma B.4, we have

$$\lim_{\substack{n \rightarrow \infty \\ \delta_r \rightarrow \infty}} \mathbb{P}(\hat{c}(\pi) \mathbb{1}_{\{\hat{u}(\pi)=j\}} < 2C) = 1. \quad (28)$$

Part 2: Prove the main result.

We first analyze $\mathbb{P}(\hat{C}_k < \hat{C}_r)$ for $k \in [p] \setminus \{r\}$, then obtain the main result by using the union bound.

Denote all permutations by $\{\pi_i : i \in [p!]\}$, and let $\hat{d}_i = \mathbb{1}_{\{\pi_i \in \hat{\Pi}\}} \in \{0, 1\}$ be a data-dependent random variable indicating whether a permutation is contained in $\hat{\Pi}$. Then, for $j \in [p]$, we can rewrite \hat{C}_j (see Algorithm 2) as

$$\hat{C}_j = \max_{i \in [p!]} \left\{ \hat{c}(\pi_i) \hat{d}_i \mathbb{1}_{\{\hat{u}(\pi_i)=j\}}, \hat{w}_j \hat{c}_{\min} \left(\prod_{l \in [p!]} (1 - \hat{d}_l \mathbb{1}_{\{\hat{u}(\pi_l)=j\}}) \right) \right\}.$$

For any $k \in [p] \setminus \{r\}$, we have

$$\begin{aligned} \mathbb{P}(\hat{C}_k < \hat{C}_r) &= \mathbb{P} \left(\max_{i \in [p!]} \left\{ \hat{c}(\pi_i) \hat{d}_i \mathbb{1}_{\{\hat{u}(\pi_i)=k\}}, \hat{w}_k \hat{c}_{\min} \left(\prod_{l \in [p!]} (1 - \hat{d}_l \mathbb{1}_{\{\hat{u}(\pi_l)=k\}}) \right) \right\} < \hat{C}_r \right) \\ &\geq \mathbb{P} \left(\max_{i \in [p!]} \{ \hat{c}(\pi_i) \mathbb{1}_{\{\hat{u}(\pi_i)=k\}} \} < \hat{C}_r, \hat{c}_{\min} < \hat{C}_r \right) \\ &\geq \mathbb{P} \left(\max_{i \in [p!]} \{ \hat{c}(\pi_i) \mathbb{1}_{\{\hat{u}(\pi_i)=k\}} \} < \hat{C}_r \right) + \mathbb{P}(\hat{c}_{\min} < \hat{C}_r) - 1, \end{aligned} \quad (29)$$

where we used the fact that $\hat{w}_k \hat{c}_{\min} \left(\prod_{l \in [p!]} (1 - \hat{d}_l \mathbb{1}_{\{k=\hat{u}(\pi_l)\}}) \right) \leq \hat{c}_{\min}$ for the first inequality.

Next, we show that

$$\lim_{\substack{n \rightarrow \infty \\ \delta_r \rightarrow \infty}} \mathbb{P} \left(\max_{i \in [p!]} \{ \hat{c}(\pi_i) \mathbb{1}_{\{\hat{u}(\pi_i)=k\}} \} < \hat{C}_r \right) = 1 \quad \text{and} \quad \lim_{\substack{n \rightarrow \infty \\ \delta_r \rightarrow \infty}} \mathbb{P}(\hat{c}_{\min} < \hat{C}_r) = 1.$$

Part 2-1: Prove $\lim_{\substack{n \rightarrow \infty \\ \delta_r \rightarrow \infty}} \mathbb{P} \left(\max_{i \in [p!]} \{ \hat{c}(\pi_i) \mathbb{1}_{\{\hat{u}(\pi_i)=k\}} \} < \hat{C}_r \right) = 1$.

Let C be the constant from Lemma B.4, we have

$$\begin{aligned} &\lim_{\substack{n \rightarrow \infty \\ \delta_r \rightarrow \infty}} \mathbb{P} \left(\max_{i \in [p!]} \{ \hat{c}(\pi_i) \mathbb{1}_{\{\hat{u}(\pi_i)=k\}} \} < \hat{C}_r \right) \\ &\geq \lim_{\substack{n \rightarrow \infty \\ \delta_r \rightarrow \infty}} \mathbb{P} \left(\max_{i \in [p!]} \{ \hat{c}(\pi_i) \mathbb{1}_{\{\hat{u}(\pi_i)=k\}} \} < 2C, \hat{C}_r \geq 2C \right) \\ &\geq \lim_{\substack{n \rightarrow \infty \\ \delta_r \rightarrow \infty}} \mathbb{P} \left(\max_{i \in [p!]} \{ \hat{c}(\pi_i) \mathbb{1}_{\{\hat{u}(\pi_i)=k\}} \} < 2C \right) + \lim_{\substack{n \rightarrow \infty \\ \delta_r \rightarrow \infty}} \mathbb{P}(\hat{C}_r \geq 2C) - 1. \end{aligned}$$

By (27), (28) and using the union bound, we have

$$\lim_{\substack{n \rightarrow \infty \\ \delta_r \rightarrow \infty}} \mathbb{P} \left(\max_{i \in [p!]} \{ \hat{c}(\pi_i) \mathbb{1}_{\{\hat{u}(\pi_i)=k\}} \} < 2C \right) = 1. \quad (30)$$

Let the first u permutations be all sufficient permutations without loss of generality, then we have

$$\begin{aligned} \mathbb{P} \left(\widehat{C}_r \geq 2C \right) &\geq \mathbb{P} \left(\max_{i \in [u]} \{ \hat{c}(\pi_i) \widehat{d}_i \mathbb{1}_{\{r=\hat{u}(\pi_i)\}} \} \geq 2C \right) \\ &\geq \mathbb{P} \left(\min_{i \in [u]} \{ \hat{c}(\pi_i) \mathbb{1}_{\{r=\hat{u}(\pi_i)\}} \} \geq 2C, \sum_{i=1}^u \widehat{d}_i \geq 1 \right) \\ &= \mathbb{P} \left(\bigcap_{i \in [u]} \{ \hat{c}(\pi_i) \mathbb{1}_{\{r=\hat{u}(\pi_i)\}} \geq 2C \}, \sum_{i=1}^u \widehat{d}_i \geq 1 \right) \\ &\geq \sum_{i \in [u]} \mathbb{P} \left(\hat{c}(\pi_i) \mathbb{1}_{\{r=\hat{u}(\pi_i)\}} \geq 2C \right) + \mathbb{P} \left(\sum_{i=1}^u \widehat{d}_i \geq 1 \right) - |u| \\ &= \sum_{i \in [u]} \mathbb{P} \left(\hat{c}(\pi_i) \mathbb{1}_{\{r=\hat{u}(\pi_i)\}} \geq 2C \right) + \mathbb{P} \left(\widehat{\Pi} \text{ contains at least one sufficient permutation} \right) - |u|. \end{aligned}$$

Hence, by (26) and Theorem 3.4, we have

$$\lim_{\substack{n \rightarrow \infty \\ \delta_r \rightarrow \infty}} \mathbb{P} \left(\widehat{C}_r \geq 2C \right) = 1. \quad (31)$$

Therefore, by combining (31) and (30), we have

$$\lim_{\substack{n \rightarrow \infty \\ \delta_r \rightarrow \infty}} \mathbb{P} \left(\max_{i \in [p!]} \{ \hat{c}(\pi_i) \mathbb{1}_{\{\hat{u}(\pi_i)=k\}} \} < \widehat{C}_r \right) = 1. \quad (32)$$

Part 2-2: Prove $\lim_{\substack{n \rightarrow \infty \\ \delta_r \rightarrow \infty}} \mathbb{P} \left(\hat{c}_{\min} < \widehat{C}_r \right) = 1$.

Recall that we let the first u permutations be all sufficient permutations without loss of generality. Then,

$$\begin{aligned} \mathbb{P} \left(\hat{c}_{\min} < \widehat{C}_r \right) &\geq \mathbb{P} \left(r \in \widehat{U} \right) \\ &\geq \mathbb{P} \left(\bigcap_{i \in [u]} \{ \hat{u}(\pi_i) = r \}, \sum_{i=1}^u \widehat{d}_i \geq 1 \right) \\ &\geq \sum_{i \in [u]} \mathbb{P} \left(\hat{u}(\pi_i) = r \right) + \mathbb{P} \left(\sum_{i=1}^u \widehat{d}_i \geq 1 \right) - u \\ &= \sum_{i \in [u]} \mathbb{P} \left(\hat{u}(\pi_i) = r \right) + \mathbb{P} \left(\widehat{\Pi} \text{ contains at least one sufficient permutation} \right) - u \end{aligned}$$

Hence, by (25) and Theorem 3.4, we have

$$\lim_{\substack{n \rightarrow \infty \\ \delta_r \rightarrow \infty}} \mathbb{P} \left(\hat{c}_{\min} < \hat{C}_r \right) = 1. \quad (33)$$

Part 2-3: Use the union bound to show the final result.

By using the union bound and combining (29), (32) and (33), we have

$$\lim_{\substack{n \rightarrow \infty \\ \delta_r \rightarrow \infty}} \mathbb{P} \left(\hat{C}_r > \max_{k \in [p] \setminus \{r\}} \hat{C}_k \right) = 1.$$

□

In the following, we give the proofs of Lemma B.3 and B.4.

Proof. (Lemma B.3) We divide the proof into two parts. In the first part, we show some results that will be used later. In the second part, we prove the main result.

Part 1: Some results that will be used later.

For a sufficient permutation π , we have

$$\mathbb{E}[\tilde{\xi}(\pi)]_{\pi^{-1}(r)} = (L_{X^\pi}^{-1}(I - B^\pi)^{-1})_{\pi^{-1}(r), \pi^{-1}(r)} \delta_r := a \delta_r \xrightarrow{\delta_r \rightarrow \infty} \infty$$

and

$$\mathbb{E}[\tilde{\xi}(\pi)]_{\pi^{-1}(k)} = 0 \quad \text{for } k \in [p] \setminus \{r\}$$

by Theorem 3.1, where $a = (L_{X^\pi}^{-1}(I - B^\pi)^{-1})_{\pi^{-1}(r), \pi^{-1}(r)}$ does not depend on δ_r .

Part 1-1: Analyze the property of $\tilde{\xi}(\pi)_{\pi^{-1}(r)}$.

For any $\epsilon > 0$ and $M > 0$, let δ_r be large enough such that $\frac{|a\delta_r|}{2} \geq M$ and $\frac{4}{|a\delta_r|^2} \leq \epsilon$. Then,

$$\begin{aligned} \mathbb{P} \left(|\tilde{\xi}(\pi)_{\pi^{-1}(r)}| \geq M \right) &\geq \mathbb{P} \left(|\tilde{\xi}(\pi)_{\pi^{-1}(r)}| \geq \frac{|a\delta_r|}{2} \right) \\ &\geq \mathbb{P} \left(|\tilde{\xi}(\pi)_{\pi^{-1}(r)} - a\delta_r| \leq \frac{|a\delta_r|}{2} \right) \\ &\geq 1 - \frac{4}{|a\delta_r|^2} \\ &\geq 1 - \epsilon, \end{aligned} \quad (34)$$

where we used Chebyshev's inequality and the fact that $\Sigma_{\tilde{\xi}(\pi)} = I$ for the second last inequality.

Part 1-2: Analyze the property of $\max_{k \in [p] \setminus \{r\}} |\tilde{\xi}(\pi)_{\pi^{-1}(k)}|$.

For any $\epsilon > 0$, let $\tilde{M} \geq \sqrt{\frac{p-1}{\epsilon}} > 0$, so $\mathbb{P} \left(|\tilde{\xi}(\pi)_{\pi^{-1}(k)}| \geq \tilde{M} \right) \leq \frac{1}{\tilde{M}^2} \leq \frac{\epsilon}{p-1}$ by Chebyshev's inequality. Therefore, by the union bound, we have

$$\mathbb{P} \left(\max_{k \in [p] \setminus \{r\}} |\tilde{\xi}(\pi)_{\pi^{-1}(k)}| < \tilde{M} \right) \geq 1 - \epsilon. \quad (35)$$

Part 2: Prove the main results.

Part 2-1: Prove $\tilde{u}(\pi) \xrightarrow[\delta_r \rightarrow \infty]{p} r$ by definition.

For any $\epsilon > 0$, taking $\widetilde{M} \geq \sqrt{\frac{p-1}{\epsilon}}$ and δ_r large enough such that $\frac{|a\delta_r|}{2} \geq \widetilde{M}$ and $\frac{4}{|a\delta_r|^2} \leq \epsilon$. Then by (34) and (35), we have

$$\begin{aligned}
\mathbb{P}(\tilde{u}(\pi) = r) &= \mathbb{P}\left(\pi(\operatorname{argmax}_{j \in [p]} |\tilde{\xi}(\pi)|_j) = r\right) \\
&= \mathbb{P}\left(|\tilde{\xi}(\pi)_{\pi^{-1}(r)}| > \max_{k \in [p] \setminus \{r\}} |\tilde{\xi}(\pi)_{\pi^{-1}(k)}|\right) \\
&\geq \mathbb{P}\left(|\tilde{\xi}(\pi)_{\pi^{-1}(r)}| \geq \widetilde{M}, \max_{k \in [p] \setminus \{r\}} |\tilde{\xi}(\pi)_{\pi^{-1}(k)}| < \widetilde{M}\right) \\
&\geq \mathbb{P}\left(|\tilde{\xi}(\pi)_{\pi^{-1}(r)}| \geq \widetilde{M}\right) + \mathbb{P}\left(\max_{k \in [p] \setminus \{r\}} |\tilde{\xi}(\pi)_{\pi^{-1}(k)}| < \widetilde{M}\right) - 1 \\
&\geq 1 - 2\epsilon,
\end{aligned}$$

which means that

$$\tilde{u}(\pi) \xrightarrow[\delta_r \rightarrow \infty]{p} r. \quad (36)$$

Part 2-2: Prove $\tilde{c}(\pi) \xrightarrow[\delta_r \rightarrow \infty]{p} \infty$ by definition.

For any $\epsilon > 0$ and $M > 0$, taking $\widetilde{M} \geq \sqrt{\frac{p-1}{\epsilon}}$ and δ_r large enough such that $\frac{|a\delta_r|}{2} \geq M\widetilde{M} + \widetilde{M}$ and $\frac{4}{|a\delta_r|^2} \leq \epsilon$. Then, by (34), (35) and (36), we have

$$\begin{aligned}
\mathbb{P}(\tilde{c}(\pi) \geq M) &= \mathbb{P}\left(\frac{|\tilde{\xi}(\pi)|_{(1)} - |\tilde{\xi}(\pi)|_{(2)}}{|\tilde{\xi}(\pi)|_{(2)}} \geq M\right) \\
&\geq \mathbb{P}\left(\frac{|\tilde{\xi}(\pi)_{\pi^{-1}(r)}| - \widetilde{M}}{\widetilde{M}} \geq M, \max_{k \in [p] \setminus \{r\}} |\tilde{\xi}(\pi)_{\pi^{-1}(k)}| < \widetilde{M}, \tilde{u}(\pi) = r\right) \\
&\geq \mathbb{P}\left(|\tilde{\xi}(\pi)_{\pi^{-1}(r)}| \geq M\widetilde{M} + \widetilde{M}\right) + \mathbb{P}\left(\max_{k \in [p] \setminus \{r\}} |\tilde{\xi}(\pi)_{\pi^{-1}(k)}| < \widetilde{M}\right) + \mathbb{P}(\tilde{u}(\pi) = r) - 2 \\
&\geq 1 - 4\epsilon,
\end{aligned}$$

which means that $\tilde{c}(\pi) \xrightarrow[\delta_r \rightarrow \infty]{p} \infty$. □

Proof. (Lemma B.4) For an insufficient permutation π , by Theorem 3.1, there must exist a set $F^\pi \subseteq [p]$ with $|F^\pi| \geq 2$ such that

$$\mathbb{E}[\tilde{\xi}(\pi)]_j = (L_{X^\pi}^{-1}(I - B^\pi)^{-1})_{j, \pi^{-1}(r)} \delta_r \xrightarrow[\delta_r \rightarrow \infty]{} \infty \quad \text{for } j \in F^\pi$$

and

$$\mathbb{E}[\tilde{\xi}(\pi)]_k = 0 \quad \text{for } k \notin F^\pi.$$

Therefore, by using similar arguments based on Chebyshev's inequality and the union bound as in the Part 1 of the proof of Lemma B.3, we have

$$\begin{aligned}
& \lim_{\delta_r \rightarrow \infty} \mathbb{P} \left(\text{the largest and second largest elements of } |\tilde{\xi}(\pi)| \text{ are both in } F^\pi \right) \\
& \geq \lim_{\delta_r \rightarrow \infty} \mathbb{P} \left(\min_{j \in F^\pi} |\tilde{\xi}(\pi)_j| > \max_{k \notin F^\pi} |\tilde{\xi}(\pi)_k| \right) \\
& = 1.
\end{aligned} \tag{37}$$

In particular, the above holds trivially in the case of $F^\pi = [p]$.

Then, denote

$$\tilde{\xi}(\pi) = L_{X^\pi}^{-1}((I - B^\pi)^{-1}(b^\pi + \varepsilon^\pi) - \mu_{X^\pi}) + L_{X^\pi}^{-1}(I - B^\pi)^{-1}\delta^\pi := u + \delta_r v,$$

where $u = L_{X^\pi}^{-1}((I - B^\pi)^{-1}(b^\pi + \varepsilon^\pi) - \mu_{X^\pi})$ is a random vector and $v = L_{X^\pi}^{-1}(I - B^\pi)^{-1}\delta^\pi/\delta_r$ is a deterministic vector whose support is F^π . Note that both terms do not depend on δ_r . Hence, for any $i, j \in F^\pi$,

$$\frac{|\tilde{\xi}(\pi)_i| - |\tilde{\xi}(\pi)_j|}{|\tilde{\xi}(\pi)_j|} = \frac{|u_i + \delta_r v_i| - |u_j + \delta_r v_j|}{|u_j + \delta_r v_j|} \xrightarrow[\delta_r \rightarrow \infty]{p} \frac{|v_i| - |v_j|}{|v_j|}. \tag{38}$$

Let

$$C = \max_{\pi \text{ is insufficient}} \max_{i, j \in F^\pi} \frac{|v_i| - |v_j|}{|v_j|} + 1.$$

Because of (38), we have

$$\lim_{\delta_r \rightarrow \infty} \mathbb{P} \left(\frac{|\tilde{\xi}(\pi)_i| - |\tilde{\xi}(\pi)_j|}{|\tilde{\xi}(\pi)_j|} \geq C \right) = 0$$

by definition. Then, since

$$\begin{aligned}
& \mathbb{P} \left(\max_{i, j \in F^\pi} \frac{|\tilde{\xi}(\pi)_i| - |\tilde{\xi}(\pi)_j|}{|\tilde{\xi}(\pi)_j|} \geq C \right) \\
& = \mathbb{P} \left(\bigcup_{i, j \in F^\pi} \left\{ \frac{|\tilde{\xi}(\pi)_i| - |\tilde{\xi}(\pi)_j|}{|\tilde{\xi}(\pi)_j|} \geq C \right\} \right) \\
& \leq \sum_{i, j \in F^\pi} \mathbb{P} \left(\frac{|\tilde{\xi}(\pi)_i| - |\tilde{\xi}(\pi)_j|}{|\tilde{\xi}(\pi)_j|} \geq C \right),
\end{aligned}$$

we have

$$\lim_{\delta_r \rightarrow \infty} \mathbb{P} \left(\max_{i, j \in F^\pi} \frac{|\tilde{\xi}(\pi)_i| - |\tilde{\xi}(\pi)_j|}{|\tilde{\xi}(\pi)_j|} < C \right) = 1. \tag{39}$$

Finally, because

$$\begin{aligned}
& \mathbb{P}(\tilde{c}(\pi) < C) \\
&= \mathbb{P}\left(\frac{|\tilde{\xi}(\pi)|_{(1)} - |\tilde{\xi}(\pi)|_{(2)}}{|\tilde{\xi}(\pi)|_{(2)}} < C\right) \\
&\geq \mathbb{P}\left(\text{the largest and second largest elements of } |\tilde{\xi}(\pi)| \text{ are both in } F^\pi, \max_{i,j \in F^\pi} \frac{|\tilde{\xi}(\pi)_i| - |\tilde{\xi}(\pi)_j|}{|\tilde{\xi}(\pi)_j|} < C\right) \\
&\geq \mathbb{P}\left(\text{the largest and second largest elements of } |\tilde{\xi}(\pi)| \text{ are both in } F^\pi\right) \\
&\quad + \mathbb{P}\left(\max_{i,j \in F^\pi} \frac{|\tilde{\xi}(\pi)_i| - |\tilde{\xi}(\pi)_j|}{|\tilde{\xi}(\pi)_j|} < C\right) - 1,
\end{aligned}$$

we have $\lim_{\delta_r \rightarrow \infty} \mathbb{P}(\tilde{c}(\pi) < C) = 1$ by (37) and (39). \square

C Supplementary materials for simulations

C.1 Simulation results illustrating the effect of v in Algorithm 2

We illustrate the benefit of using a large number of random permutations v in Algorithm 2 through a simulation.

We consider a setup with a random DAG and uniform errors following the distribution $U(-5, 5)$, as described in Section 4.1. The number of variables is $p = 50$, the sample size is $n = 200$, the intervention strength is $\delta_r = 8$, and the sparsity level is $s = 0.4$. We generate $m = 1000$ interventional samples (see Section 4.1 for more details) and apply Algorithm 2 with $v = 1$ and $v = 10$ to these samples.

The CDFs of the root cause rank of these two methods (see Section 4.3 for more details) are shown in Figure 10 (a). We can see that using $v = 10$ yields better results than using $v = 1$.

We investigate the results a bit more closely. Among the 1000 interventional samples, the root cause ranks differ between $v = 1$ and $v = 10$ in 589 samples. We then calculate the rank difference between $v = 1$ and $v = 10$ for these 589 samples. A large positive difference indicates that using $v = 1$ yields a much worse rank than using $v = 10$, while a small negative difference suggests the opposite. Figure 10 (b) shows the histogram of the rank differences, which is clearly right-skewed, indicating that it is more likely to obtain a much worse score with $v = 1$ than with $v = 10$. For example, there are 29 samples where the rank difference exceeds 20, but only one sample where the rank difference is less than -20 . This is largely due to the fact that using only one permutation leads to more cases where the root cause lies outside \hat{U} , resulting in a lower score. In particular, when using $v = 1$, the root cause lies outside \hat{U} in 195 samples, while this happens in 87 samples when using $v = 10$.

C.2 More simulation results for Section 4.3

The simulation results for the hub DAG with Gaussian errors, the random DAG with uniform errors and the random DAG with Gaussian errors are shown in Figures 11, 12 and 13, respectively. The results and information in these plots are similar to those in Figure 4; see Section 4.3 for related discussions.

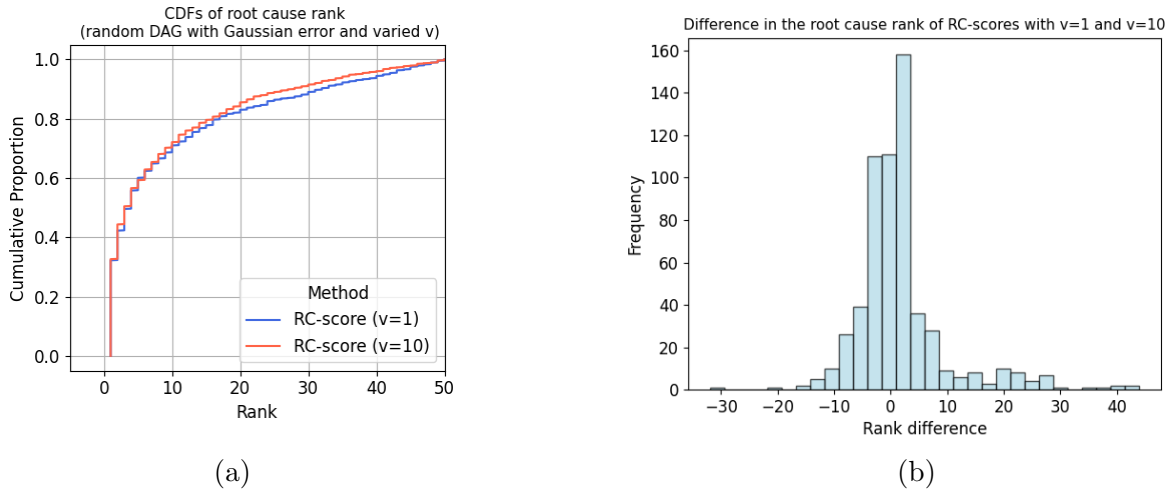


Figure 10: (a) CDFs of the root cause ranks using the RC-score with $v = 1$ and $v = 10$ in the setting with a random DAG and uniform errors. (b) Histogram of the differences in the root cause ranks between $v = 1$ and $v = 10$ for the 589 samples for which these two methods lead to different ranks for the root cause.

C.3 The optimal thresholds for the LiNGAM-opt approach

In Figure 14 and 15, we show the optimal thresholds used in the LiNGAM-opt approach for hub and random DAGs, respectively. We observe that the optimal thresholds vary significantly across the 1000 interventional samples in each setting, indicating that no single fixed optimal threshold exists.

C.4 Score plots for all patients in real applications

We show the raw transformed gene expression levels, squared z-scores, and RC-scores of genes for all 58 patients in Figures 16, 17, 18, 19, 20, 21, 22, 23, 24, 25, 26, and 27.

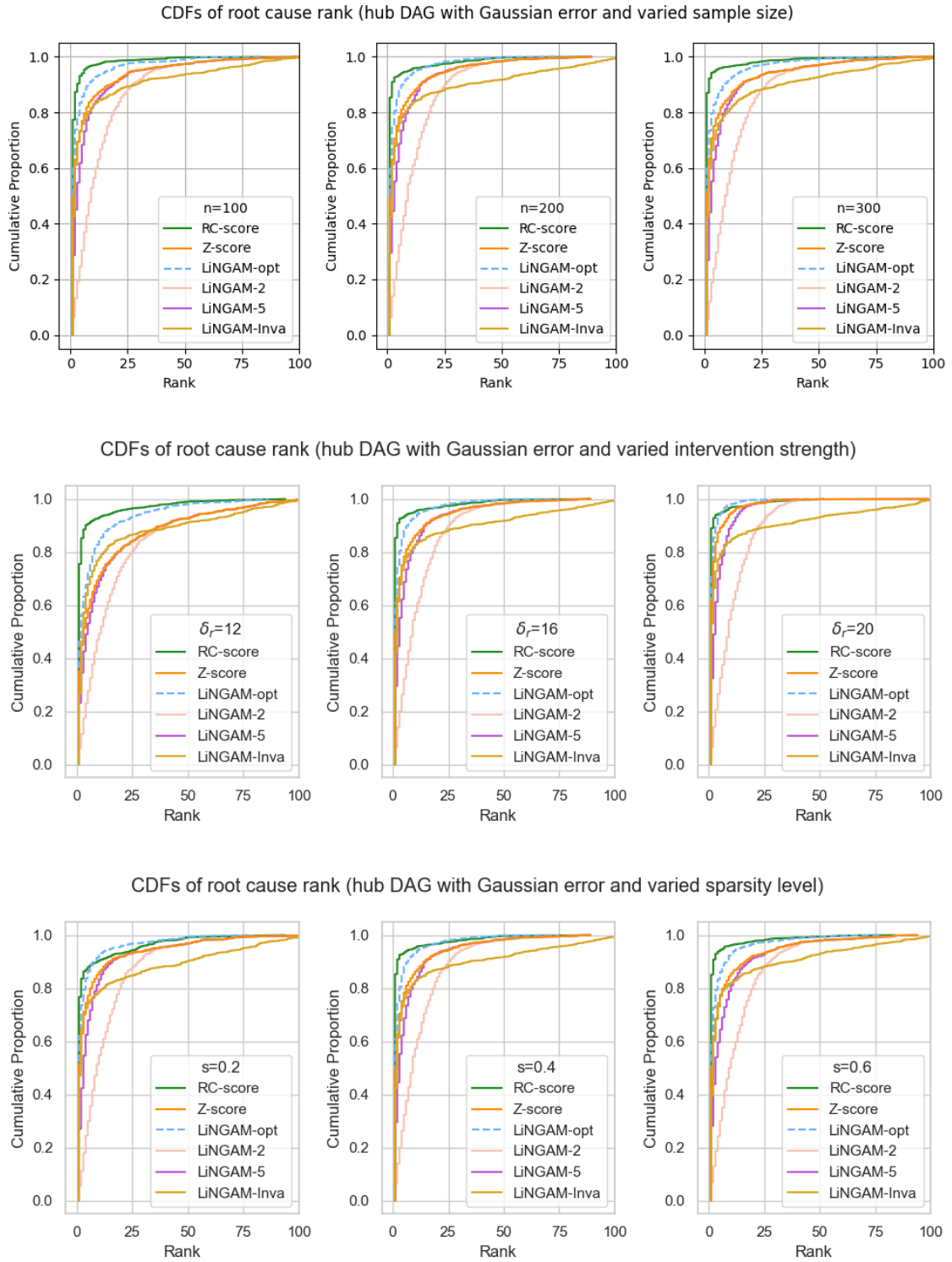


Figure 11: CDFs of the root cause rank using the squared z-score, RC-score, and LiNGAM-based approaches in the setting with a hub DAG and Gaussian errors. The top, middle, and bottom plots display results for varying sample sizes, intervention strengths, and sparsity levels, respectively.

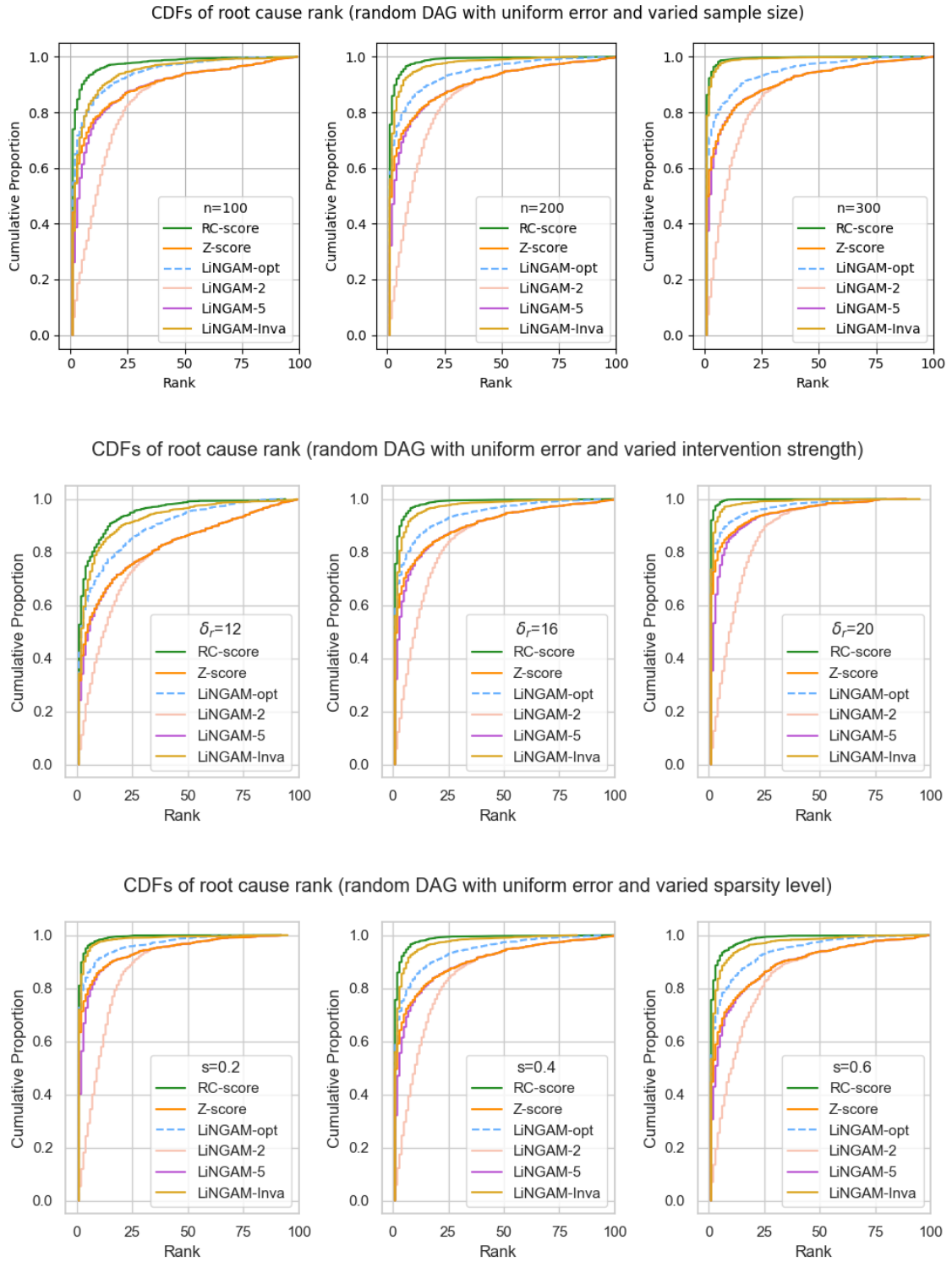


Figure 12: CDFs of the root cause rank using the squared z-score, RC-score, and LiNGAM-based approaches in the setting with a random DAG and uniform errors. The top, middle, and bottom plots display results for varying sample sizes, intervention strengths, and sparsity levels, respectively.

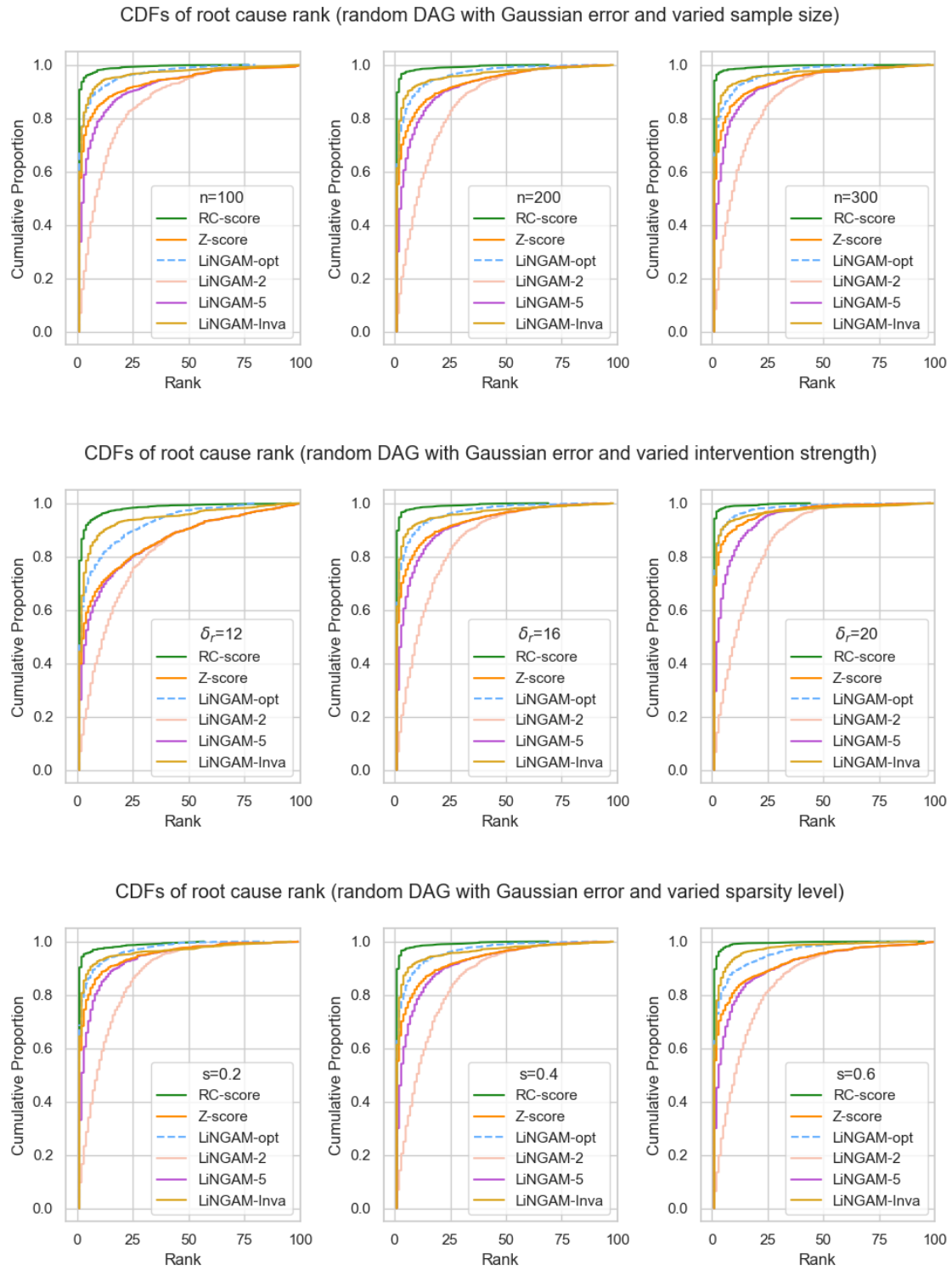


Figure 13: CDFs of the root cause rank using the squared z-score, RC-score, and LiNGAM-based approaches in the setting with a random DAG and Gaussian errors. The top, middle, and bottom plots display results for varying sample sizes, intervention strengths, and sparsity levels, respectively.

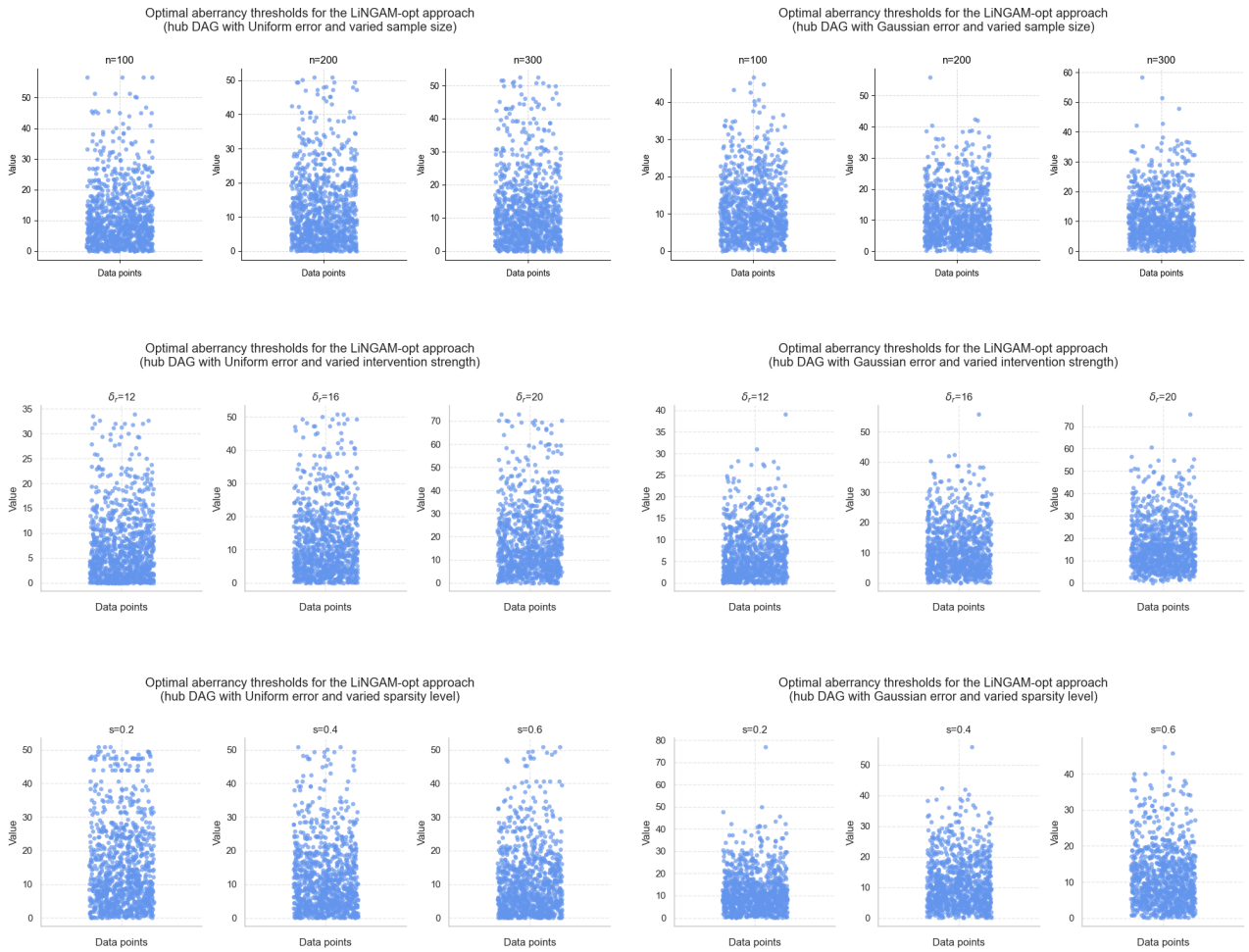


Figure 14: The optimal thresholds used in the LiNGAM-opt approach for simulation settings with hub DAG. The error types are described in the subtitle of each plot.

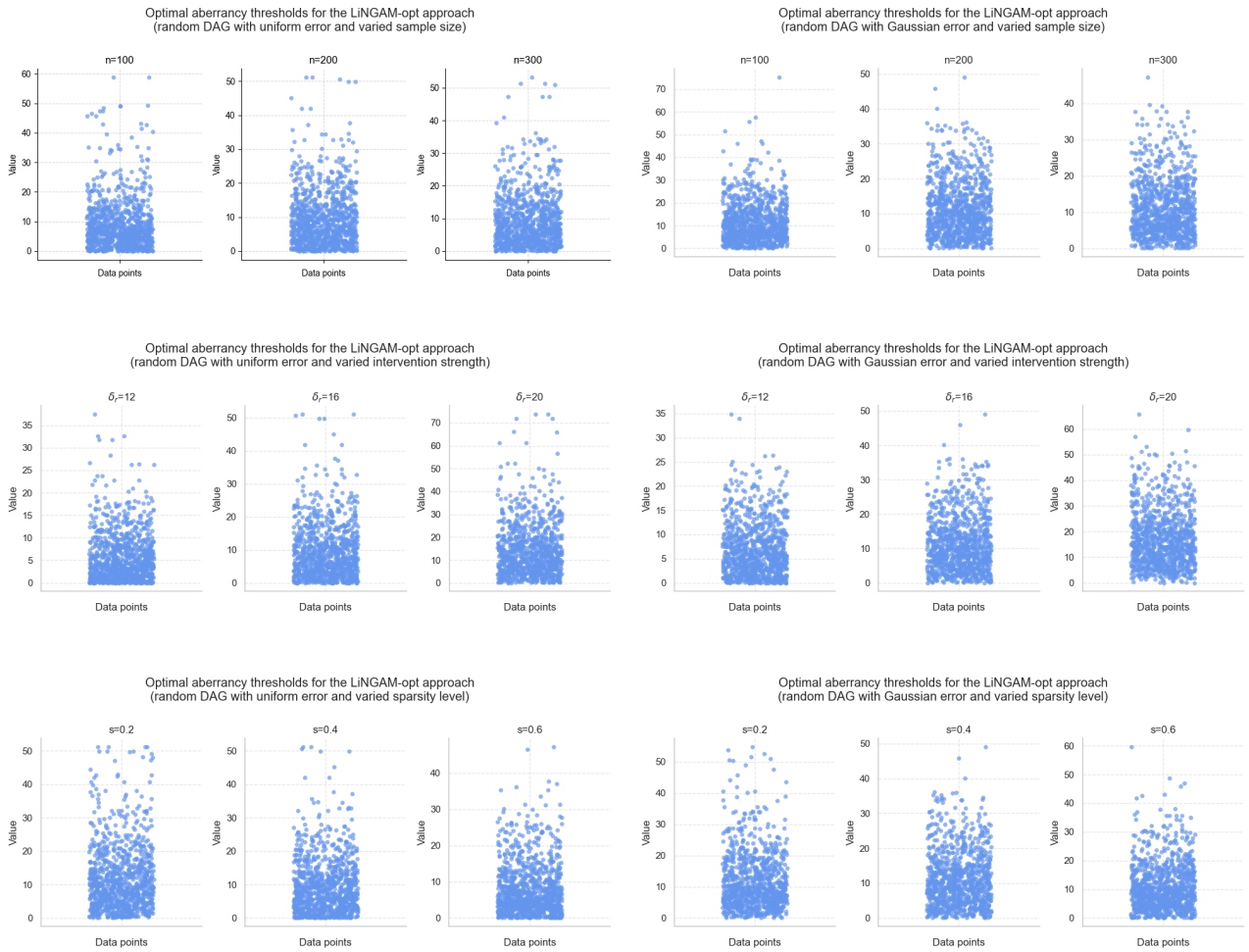


Figure 15: The optimal thresholds used in the LiNGAM-opt approach for simulation settings with random DAG. The error types are described in the subtitle of each plot.

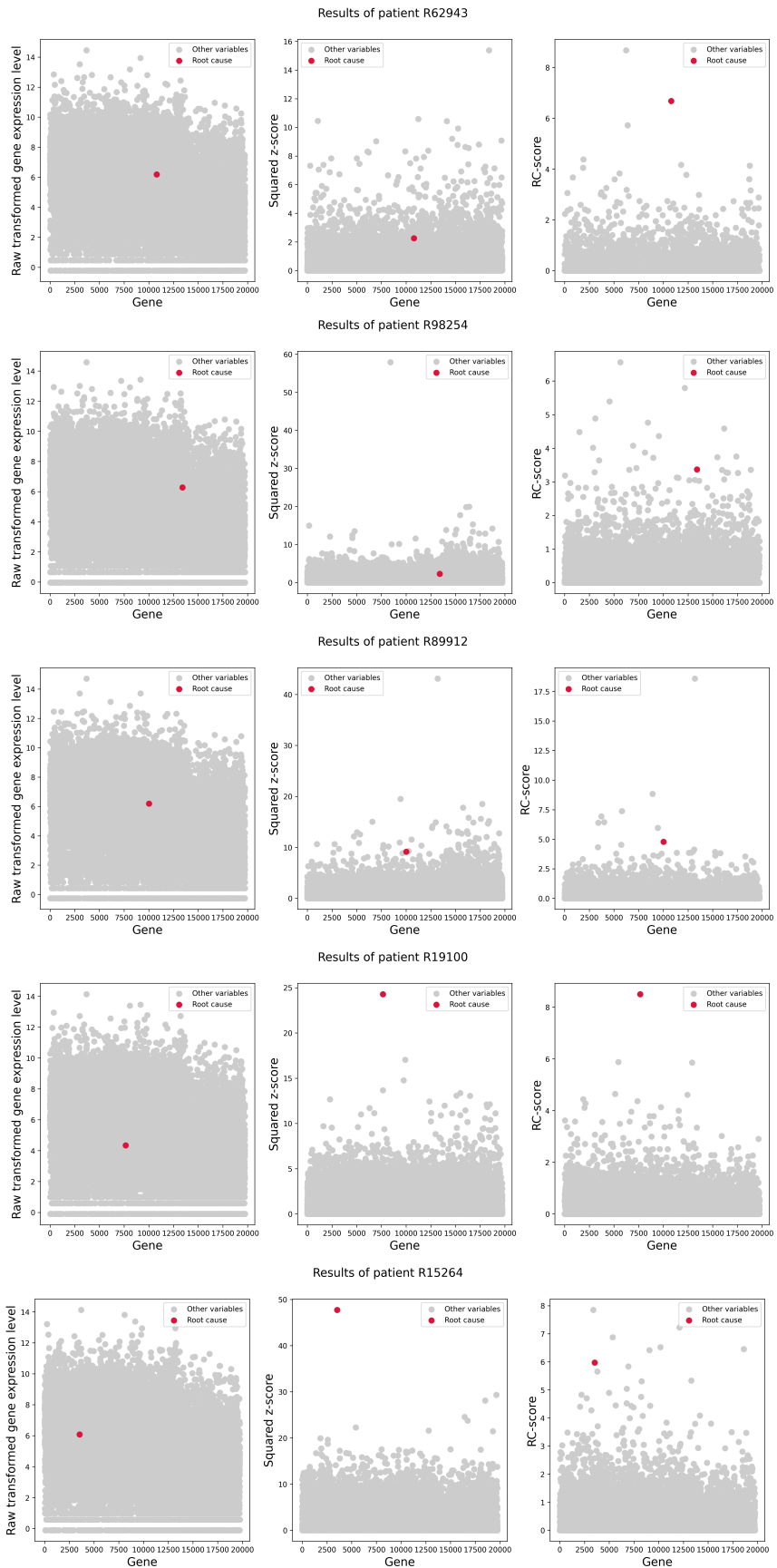


Figure 16: The raw transformed gene expression levels, squared z-scores, and RC-scores of genes for patients *R62943*, *R98254*, *R89912*, *R19100*, and *R15264*.

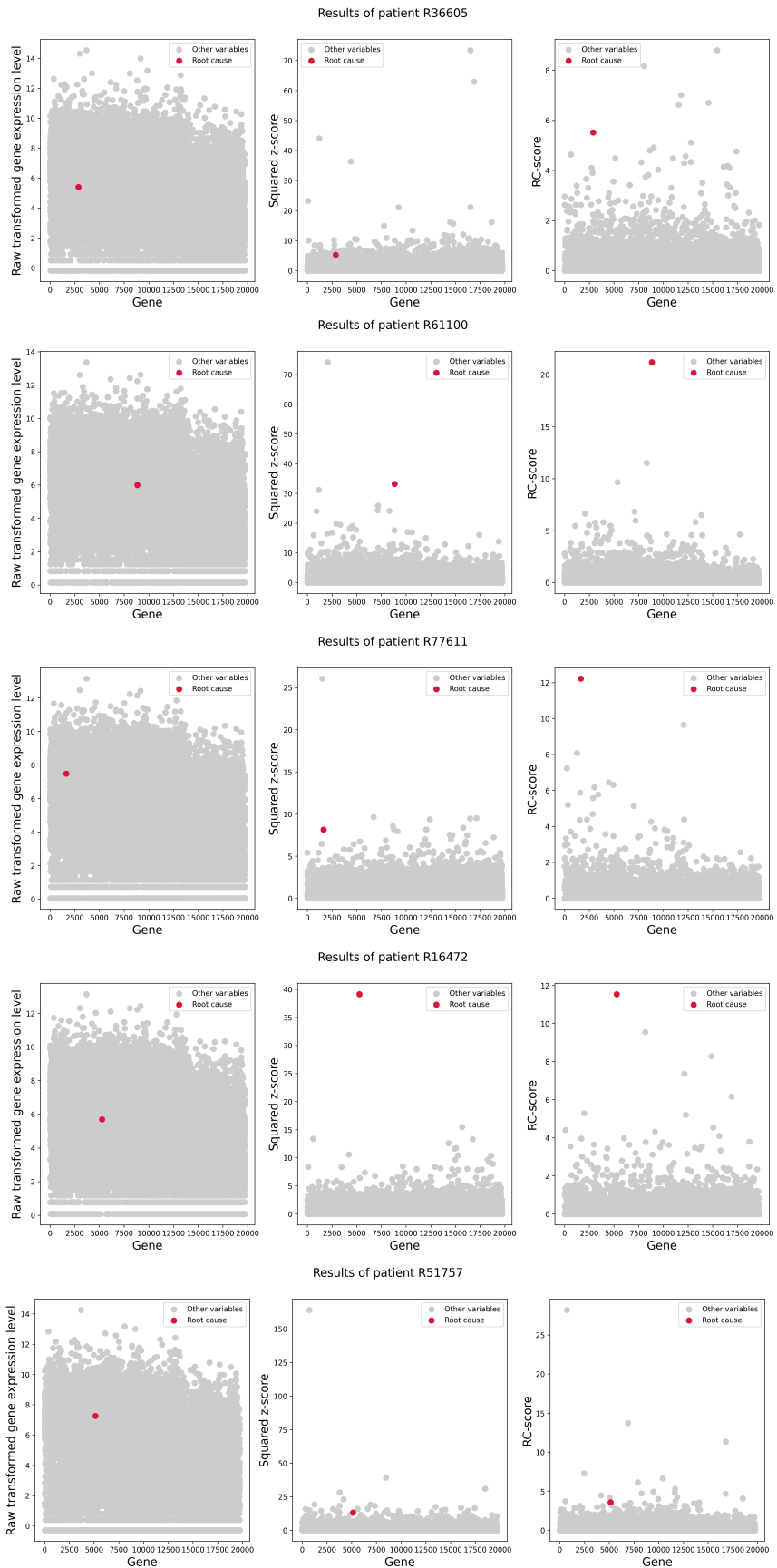


Figure 17: The raw transformed gene expression levels, squared z-scores, and RC-scores of genes for patients $R36605$, $R61100$, $R77611$, $R16472$, and $R51757$.

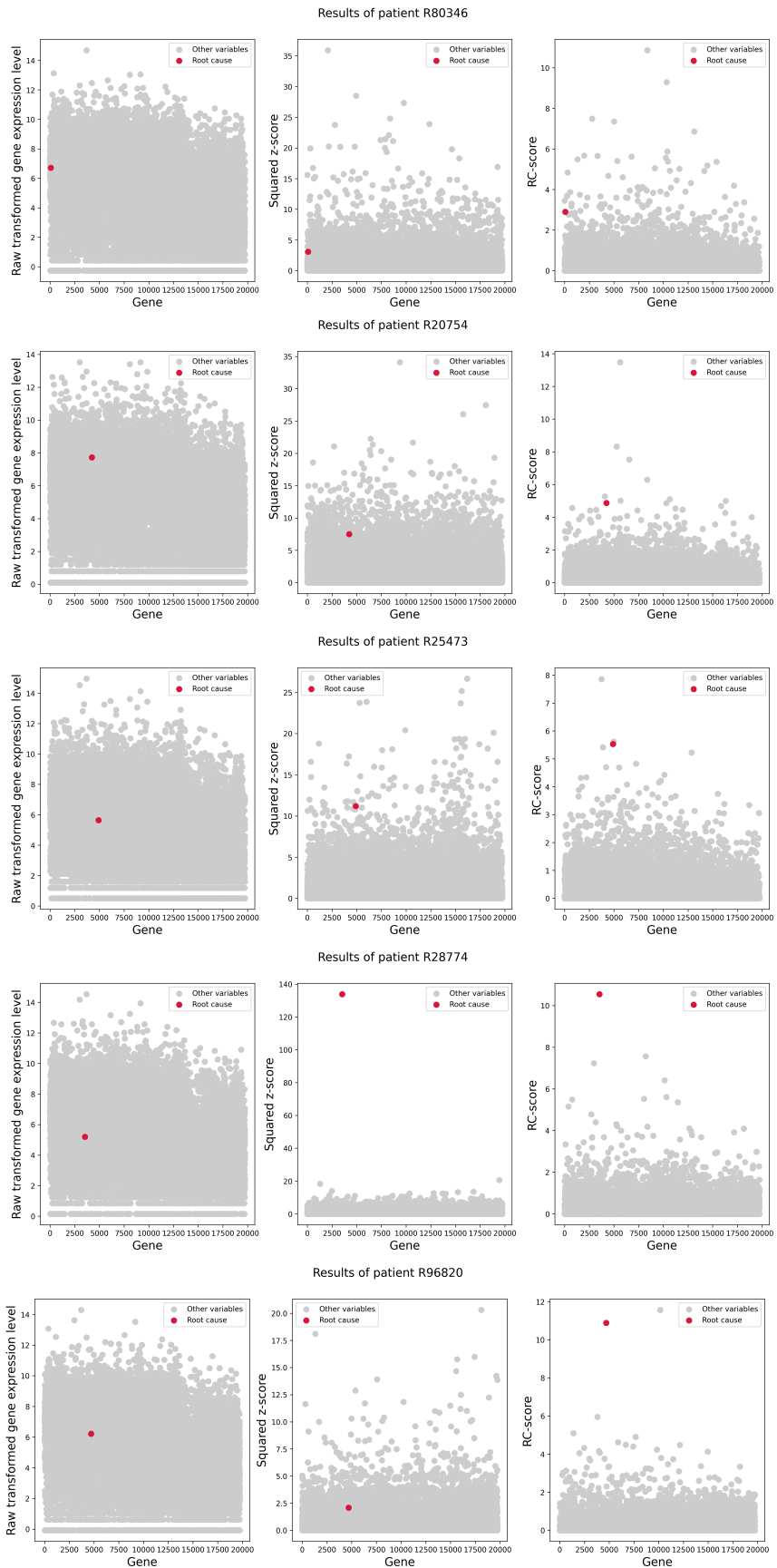


Figure 18: The raw transformed gene expression levels, squared z-scores, and RC-scores of genes for patients *R80346*, *R20754*, *R25473*, *R28774*, and *R96820*.

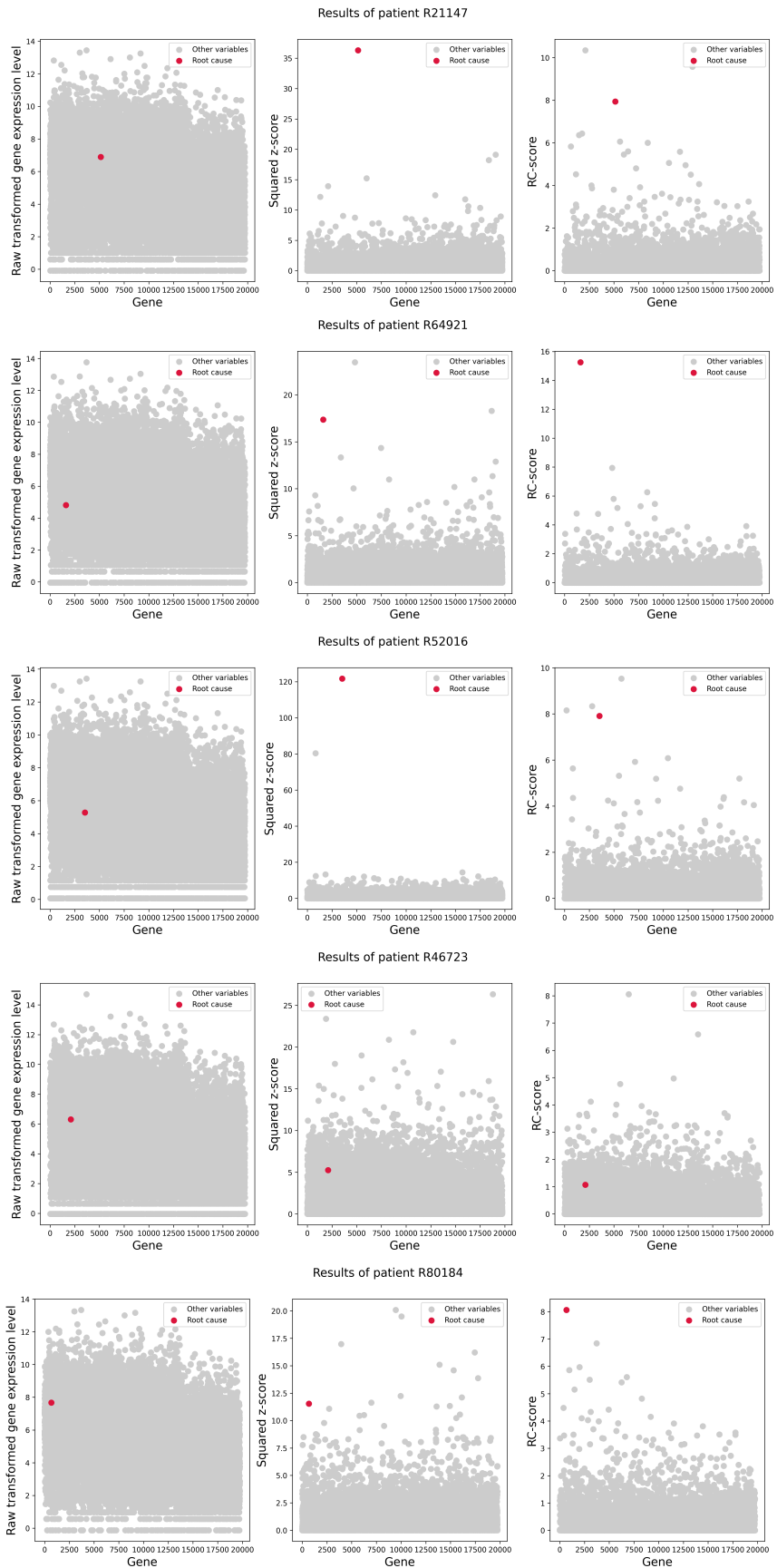


Figure 19: The raw transformed gene expression levels, squared z-scores, and RC-scores of genes for patients $R21147$, $R64921$, $R52016$, $R46723$, and $R80184$.

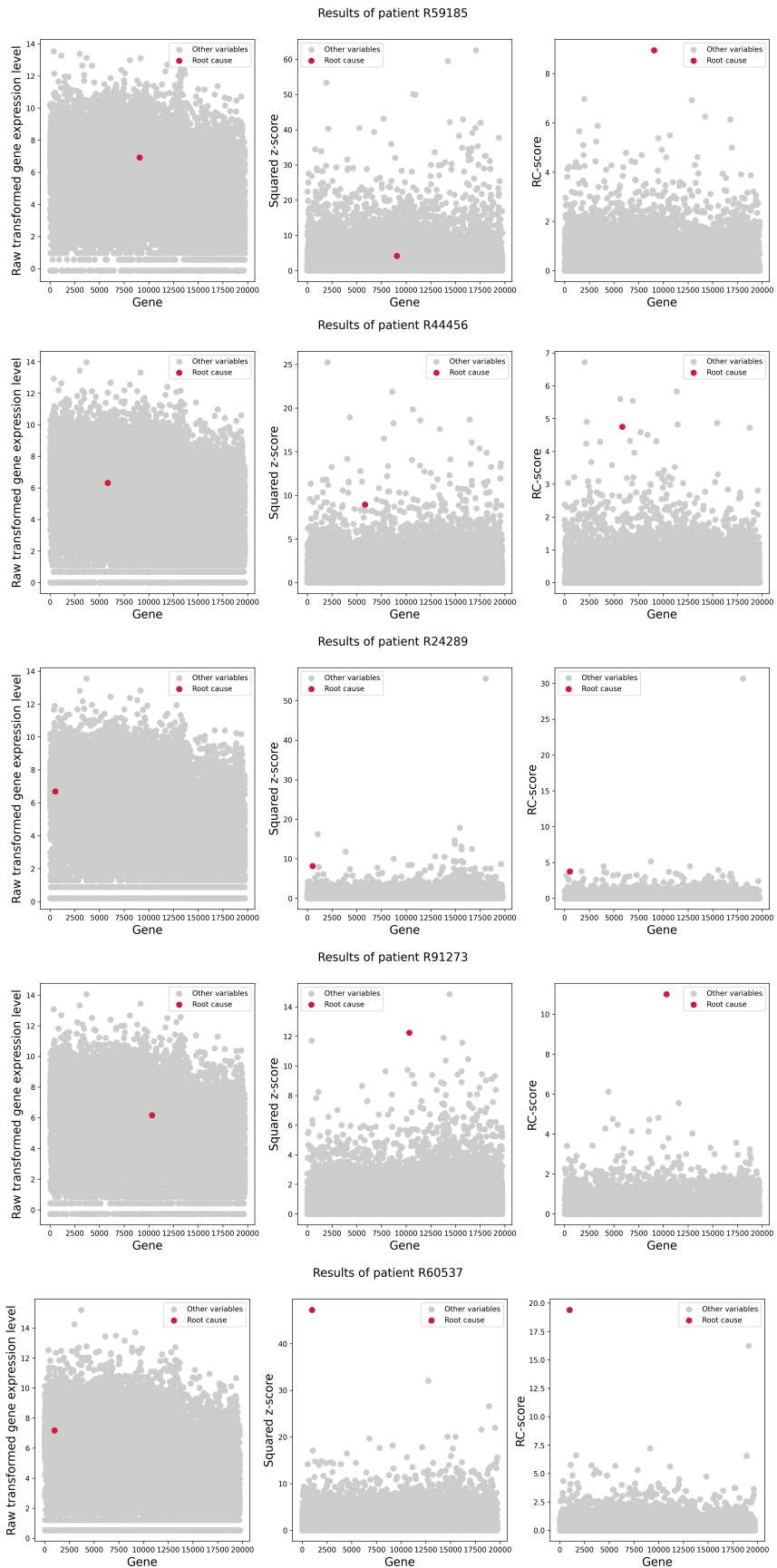


Figure 20: The raw transformed gene expression levels, squared z-scores, and RC-scores of genes for patients $R59185$, $R44456$, $R24289$, $R91273$, and $R60537$.

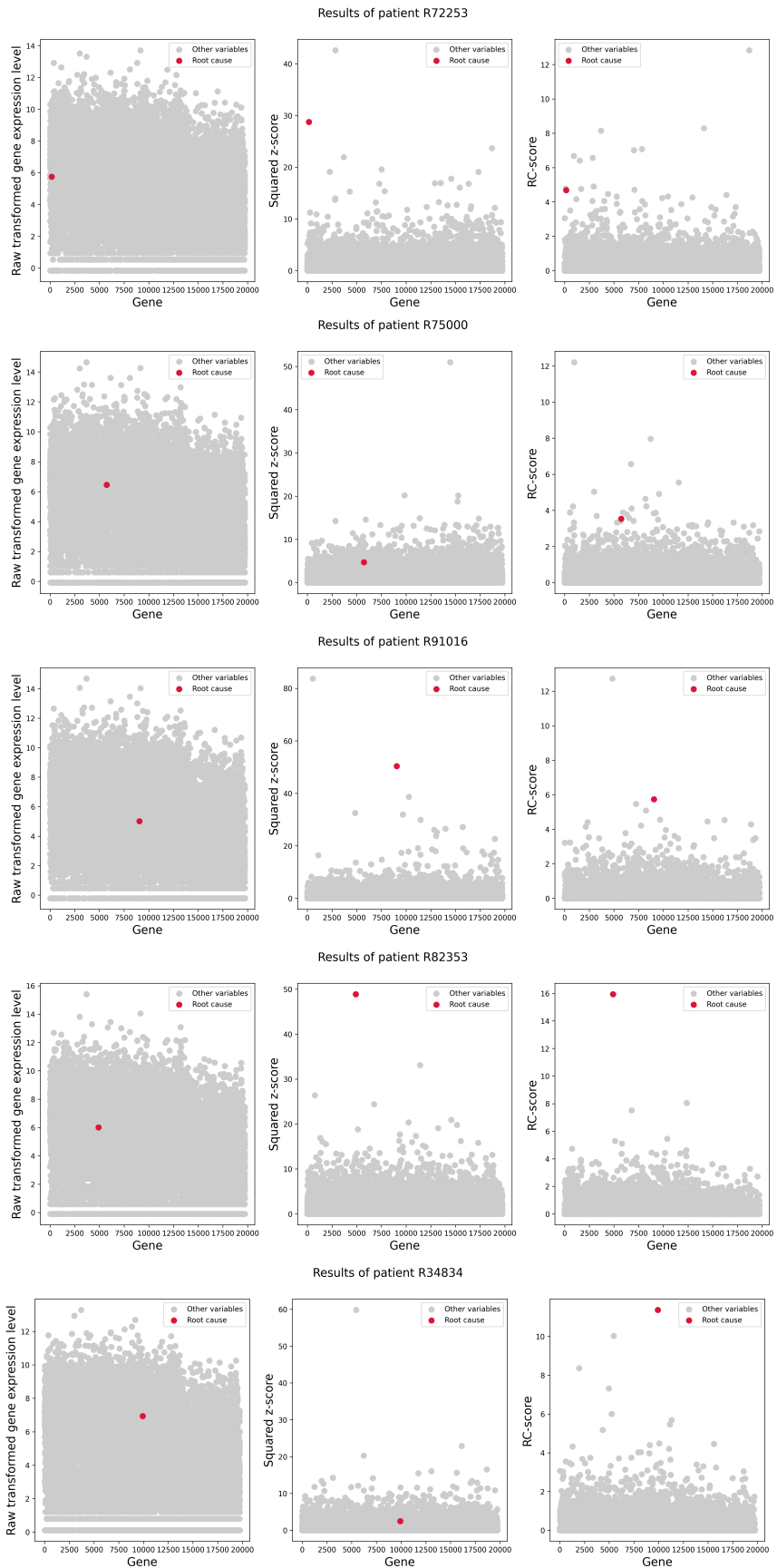


Figure 21: The raw transformed gene expression levels, squared z-scores, and RC-scores of genes for patients *R72253*, *R75000*, *R91016*, *R82353*, and *R34834*.

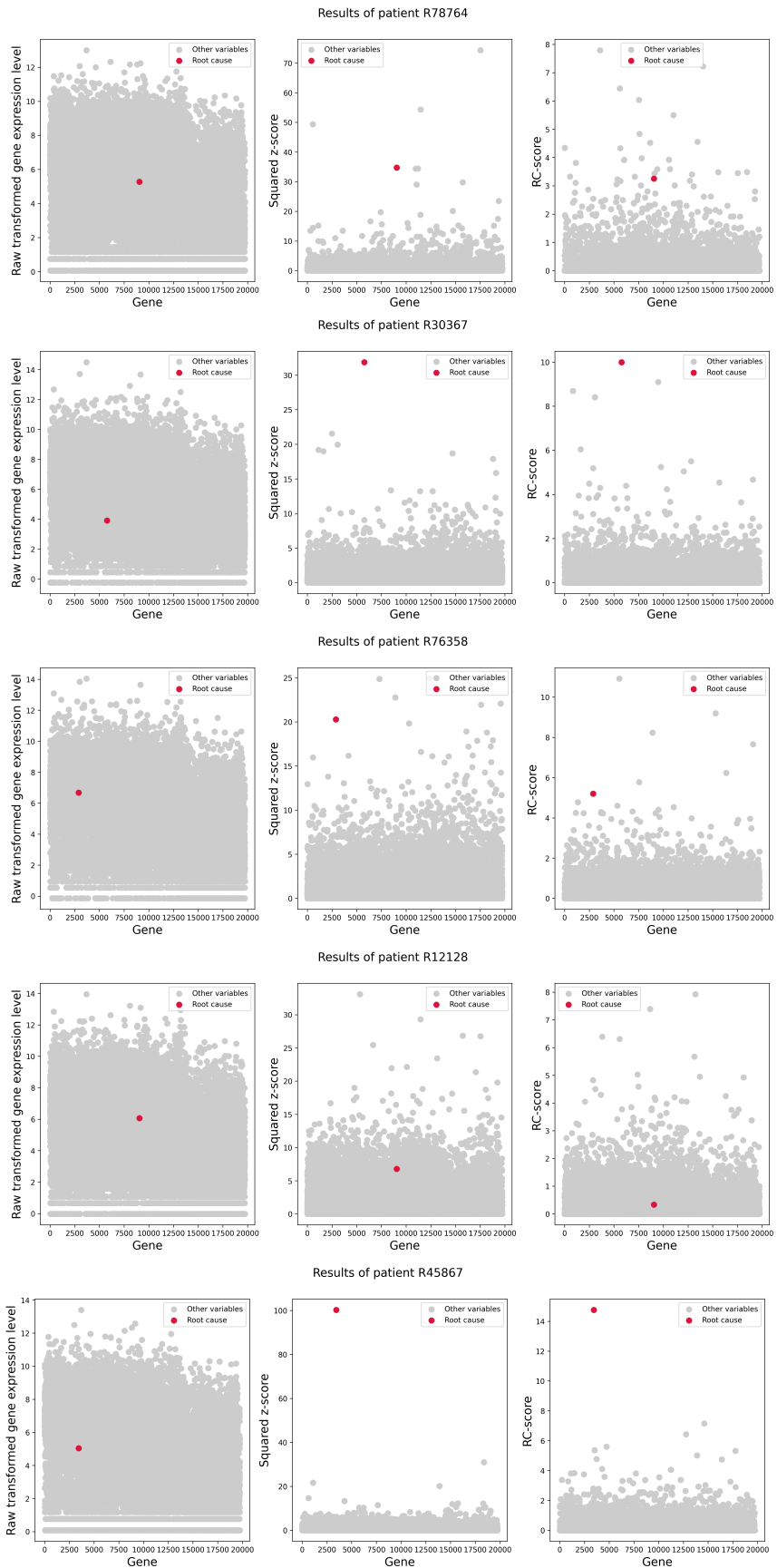


Figure 22: The raw transformed gene expression levels, squared z-scores, and RC-scores of genes for patients *R78764*, *R30367*, *R76358*, *R12128*, and *R45867*.

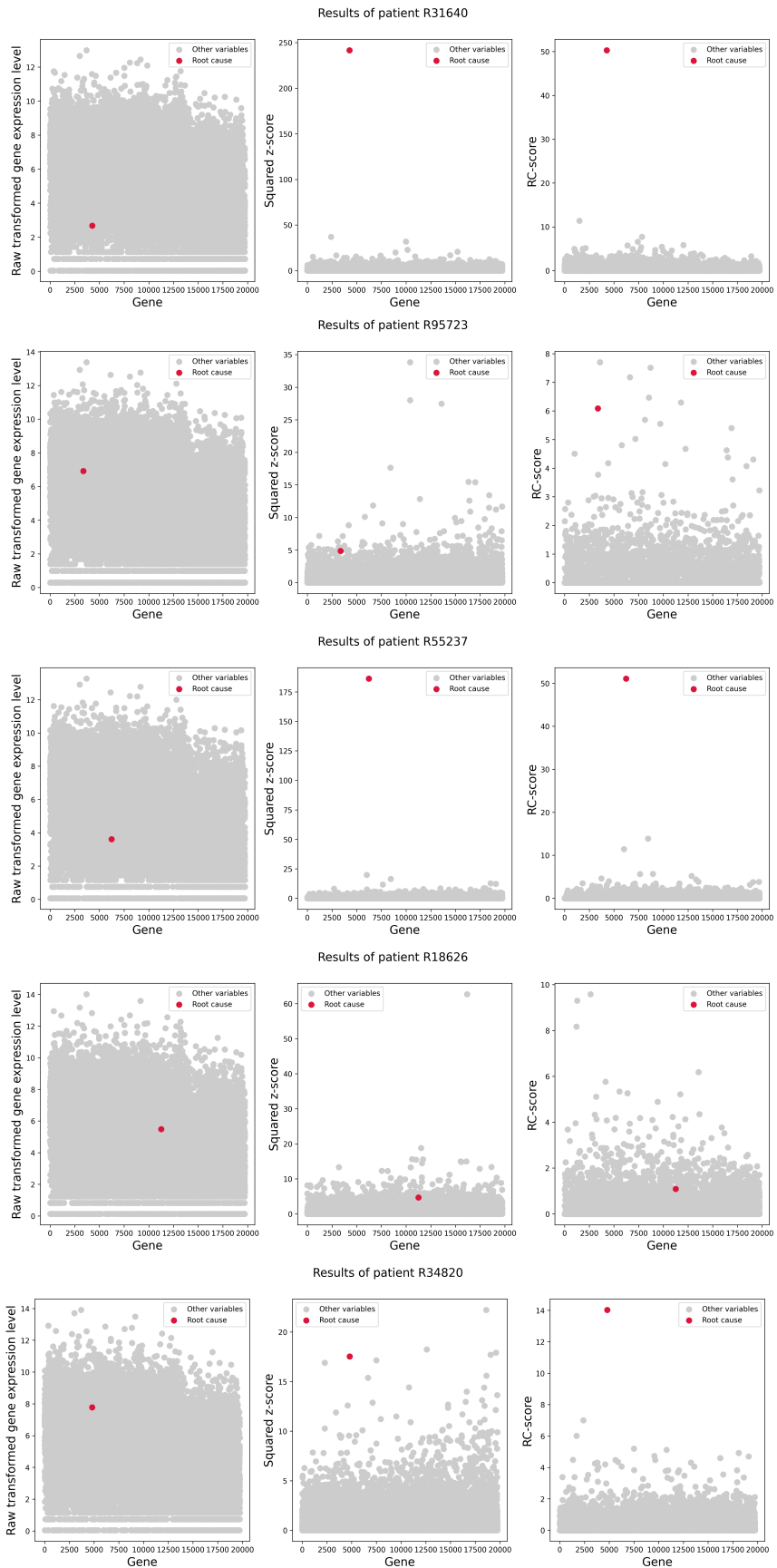


Figure 23: The raw transformed gene expression levels, squared z-scores, and RC-scores of genes for patients *R31640*, *R95723*, *R55237*, *R18626*, and *R34820*.

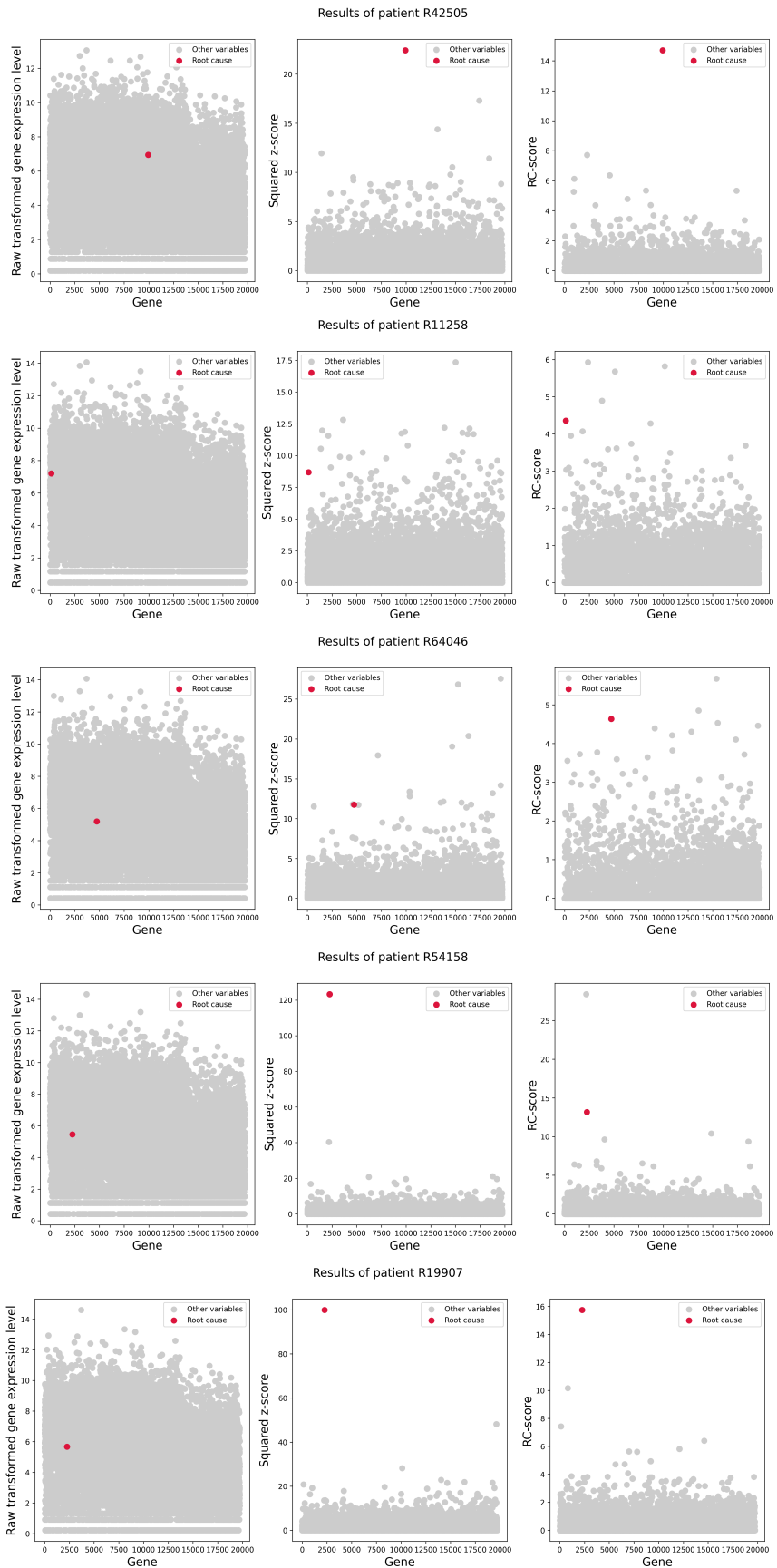


Figure 24: The raw transformed gene expression levels, squared z-scores, and RC-scores of genes for patients *R42505*, *R11258*, *R64046*, *R54158*, and *R19907*.

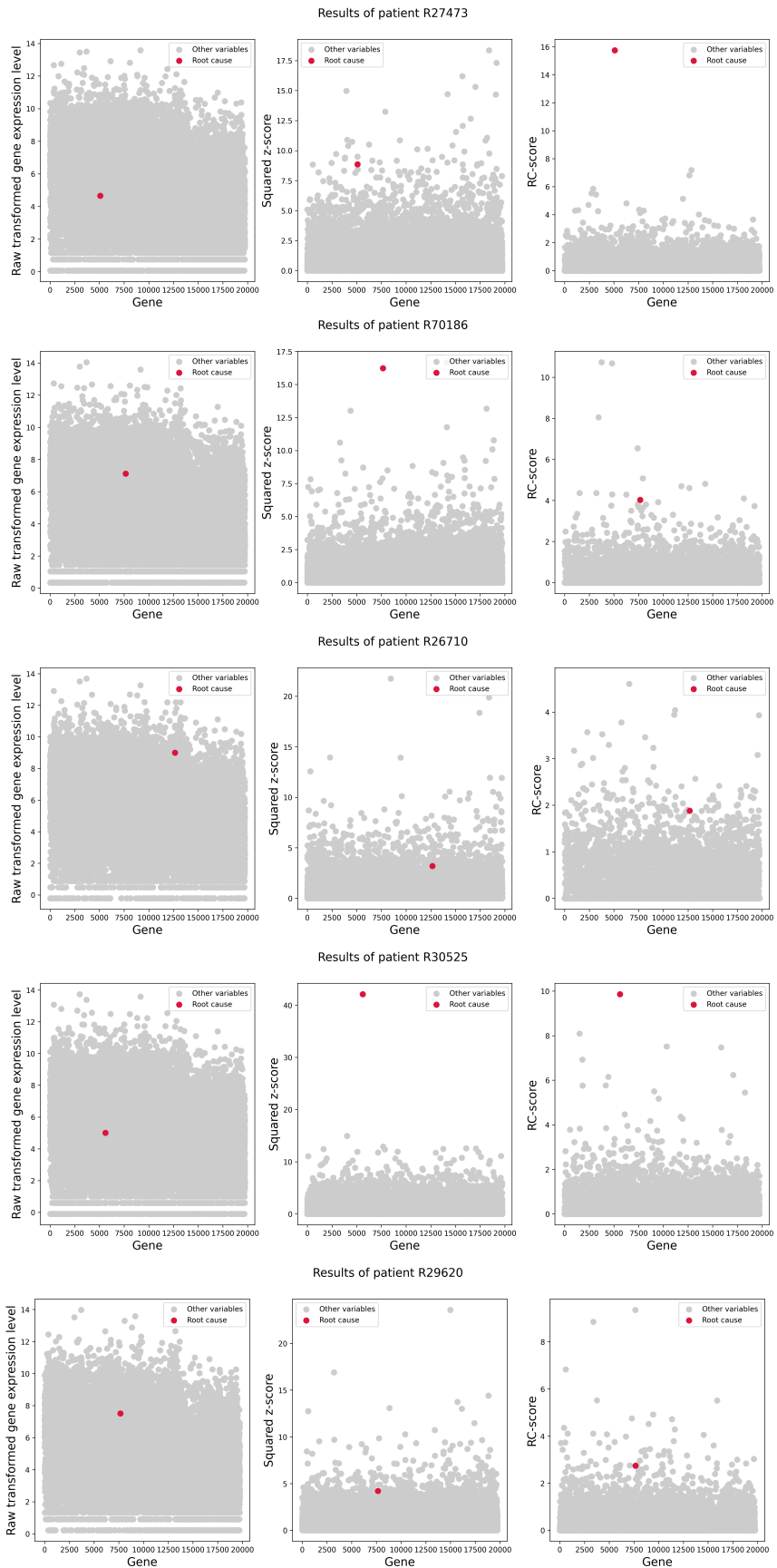


Figure 25: The raw transformed gene expression levels, squared z-scores, and RC-scores of genes for patients *R27473*, *R70186*, *R26710*, *R30525*, and *R29620*.

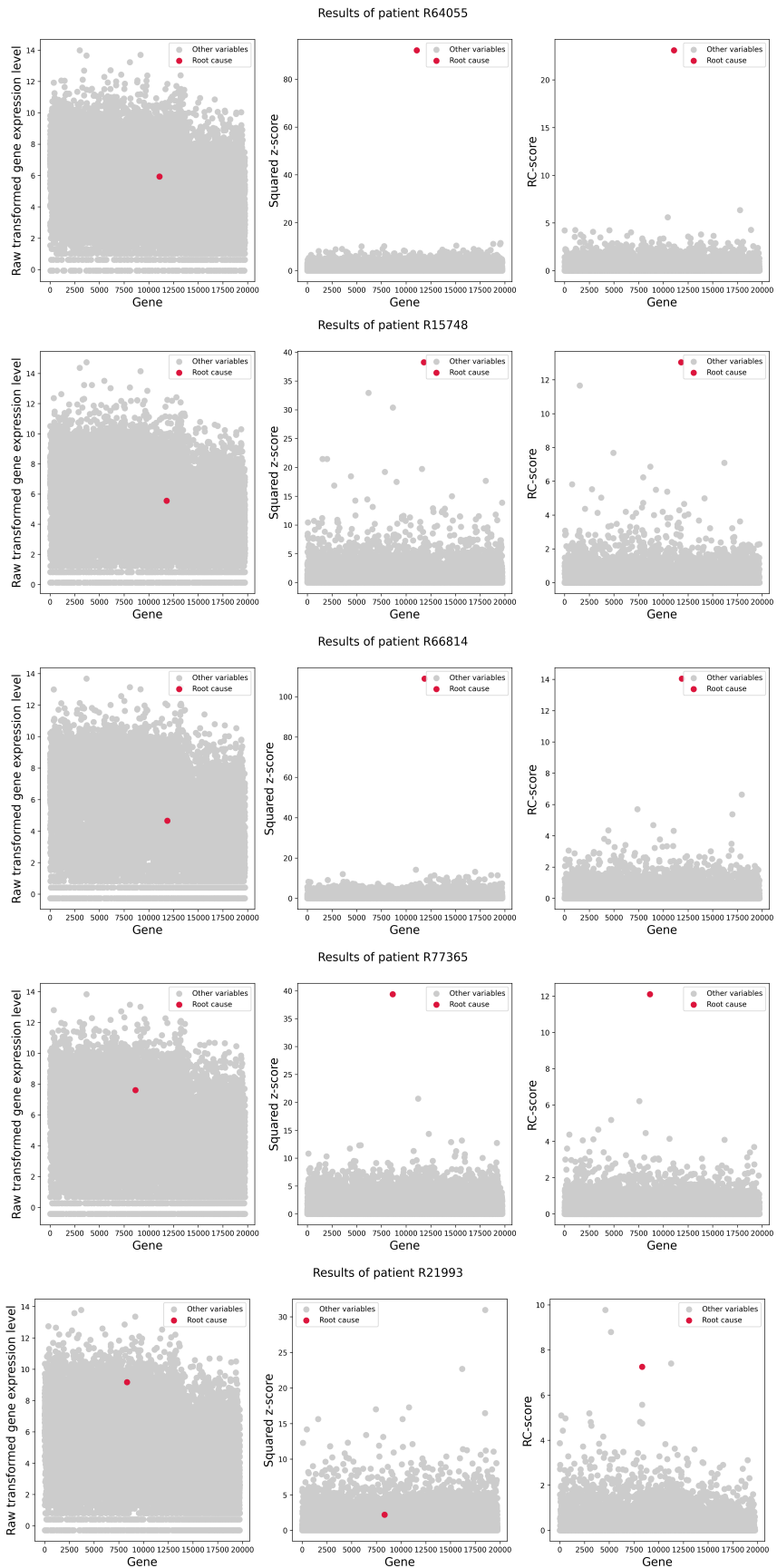


Figure 26: The raw transformed gene expression levels, squared z-scores, and RC-scores of genes for patients *R64055*, *R15748*, *R66814*, *R77365*, and *R21993*.

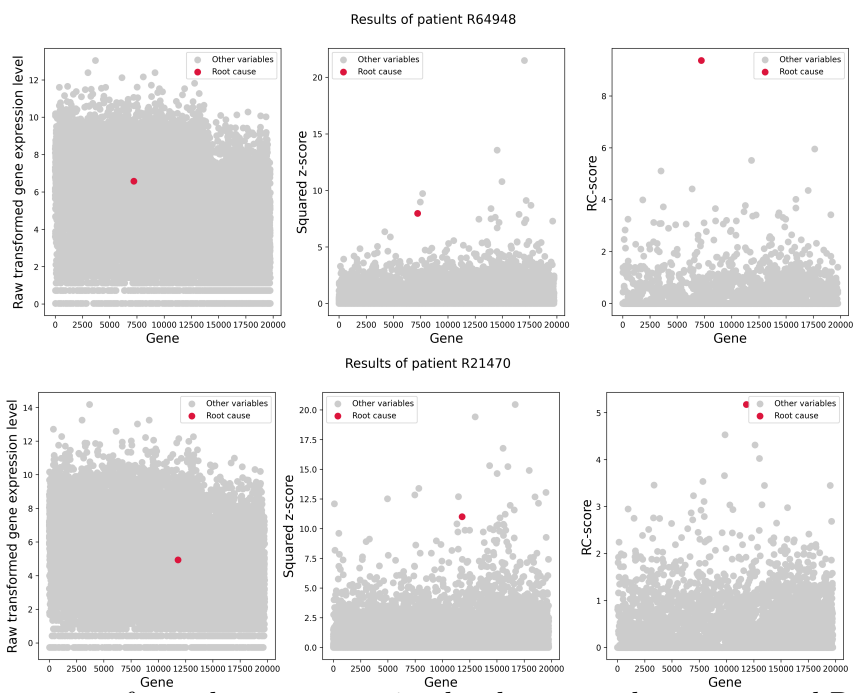


Figure 27: The raw transformed gene expression levels, squared z-scores, and RC-scores of genes for patients *R64948* and *R21470*.